SPECTRAL SHAPING IN DC-DC CONVERTERS USING MAXIMUM ENTROPY RANDOM PULSE WIDTH MODULATION

A Master's Dissertation by

Albert Dove

in the
Faculty of Engineering and the Built Environment
School of Electrical and Information Engineering

16 February 2018

Declaration of Authorship

I, Albert Dove, declare that this thesis titled, 'SPECTRAL SHAPING IN DC-DC CONVERTERS USING MAXIMUM ENTROPY RANDOM PULSE WIDTH MODULATION' and the work presented in it are my own. I confirm that:

- This work was done wholly or mainly while in candidature for a research degree at this University.
- Where any part of this thesis has previously been submitted for a degree or any other qualification at this University or any other institution, this has been clearly stated.
- Where I have consulted the published work of others, this is always clearly attributed.
- Where I have quoted from the work of others, the source is always given. With the exception of such quotations, this thesis is entirely my own work.
- I have acknowledged all main sources of help.
- Where the thesis is based on work done by myself jointly with others, I have made clear exactly what was done by others and what I have contributed myself.

Signed: _____

Date: _____

Abstract

This work investigates the impact of probability distribution functions (PDF) on spreading the harmonic power in the power density spectrum (PSD) of Random PWM (RPWM) switching signals. Periodic switching is known to result in conducted electromagnetic interference (EMI) in switched-mode power converters. The main benefit of using RPWM signals is the ability to reduce the amplitudes of harmonics that cause conducted EMI. This helps in minimizing the dependence on sophisticated EMI filters that are typically used for mitigating this problem. This contributes to reduced volume and cost of power converters. With these benefits, a RPWM signal with the *'most reduced'* harmonics, and results in the desired power conversion, can be considered an ideal switching signal. In the PSD of RPWM signals, the reduction in the amplitude of harmonics does not imply that their harmonic power is lost. Instead, it is spread throughout the spectrum. This phenomenon establishes the relation that spreading out harmonic power reduces the high amplitude harmonics. As a result, it can be similarly said that *maximally* spreading out harmonic power in the PSD is an ideal requirement. This requirement is a key property that this research seeks to achieve, while ensuring that the RPWM signal maintains its properties that allow it to be used in a DC-DC converter the same way a traditional PWM would be used to convert electrical power. This is a constraint that is mostly governed by the duty ratio and, in the case of RPWM signals, by the nominal duty ratio. RPWM behaviour is governed by probability distribution functions that determine the nominal behaviour of the signal. This means that by using PDFs, the ability to alter both the time-domain nominal properties and frequency domain properties (in the PSD) is granted. The Method of Maximum Entropy in itself grants the very ability to obtain a PDF that has a maximally spread out distribution of probability while maintaining those time-domain nominal switching constraints. This idea ignited the initial investigation into how Maximum Entropy probability distributions result in the maximal spreading out of the PSD, given time-domain constraints. Before this, an investigation into the relationship between spreading out of probability in the PDFs and spreading out of harmonic power in the PSD is presented. Where it was found that increasing spreading of probability (quantified by entropy) of RPWM causes more spreading out of harmonic power in the PSD. This finding then qualified the use of Maximum Entropy (MaxEnt) PDFs to maximally spread out harmonic power, while maintaining time-domain constraints. With this, a method for computing MaxEnt PDFs given the time domain constraints - was formulated, and their ability to spread out harmonic power and yet maintain the constraints - was demonstrated. Additionally, MaxEnt PDFs coupled with varying the strength of time-domain constraints, revealed the limitations of spectral spreading using RPWM PDFs. Wherein stronger time-domain constraints of the PDFs restricted the maximum spreading level that can be obtained in the PSD.

Acknowledgements

I would truly like to thank my supervisor Professor Ivan Hofsajer for his support, motivation and guidance. It has been an honour to work with him and get to be supervised by him. His comprehensive lessons about 'creating new knowledge' are highly appreciated as they are the cornerstone of this work.

I would also like to wholeheartedly thank my co-supervisor Jacques Naudé for his providential guidance and enthusiastic discussions, especially for validating some of the analytical arguments presented in this work.

A huge thank you to my siblings for their unwavering support and encouragement.

Lastly, I'm eternally grateful to The Lord Jesus. For all things that have worked together for good.

To my siblings; Sandy, Sam, Violet, Shaun and Olga

Contents

List of Figures

List of Tables

Chapter 1

Introduction and Outline

1.1 Introduction

The research in this dissertation relates to Random Pulse Width Modulation (RPWM) in switched-mode power converters. The emphasis is on spectral shaping for the purpose of Electromagnetic Interference (EMI) reduction. Spectral shaping is concerned with using random modulation techniques to design and shape the Power Spectral Density (PSD) of a PWM signal.

The purpose of this chapter is to introduce the reader to the concept of a random PWM and to motivate for the significance of this research. The background is first discussed, which entails the problem of EMI and its abatement in switched-mode power converters. This then leads to a discussion of RPWM and its impact on the spectral content of a converter. The time-domain properties, as well as the spectral properties of RPWM signals, are discussed. A description follows of some of the issues in spectral shaping, which lay the foundation for the motivation of this research. A problem statement, as well as the scope and focus of the research, is then discussed. An outline of the rest of the dissertation concludes the chapter.

1.1.1 Background

With growing technologies in renewable energy, well-designed DC-DC converters are essential in maximising the harvest of energy from renewable energy sources [1, 2]. The advancement of power electronics determines how well this energy can be harvested. However, certain issues arise with the increasing effort to efficiently convert electrical

power. It is known pragmatically that switching is mandatory in order to efficiently convert electrical energy. However, EMI is a by-product of this conversion process.

EMI can be generally described as electromagnetic energy released from a source through a coupled path to any susceptible device or victim. There are two main types of EMI characterised by the type of coupling mechanism, namely conducted EMI, which is through conducting wires, and wirelessly, as radiated EMI [3–7]. It is important for designers to mitigate this and to ensure that electrical equipment meets Electromagnetic Compatibility (EMC) regulations. This ensures that the switching circuits do not interfere with other linked circuits, ensuring proper uninterrupted functionality [3].

The most important contributing factor to conducted EMI generation is the production of harmonics resulting from the periodic switching pattern of switching circuits [3, 8]. A periodic PWM that drives the switching process follows a constant switching frequency with a given duty ratio. Consequently, the EMI spectrum contains high amplitude peaks concentrated at the switching frequency and at multiples of this switching frequency [7, 8]. In the case of inverter-fed motor drives, this constant switching pattern induces mechanical vibrations and harsh-to-hear acoustic noise [9–12].

Traditionally, EMI is mitigated by using numerous varieties of carefully designed EMI filters. Inserting filters at the supply, as well as at the output of the converters, has been the primary means of attenuating conducted EMI in order to reduce its impact and also to adhere to EMC standards [3, 8]. However, EMI filters are not ideal. Designing a better performing EMI filter results in an increased overall volume, which effectively decreases the volumetric power density of the converter, which furthermore leads to an increased overall cost of constructing the filters [3, 5, 13, 14].

It is these challenges which led to the development of new research focuses in power electronics, where the aim is to reduce the high amplitude harmonics without extensive use of EMI filters. Significant amounts of research have gone into using RPWM techniques, where it has been shown that by introducing a form of controlled-randomness to the switching pattern (to maintain the nominal switching pattern) in order to weaken the periodicity and relax the concentration of harmonic power, the high amplitude peaks that cause conducted EMI can be reduced [15–26].

The work presented in this dissertation forms a piece of the puzzle that contributes to achieving these aims. The aim is now to develop this knowledge further by investigating the limitations of how far this harmonic power can be reduced and what the associated

trade-offs are. More importantly, to understand the general impact of probability distribution functions (PDFs) that govern the RPWM strategy on both the time-domain and spectral-domain properties.

1.1.2 Random Pulse Width Modulation

It is known that the switching pattern in a deterministic PWM contains harmonics in the frequency spectrum. Due to the injection of randomness to the switching pattern or to the PWMs reference signal, the harmonic power is (partially) redistributed over a wider frequency range, which is typically observed and analysed from the PSD of the PWM signal, or the (input or output) terminals of a power converter. This method dates back to as early as around 1970, where Clark showed the abatement of acoustic noise in a DC-DC converter by the injection of noise to the reference voltage [27].

1.1.2.1 Basic Principle of Random PWM

A time-domain PWM signal is fundamentally characterised by three parameters: the Pulse Width W, the Pulse Period T and the Delay Δ as shown in Figure 1.1. Randomisation of a parameter means that at every switching cycle k, after some time t_k, the value that W_k, T_k and/or Δ_k will take is chosen at random from a given pool of possible values. The outcome will make up the pulse as shown in Figure 1.1A. The entire switching signal is therefore parameterised as (adopted from [17])

$$x(t) = \sum_{k=-\infty}^{\infty} u(t - \xi_k, W_k), \tag{1.1}$$

where the function u takes W_k as the input and produces a pulse with width W_k and time shifted by ξ_k. The variable ξ_k is a function of T_k and Δ_k. The switching function $x(t)$ is as shown in Figure 1.1B.

The randomisation must occur under the constraint that the desired PWM is obtained – on average – to ensure that the required energy conversion is achieved. For this, randomisation follows a predefined probability distribution that determines how the discrete values in the pool are chosen. This in turn affects the spectral properties of the PWM signal.

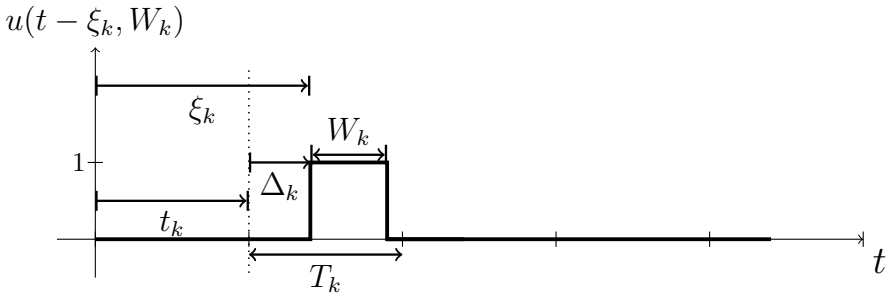

(A) Switching pulse function for a single pulse (at some switching cycle k).

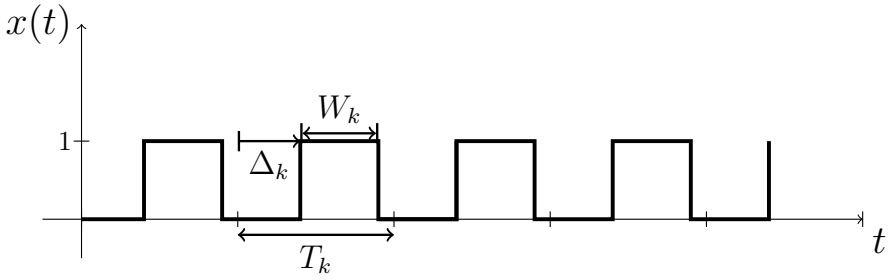

(B) Simplified PWM pulse train with three characteristic parameters W, T and Δ. It is composed of time-shifted pulses represented as u.

FIGURE 1.1: Showing fundamental parameters that characterise a PWM switching signal.

1.1.2.2 Impact of Probability Distribution Functions of RPWM on Power Spectral Density

In any RPWM strategy, a PDF of PWM parameters is required from which to sample the random PWM values. From this perspective, a PDF can be thought of as an input function to control the random switching pattern. Altering the switching pattern alters the RPWM signals spectrum (which essentially is the spectral content that is introduced by the switching device into the power converter circuitry) [15–21].

In a review of the impact of RPWM on converter-fed drives, the authors showed that randomisation of different parameters alters the PSD [7]. Lee *et al.* [28], give a performance characterisation of current (year 2016) state of the art RPWM methods in industrial adjustable speed drives based on various performance indicators including harmonics producing audible noise. Tse *et al.*[29], on the other hand, presented a detailed analysis of the random pulse period (or random carrier frequency) modulation, where this technique was proven to suppress conducted EMI in a switched-mode power supply.

The key idea in all these publications is that every randomisation strategy and other 'customised' strategies have been shown to alter the PSD in some form or another.

Further RPWM papers demonstrate this [21, 24, 30–32].

1.1.2.3 Spectral Shaping using PDF

The studies on using RPWM for altering the spectral content of a converter create an opportunity to manipulate – to some extent – the spectrum by manipulating the PDFs that govern the RPWM. The general approach to the spectral shaping problem is from an optimisation perspective, where a PDF must be found that satisfies the following requirements: 1) It must minimise a certain objective function or meet some spectral specifications, and 2) it must minimise this objective function within a certain region of time-domain constraints [17, 22–26]. For example, this objective function can be the total power in a certain frequency band of the PWM signal, and the constraints could be an average duty ratio that results in the desired power conversion. The spectral specification with which this dissertation is concerned is reducing the harmonic amplitudes in the PSD.

1.1.2.4 Spectral Spreading Link to Spectral Amplitude Reduction

Studies that are concerned with reducing EMI using random modulation, establish a visually observable impact of random modulation, where spreading the harmonic power over other frequencies results in a reduction in the harmonic peaks when either the pulse width (W), pulse period (T) or pulse position (Δ) are randomized [5, 7, 21, 24, 33].

Publications [5, 33] demonstrate how increasing the range of the frequencies in the random frequency pool (which are equivalent to the pulse periods), causes the harmonic power in the PSD to spread over a wider frequency range. It was then shown that, as a result of the spreading out, the EMI amplitudes where reduced. This applied to both random modulation with varying and with constant duty ratio.

According to Tse *et al.* randomising W produces discrete harmonics at multiples of the switching frequency as well as a continuous component over the frequency spectrum [21]. It was also demonstrated that randomising Δ can be categorised into two types, lead and lag random pulse positions [7, 21, 24]. According to these authors, randomising Δ results in each harmonic amplitude being reduced accordingly and the power lost being transferred to the continuous spectrum. However, the harmonics still have relatively high amplitudes, but are progressively smaller for higher order harmonics.

If T is randomised while keeping W constant then the duty cycle changes accordingly [21]. This is referred to as random carrier frequency with variable duty modulation (RCFVD). If the width is allowed to vary by the same proportion as the period, then it becomes a random carrier frequency with fixed duty modulation (RCFFDM). The PSDs of RCFVDM and RCFFDM have a continuous spectrum due to the switching frequency itself being randomised (the concept of a continuous and a discrete spectrum will be later revisited in detail).

Randomisation of the switching frequency flattens the discrete harmonics into the continuous spectrum [7], but the low frequency harmonics in RCFVDM have higher amplitudes than in RCFFDM [21]. This makes RCFFDM the best among the three fundamental random modulation techniques when it comes to spreading harmonic power [21].

Studies that are primarily concerned with three phase inverters, also observe the spread spectrum effects, and these effects are reported to result in improved acoustic and vibration performance, due to the reduced harmonic amplitudes caused by periodic PWM [5, 34–43].

Many of these studies, therefore, use the term 'spreading' synonymously with high amplitude harmonic reduction, due to this phenomenon being visually observable from the PSD, as well as its physical effects being evident. In other words, there is an underlying assumption that spreading out invariably leads to harmonic reduction. However, no formal definition of spreading is provided except for the visually observed effect. Although there exist statistical measures of spreading, such as the harmonic spread factor [44], that aim at obtaining a performance measure of this spreading effect. This publication neither describes nor defines the relation between the two, nor do many other publications. To the authors knowledge, the few publications that are closest to describing the link between reduction and spreading are by Stanković and Bech [17, 45]. Their respective researches show, analytically, how a PSD is composed of a discrete (high amplitude) harmonic component and a continuous component, and that, as the RPWM signal is randomised, the discrete component loses its power to the continuous component, thereby reducing its high amplitudes.

For this dissertation, and similar to published material, the general notion that spreading results in reduction is adopted. However, a description and quantification of spreading will be proposed that could be useful for further analysis.

1.1.3 Theoretical Issues in Spectral Spreading

Having discussed that one of the goals of spectral shaping is to spread the harmonic power in the PSD in order to reduce conducted EMI, a spectrum with the most spread out harmonic power is, from an EMI perspective, the 'best spectrum'.

Therefore, computing an ideal PDF for RPWM, which will result in this desired performance, is of great significance and has not been solved. It is not known if there exists a method to find the 'best possible' PDF that can satisfy the PSD spreading out requirements. The closest attempts were made by Kirlin *et al.* [19], where an optimal approach was presented. The objective was to find a PDF for a carrier frequency-based RPWM that would maximise the power in the continuous spectrum. However, the authors stated that the adjective 'optimal' does not refer to 'the best possible' and, as a result, the optimisation does not truly yield a best solution. This is true, considering that not all three random parameters were candidates for random strategies.

Other optimisation attempts were aimed at selecting the best suited pool of possible frequencies [25], or at optimising for the total harmonic distortion (THD) with carrier frequency-based RPWM techniques [23]. However, not much attention has been given to the impact of probability distribution function of all three the PWM parameters (jointly) on spreading out the harmonic power in the PSD. Such an investigation would bring the benefit of using PDFs of all three random parameters as the fundamental control variables to manipulate the spectral content of a PWM, as well as knowing the limits of these RPWM techniques based on their PDFs, and the ability to find a 'best possible' PDF suited for obtaining the 'most spread out' spectrum, given certain PWM specifications or constraints.

1.2 Research Problem

1.2.1 Problem Statement

The following problems are thus summarized:

(1) *The limiting factors of PDFs on spectral spreading are not sufficiently known.*

It is important to know what prevents a PDF from spreading the spectrum wider than it already does. It is hypothesised that having certain specifications, such as duty ratio or a limited RPWM pool, will affect the spreading out capabilities due to

limiting the degrees of freedom. This is intuitive, but a theoretical framework is of great significance.

(2) *There are currently limited methods of finding the best PDF which will result in a maximally spread out PSD given PWM time-domain constraints.*

Literature that is concerned with optimising for a PDF that will maximally spread the PSD typically use a single parameter among the three, with random carrier frequency being the most common [4, 19, 43]. This leaves the joint randomisation of the three unexplored. Thus any method that attempts to optimise for random PWM must take all three into consideration (see 5.4.4.3). This (to the authors knowledge) has not been explored in depth. Assuming that a PDF is the only means used to alter the PSD, then the best possible PDF must yield the best possible PSD. The best possible PSD is defined as the maximally spread out spectrum possible. As acknowledged previously, it is possible that certain PWM specifications might limit the PDF from spreading the PSD any wider. In other words, the very same PWM specifications given by converter designers might become the limiting factors to spreading the spectrum any wider. However, it would be beneficial to maximally spread the PSD within the given constraints or limitations; i.e. due to these limiting factors, the resulting PSD would be the best spread out possible – given the constraints.

1.2.2 Proposed Solution

The Method of Maximum Entropy [46] is a method that can be used to compute probability distribution functions (of a random variable) with maximally spread out probabilities, yet satisfy any constraints placed on it.

If there is a relationship between spreading out of probability and spreading out in the PSD, then this creates an opportunity to use the Method of Maximum Entropy to spread the probability distributions of the RPWM, while maintaining nominal switching constraints, and effectively spread the PSD. Additionally, understanding this relationship would allow for an investigation into the limiting factors of spectral spreading.

The research question is, therefore, stated as a two-part question, as follows:

"What is the relationship between spreading out of probability and spreading out of the power density spectrum of a Random PWM signal? To what extent do Maximum Entropy probability distributions of random PWM subject to constraints, result in a maximally spread out PSD?"

1.2.3 Hypothesis and Research Objectives

There are a few prerequisites to answering the research question. Firstly, the random PWM signal must be characterised using probability. From this, spreading out in the PSD must be quantified and its relationship to probability spreading can be investigated.

When considering random carrier frequency modulation (which can be referred to as random pulse period), it is intuitive that a probability distribution describing the likelihood of choosing certain switching frequencies will - most likely - introduce the frequencies with the highest probability into the PSD (see Appendix A in the 'model problem' as it also establishes this intuition). And thus introduced frequencies (under some constraints) may appear to spread out the PSD.

The major hypothesis is therefore: Increasing the spreading out of probability will increase the spreading out of harmonic power in the PSD.
[1]

An important role of this hypothesis is that it allows the Method of Maximum Entropy to be stated as a proposed solution to maximal spectral spreading, provided the hypothesis is true. The research objectives are thus summarised as follows:

- To define the general behaviour of a RPWM by using PDFs
- To prove the relationship between spreading out the probability distribution and spreading in the PSD
- To compute maximum entropy probability distribution functions for RPWM that will lead to maximally spread PSD, taking into consideration the time-domain probability constraints
- To determine the factors that limit spreading out in the PSD using PDFs
- To provide theoretical framework on how to obtain the most spread out spectrum given certain RPWM specifications

[1] Although not explicitly, the work presented by Bech [34] Kirlin [47] and Covic [48] hint this hypothesis as their work shows how spreading in the PSD is increased by addition more random carrier frequencies in the pool. Adding more frequencies implies spreading out the distribution of probability to other frequencies. This is true considering the nomalisation constraint of probability distribution functions that all probabilities sum to 1 (this is discussed in detail in succeeding chapters).

1.2.4 Research Constraints

The main motivation for this research is the mitigation t of conducted EMI in DC-DC converters. This is tackled from the perspective of spectral shaping. Although it is possible to extend the work for application in inverters, as well as reduction of vibrations and audible noise in inverter-fed drives, such aims are beyond the intended scope of this research. It should also be noted that using RPWM and spectral shaping in converters to comply with EMC standards is not the main focus of this research. Although the work may be extendible and beneficial to such aims, it will not be the main contribution of the methods presented in this dissertation.

The following research constraints also apply:

- The research will only focus on the fundamental RPWM methods characterised by the three parameters (Δ, W and T as introduced in Section 1.1.2) .
- The focus is on the time and spectral domain properties of a PWM signal meant for an ideal single switch DC-DC converter.
- The research only focusses on conducted EMI and not radiated EMI.
- Issues concerning trade-offs between switching losses due to rates of switching and EMI are not considered.

This research is only focused on an ideal PWM square wave function. This makes for a contribution to the nature and function of a PWM signal. As such it is theoretically rooted, and is heavily reliant on probability theory. Due to this theoretical nature, analytical and simulated illustrations are used to verify findings. As introductory material, the reader may refer to Appendices A and B, which include a 'model problem' that is a significantly smaller scale version of the RPWM theory contained in this dissertation.

1.2.5 Dissertation Outline

This dissertation is outlined as follows:

- Chapter 2 focuses on developing a general description of a random PWM by using probability distributions of the three RPWM parameters.

- Chapter 3 introduces the Method of Maximum Entropy and how it relates to the idea of defining and quantifying 'spreading'.
- Chapter 4 gives a background on how the formula for analytically determining the PSD is derived. This is important, as the formula is extensively used in the succeeding chapters.
- In Chapter 5 focus is placed on justifying the use of maximum entropy by arguing for the relationship between spreading out in probability and spreading out in the PSD. The argument is founded on the PSD formula for a theoretical backing, and on simulated data for evidence-based arguments.
- Chapter 6 is dedicated to using maximum entropy to spread the PSD, while maintaining nominal switching constraints. An analysis of the impacts and limitations of spreading in RPWM is also provided.
- Chapter 7 offers a summary of the research presented.

1.3 CONCLUSION

This introductory chapter presented three important discussions: the motivation for the research, a background on random modulation and the problem that this research tackles. A background on EMI and EMI reduction was first provided. The use of random modulation for mitigating conducted EMI was then introduced, where the basic principle of RPWM was described and it was highlighted that from the power density spectrum point of view, random modulation reduces the harmonic peaks that otherwise come from periodic PWM. A discussion on spreading out the harmonic power versus reduction in high amplitude harmonics was given, where it was shown how literature accepts pragmatically that random modulation spreads out the harmonic power in the PSD, and that this spreading out leads to a reduction in the harmonic peaks. Due to this phenomenon, in order to reduce EMI, then maximally spreading the harmonic power, while maintaining the time-domain constraints, was considered as an ideal requirement. It was then hypothesised that spreading out probability leads to spreading out of this harmonic power. Following this hypothesis, the Method of Maximum Entropy was proposed to maximally spread the PSD and maintain the constraints. This led to a summary discussion of the main problems that this dissertation aims to solve, which are: providing knowledge about the factors that limit PDFs from spreading the PSD, to describe the relationship between PDFs and PSD, and how maximum entropy PDFs

can be used to find the best possible PDF that will maximally spread out the PSD given PWM time-domain constraints.

Chapter 2

Analysis of Random PWM Probabilistic Behaviour

2.1 Introduction

The ability to describe a random PWM signal using probability is important and useful. A pseudo-random generator samples objects from a predefined probability distribution, and as a result the samples should possess properties that are characterised by the distribution itself. In the same manner, the characteristics and behaviour of a random switching signal can be described by a probability distribution.

This chapter seeks to describe the overall dynamics of generating a random PWM signal, as well as the properties of the PDFs that govern the random behaviour. Since each pulse in the PWM makes up the random PWM signal, each pulse must meet certain requirements to ensure the random PWM signal is suitable to drive a switched-mode converter and to ensure that it results in the desired power conversion. Among these requirements, an added requirement is for the random PWM signal to possess certain spectral properties; particularly, that the random PWM spectrum is spread out for EMI reduction purposes, although, in this chapter, focus is placed mostly on the time-domain properties and constraints.

There exists some literature that has investigated the impact of pseudo-random generators on both the time-domain and spectral properties of random PWM signals [12, 31, 49, 50]. One such example is where an M-sequence (maximum length sequence)

pseudo-random generator is employed and the resulting power spectrum density is analysed [50]. However, as opposed to such research, this chapter seeks to provide a generic overview of the characteristics of a random PWM despite the pseudo-random generation strategy, as well as to provide a starting point by describing factors that need to be considered when analysing random PWM PDFs. Therefore, it should be noted that the presented characterisation is from a purely functional or high-level perspective. Thus, any controlled strategy for a DC-DC converter that exists in literature will likely follow the generic process presented in this chapter in one form or another.

2.2 Aspects of Probability

In the process of describing probability distributions that govern random PWM, a choice needs to be made as to whether to use discrete or continuous probability distribution functions. The statistical properties of the probabilities must also be defined.

2.2.1 Discrete vs. Continuous Probability Distribution Functions

Michael M Bech [17] provided an in-depth comparison of advantages and disadvantages of using continuous and discrete probabilities. The discussion here summarises Bech's comparison along with other researchers that have highlighted the benefits of using discrete probabilities. These are centred around the smoothing effects on the spectrum, optimizsation and implementation.

2.2.1.1 Smoothing the Spectrum

According to experiments done by Bech [34] and acknowledged by Bech *et al.* [16], a random PWM signal governed by a continuous probability distribution produces a smoother output voltage spectrum. This is desirable since it implies smaller harmonic amplitudes. With a discrete probability, the same cannot be assured despite the randomisation strategy. However, according to Kirlin *et al.* [47] and as demonstrated by Covic [51] (where they concluded that the number of possible random pulse periods can be as small as five) the size of the pool or sample space of randomisation can be carefully selected such that this smoothing is obtained, resulting in reduced amplitude harmonics, except for the fundamental one.

2.2.1.2 Optimisation

In spectral shaping, the PDF must be computed such that it achieves or minimises a certain objective function. Thus, spectral shaping is an optimisation problem. With a discrete PDF, or more accurately, a probability mass function (PMF), the probabilities of each possible state in the pool are the free parameters which can be used in the optimisation process [19]. In the continuous probability case, it is convenient to first consider a parameterised family of PDFs and then optimise for the parameters against constraints [17]. For example, a Gaussian distribution can be considered as the general PDF, and the mean and the variance become the parameters to be optimised. However, this already reduces the number of possible PDFs that could be candidates. Thus, such an optimisation process cannot guarantee that the computed PDF is truly the optimum possible. Compared to this, a discrete PDF (or PMF), can be more general as, since no family must be selected, the probabilities themselves determine the shape of the PDF.

2.2.1.3 Implementation

The most important advantage is that discrete PDFs are digitally realisable. Furthermore, if one desired to approximate a continuous distribution, then the interval spacings between the values in the pool of the random parameters can be decreased. Thus, there are no implementation issues, except for computational limitations such as the resolution and memory [51].

In later sections, a detailed discussion is given as to how the pool affects the spreading out capabilities. For now, it is assumed that a limited pool is available.

2.2.2 Stationarity

Similar to Stanković's analysis [45], only stationary randomisation is considered in this research. This means the probabilities do not change over time, they remain stationary at every switching cycle. This also characterises the randomisation for DC-DC converters, where the reference signal does not change over time since a constant duty ratio is maintained. Each switching cycle k is, therefore, independent of the future or past cycles.

It is possible, however, to obtain a more general randomisation that need not be stationary. This is achievable by using Markov Chains, as it takes into account a time

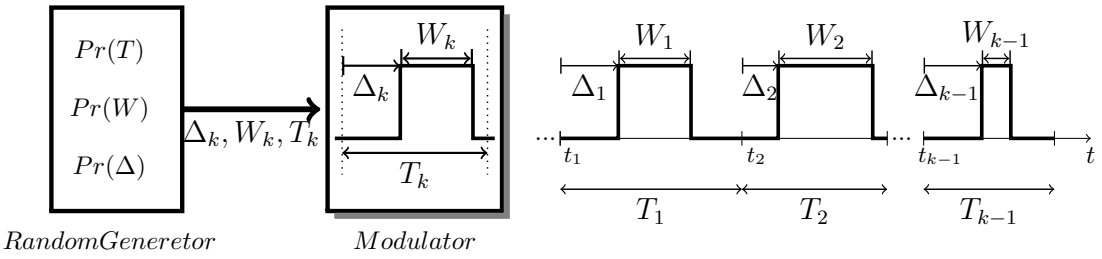

FIGURE 2.1: Showing generic process for computing a random PWM signal for a single switching cycle

dependence, or in this case a switching cycle dependence [52, 53]. However this approach is reported to add some complexity to the random PWM problem, especially for spectral analysis [17].

2.2.3 PMF versus PDF

The term 'probability distribution function (or PDF)' is a generic term, regardless of whether the function is discrete or not. Thus a probability mass function is technically a type of a PDF, which is in this case a discrete PDF. Therefore, to be more specific, the term/abbreviation 'PMF' will be used throughout the text. And since only discrete PDFs are considered for random PWM, the term 'distribution of probability' or 'probability distribution' can be taken to refer to a PMF.

2.3 Random PWM Process

There are two major components that are used here to describe the process of computing a random PWM signal - the random generator component, as well as the pulse generation component which is dubbed the 'modulator'. Figure 2.1 illustrates this process.

2.3.1 Random Generator

The random generator produces numerical values that each random parameter will posses. This occurs at every switching cycle k. The values are produced as triplets (T_k, W_k, Δ_k) with each member of the triplet sampled randomly from a predetermined probability distribution. Thus, each random parameter is sampled from its own PMF denoted $\Pr(T)$, $\Pr(W)$ and $\Pr(\Delta)$, as shown in Figure 2.1. Once the numerical values

are determined, they are passed to the modulator which then creates the pulse possessing those values. The three parameters need not all be random (depending on the preferred random strategy). Note that deterministic PWM switching is contained as a special case of this process. The PMF will have a probability of 1 for a deterministic PWM parameter.

2.3.2 Pulse Generation (Modulator)

The 'Modulator' uses the numerical values produced by the random generator to create a pulse. The modulator thus creates a time-domain pulse which was described as the function $u(t - \xi_k, W_k)$ in Chapter 1. The individual pulses are then summed up to produce a pulse sequence.

2.3.3 Random PWM Generation Constraints

The time-domain constraints also determine the random behaviour of the switching pattern. The PMFs of each random parameter have the respective pools

$$T \in \{T_1, T_2, ..., T_i, ..., T_{N_T}\}, \quad i = 1, 2, ..., N_T, \tag{2.1a}$$

$$\Delta \in \{\Delta_1, \Delta_2, ..., \Delta_j, ..., \Delta_{N_\Delta}\}, \quad j = 1, 2, ..., N_\Delta, \tag{2.1b}$$

$$W \in \{W_1, W_2, ..., W_r, ..., W_{N_W}\}, \quad r = 1, 2, ..., N_W, \tag{2.1c}$$

where N, with its corresponding subscript, represents the total number of values in the pool of each parameter. The corresponding subscripts i, j and r each represent the index of each value in the pool. Therefore, at every k^{th} selection cycle, a value for each random parameter is selected with a selection likelihood determined by the parameter's PMF, which from now onwards will be denoted as $\Pr(T_i)$, $\Pr(\Delta_j)$ and $\Pr(W_r)$. The PMFs remain the same for all selection cycles to ensure that the PWM is wide-sense stationary. It follows that the respective pools also remain unchanged from cycle to cycle.

A set of constraints that each selection cycle must obey are now defined. This set of constraints will be referred to as the primary constraints, as they are essential to producing a valid PWM signal i.e. posses non-overlapping pulses and ensure an amplitude of unity. These are defined as

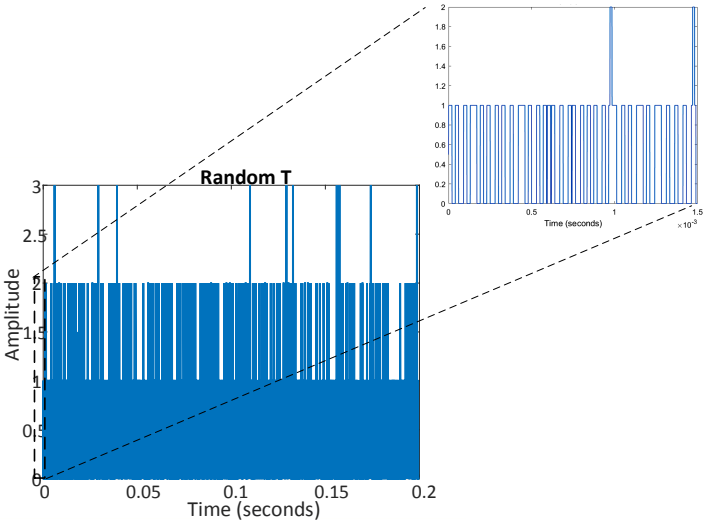

FIGURE 2.2: Showing RPWM signal for random T with undesired overlapping pulses that add up resulting in higher amplitudes (zoomed)

Primary Constraints

$$0 \leq \Delta_k < T_k \quad , \tag{2.2a}$$

$$0 \leq W_k < T_k \quad , \tag{2.2b}$$

$$\Delta_k + W_k < T_k \quad , \tag{2.2c}$$

where constraint 2.2c already encompasses constraint 2.2a and 2.2b. However, both 2.2a and 2.2b have been stated explicitly for clarity. These constraints ensure that the pulse always exists within the magnitude of the pulse period. Therefore, every probability distribution function must be defined such that, when PWM parameters are sampled from the probability distribution, the primary constraints are obeyed. Figure 2.2 depicts a simulated random PWM signal with the undesired overlapping pulses. Thus, obeying the primary constraint is imperative as it maps the physical switching that occurs in the converter.

Another set of constraints are defined here as the secondary constraints. These are the traditional constraints for a deterministic PWM that determine the DC-DC conversion (the switching speed and duty ratio). For random PWM these are specified as the averages

Secondary Constraints

$$\overline{T} = \zeta \quad , \tag{2.3a}$$

$$\overline{W} = \gamma \quad , \tag{2.3b}$$

$$\overline{\Delta} = \alpha \quad , \tag{2.3c}$$

where the bar symbol denotes *average* outcome. The symbols ζ, γ and α represent the numerical constants for the respective PWM parameter averages. The secondary constraints are meant to ensure that the average duty ratio d, which is $\frac{\gamma}{\zeta} = d$ is kept constant. This ensures that the desired power conversion is maintained - at least on average.

2.4 Random PWM Probability Distribution Functions

2.4.1 Random PWM General Probability Distribution Requirements

It is possible that one may desire to randomise all three parameters, or only one of them. In any case, the PMF that is given to the 'Random Generator' can be given as a joint PMF, that determines how T, Δ and W jointly behave. From the joint PMF, the marginal PMF for each parameter can be computed. Therefore, given a pool for T, Δ and W, the joint PMF must ensure the following:

- That the desired power conversion occurs, and the primary and secondary constraints are obeyed
- That, for the DC-DC converter, the joint PMF and the marginal PMFs are stationary
- That the objective is met (which is maximally spreading out the PSD) taking into account both primary and secondary constraints

The reasoning behind these requirements is discussed in depth next.

2.4.2 Random PWM General Probability Distributions

The probability that governs the randomisation can generally be expressed as a joint probability distribution of all the three parameters $\Pr(T_i, W_r, \Delta_j|D)$, where the probability is conditional on the given Data D, which includes the constraints. To facilitate characterising the probabilities, the discussion is divided into two cases:

- Univariate randomisation
- Multivariate (or trivariate) randomisation

2.4.2.1 Univariate Randomisation

If only one parameter is randomised, then the probability that describes random PWM is one of three PMFs. Therefore, the joint probability will either be

$$\Pr(T_i, W_r, \Delta_j|D) = \begin{cases} \Pr(T_i|W, \Delta, D), & \text{for random } T\text{, fixed } W \text{ and } \Delta, \\ \Pr(W_r|\Delta, T, D), & \text{for random } W\text{, fixed } T \text{ and } \Delta, \\ \Pr(\Delta_j|T, W, D), & \text{for random } \Delta\text{, fixed } W \text{ and } T. \end{cases} \tag{2.4}$$

Thus, if two other parameters are fixed, then the PMF of the random parameter is conditional on the fixed ones so that the primary constraints can be obeyed. The PMFs can generally be expressed as a sum of Dirac delta functions, with the weightings (probability mass) determining the probability of choosing some value in the pool as

$$\Pr(T_i, W_r, \Delta_j|D) = \begin{cases} \sum_{i=0}^{N_T} p_i \delta(T - T_i), & \text{for random } T\text{, fixed } W \text{ and } \Delta, \\ \sum_{r=0}^{N_W} p_r \delta(W - W_r), & \text{for random } W\text{, fixed } T \text{ and } \Delta, \\ \sum_{j=0}^{N_\Delta} p_j \delta(\Delta - \Delta_j), & \text{for random } \Delta\text{, fixed } W \text{ and } T, \end{cases} \tag{2.5}$$

where p_i, p_r and p_j are the probability masses for the members of the pools in each corresponding random parameter.

For the special case of random T with fixed duty ratio from cycle to cycle, W is calculated at every k^{th} cycle given the desired duty d and the random outcome of T. And so W can be calculated as

$$W_k = dT_k. \tag{2.6}$$

2.4.2.2 Trivariate Randomisation

As an extreme case, assume all three random PWM parameters are randomised. Then, to ensure that the primary constraints are obeyed, randomisation of one random PWM parameter is dependent on the other two random PWM parameters. This dependence

can be maintained by randomising the parameters in a subsequent order. In one switching cycle, one parameter (out of all the three random PWM parameters) must be randomised at a time. The outcome of the first randomised parameter will determine the PMF of another parameter's constraints, and the outcome of *this* random selection will determine the constraints placed on the PMF of the succeeding random parameter. This means that the PMF of the final random selection is conditional on the previous selection. Once the values that the three parameters will take have been found, then the pulse that is made up of those values can be generated. The subsequent switching cycle will go through the same procedure. To illustrate this, consider the example of rolling three dice next.

Rolling Three Dice

Suppose there are three (6 sided) dice, each representing one of the random parameters T, W and Δ labelled D_T, D_W and D_Δ (the symbol D is borrowed for this dice example). Let each dice be 'fair', i.e. equally weighted sides. It is required that the three dice be rolled. And suppose the primary constraint is this; *in the outcome of rolling the three dice, dice* D_Δ *must be less than both* D_W *and* D_T*, and also* D_W *must be less than* D_T. One of the ways that this can be easily achieved is by rolling each dice subsequently. Starting with dice D_T since it has not been constrained. Once D_T is rolled, its outcome will restrict the possible outcomes of D_W, as some sides of D_W will not be allowed if they are greater than the outcome of rolling D_T. In that way, the probability distribution of D_W is conditional on D_T. The same principle applies for rolling dice D_W and D_Δ.

Trivariate Random PWM Example

In the same manner as in the dice illustration, suppose it is required that all the three random PWM parameter be randomised. And in every cycle, T is chosen first, followed by W and lastly Δ. The process would be carried out as follows:

Selection 1: *Randomly select* T

Probability is $\Pr(T_j|D)$,

Outcome is T_1.

Selection 2: *Randomly select* W *given* T *s.t. primary constraints are obeyed*

Probability is $\Pr(W_r|T = T_1, D)$,

Outcome is W_1 where $0 < W_1 < T_1$.

Selection 3: *Randomly select* Δ *given* T *and* W *s.t. primary constraints are obeyed*
Probability is $\Pr(\Delta_l | T = T_1, W = W_1, D)$,
Outcome is Δ_1 where $0 < \Delta_1 + W_1 < T_1$.

The above selection process would occur at every switching cycle k and would ensure that the primary constraints are obeyed. This type of stochastic model is referred to as a Markov Model [54].

The conditional PMFs thus depend on the order of selection.

If the order of selection is Δ, W and then T, denoted $\Delta \to W \to T$, the joint PMF can be expanded using the product rule as:

$$\Pr(T_i, W_r, \Delta_j | D) = \Pr(\Delta_j | D) \Pr(W_r | \Delta, D) \Pr(T_i | W, \Delta, D), \tag{2.7}$$

For the order $\Delta \to T \to W$:

$$\Pr(T_i, W_r, \Delta_j | D) = \Pr(\Delta_j | D) \Pr(T_l | \Delta, D) \Pr(W_r | T, \Delta, D), \tag{2.8}$$

For the order $T \to W \to \Delta$:,

$$\Pr(T_i, W_r, \Delta_j | D) = \Pr(T_i | D) \Pr(W_r | T, D) \Pr(\Delta_j | W, T, D), \tag{2.9}$$

For the order $T \to \Delta \to W$:

$$\Pr(T_i, W_r, \Delta_j | D) = \Pr(T_i | D) \Pr(\Delta_j | T, D) \Pr(W_i | \Delta, T, D), \tag{2.10}$$

For the order $W \to \Delta \to T$:

$$\Pr(T_i, W_r, \Delta_j | D) = \Pr(W_r | D) \Pr(\Delta_j | W, D) \Pr(T_i | \Delta, W, , D), \tag{2.11}$$

For the order $W \to T \to \Delta$:

$$\Pr(T_i, W_r, \Delta_j | D) = \Pr(W_r | D) \Pr(T_i | W, D) \Pr(\Delta_j | W, T, D), \tag{2.12}$$

Therefore, the product expansion is conditional on the order of dependence. The above equations are general, and assume that all three parameters are randomised. In all the above equations, if one parameter is fixed (non-random), then its probability distribution reduces to 1 for the determined outcome, and zero other wise.

Alternatively, if the random PWM parameters are independently randomized, then their PMFs are not conditional on other parameters. In that case, the probability is expanded as:

$$\Pr(T_i, W_r, \Delta_j|D) = \Pr(T_i|D)\Pr(W_r|D)\Pr(\Delta_j|D) \tag{2.13}$$

where the marginal probabilities on the right hand side are only dependent on the secondary constraints (which are the average values of the random PWM outcomes).

The issue with the case of Equation 2.13 is that there is a possibility that the primary constraints will not be obeyed, since the PMF of any parameter is not aware of the outcome of another PMF.

A possible solution to this is that the pools of each random PWM parameter can be 'pre-set' such that they already obey the primary constraints. For example, if W has 5 possible states or outcomes, then the possible states for W must all be less than all 5 possible states of T. This would ensure that the primary constraints are obeyed while randomising the parameters independently. However, this still has one major issue. Some duty ratios will not be impossible to obtain if all 5 states of W are less than all possible states of T. Independently randomising the three parameters is thus too restricted. Especially for this particular problem were a limited pool is available.

Note that all the probabilities functions presented throughout this work are implicitly conditional on D. Thus, from here onwards, D will be omitted for convenience.

2.4.3 Final Remarks

The PMFs that characterise the random PWM signal can depend on how one decides to randomise the parameters. The possible PMFs are as given from Equation 2.4 for randomising one parameter, right through to Equation 2.13, when randomising more than one parameter, independently or interdependently, where independently randomising the parameters limits the duty ratios that can be obtained.

The idea of choosing the order of randomisation when randomising all three the parameters shall be revisited in later chapters to introduce a more general approach that is not dependent on the order of selection, but instead considers all possible orders of selection as combinatorial outcomes of triplets of (T_i, W_r, Δ_j). The current approach illustrated the importance of the primary constraints and how they introduce conditional PMFs.

At this stage, the description of how the PMFs will ensure that the secondary constraints are obeyed, as well as how they will ensure that the resulting random PWM spectrum is maximally spread out, has not yet been given. This follows in the next chapter.

2.5 Conclusion

This chapter was focused on describing the properties of PDFs that are suitable for random PWM. Firstly, a discussion on the type of PDF to be used for analysis between a continuous and discrete PDF was given, where a discrete PDF (PMF) was preferred, mainly due to its practicality for digital implementation. The process of generating a random PWM signal was then given, which led to a discussion on characterising the generic PMFs that generate the random PWM signal. These characteristics include the constraints that the PMFs must obey, and the associated requirements for obtaining a valid random PWM signal that can be used for DC-DC converter. The discussion on characterising the random PWM PMF concluded with providing general joint PMF functions that are based on the parameters being randomised and on the relationship between the random parameters. This leads to the following chapter which focuses on solving for the PMFs that meet all the given requirements.

Chapter 3

Maximum Entropy Probability Distributions

3.1 Introduction

Maximum Entropy is a method that assigns probabilities that maximise the spreading out of probability and ensures that the constraints that are specified are maintained. The goal of this chapter is to introduce the Method of Maximum Entropy and how it is proposed to be used for spectral spreading. It also seeks to qualify the application of maximum entropy given the ultimate goal of randomising a PWM such that the harmonic power in the PSD is maximally spread out. The notion of different levels of constraints that describe the degree of freedom of randomisation is also introduced.

3.2 Definition of Entropy

In thermodynamics and statistical mechanics, entropy has been defined more generally, as the measure of the amount of chaos or disorder [55]. In information theory, informational entropy is a quantity that describes the amount of information content of a random variable [48, 55]. However, Jaynes'[56] contribution was crucial as it led to the insight that Shannon's entropy was not limited to information theory in communication channels, nor is it limited to interpretations of thermodynamic systems [46, 56, 57]. Jaynes argued that entropy is a method of inference, not necessarily a physical quantity and that it could be used irrespective of being interpreted as heat loss, disorder or uncertainty [56, 57].

3.2.1 Shannon's Entropy Definition

Given a random variable with the pool $X \in \{x_1, x_2, x_3, ..., x_N\}$ and discrete probabilities $p_i = \Pr(x_i)$. The Shannon's entropy H of probability is defined as [57]

$$H[\Pr(x_i)] = -\sum_{i=1}^{N} p_i \log p_i. \tag{3.1}$$

In information theory, Equation 3.1 measures the uncertainty of the random variable X. It can also be said that it measures the amount of missing information one has about X [48, 57]. In other words, the more information one obtains about X, the more certain (less uncertain) one is about X - the higher the certainty, the lower the entropy.

In this work, the logarithm in Equation 3.1 is used with the base e.

3.2.2 Entropy as 'Spreading'

The notion of entropy as a measure of certainty is now extended further to describe spreading out of probability as entropy as well.

Note that a probability distribution holds the normalisation constraint that the sum of all probabilities must be 1 ($\sum_i p_i = 1$). Then the total probability of 1 is always shared or distributed to each element of the pool. This means that, if there exists a low uncertainty (high certainty), then most of this probability mass is allocated to the elements that possess a higher certainty. The shape of the PMF would have a higher probability density for the elements with higher certainty. In this case, the probability mass is more concentrated at the elements with a high degree of certainty. High certainty corresponds to lower entropy. On the other hand, low certainty (or high uncertainty), is represented by a 'flatter' PMF, with a wider (more even) distribution of probability across the elements of the pool.

These two cases are demonstrated by Figure 3.1 and Figure 3.2 with a random variable F possessing 5 elements $f_1 - f_5$. Equation 3.1 was used to calculate the entropic value of each PMF. In Figure 3.1, the elements with higher probability have essentially 'gathered' most of the probability. This is where there is a higher degree of certainty. In Figure 3.2 the probability has been more distributed or 'spread out' to other elements. This spreading out of probability is an indication of less certainty (or high uncertainty) as its entropy is higher than in Figure 3.1.

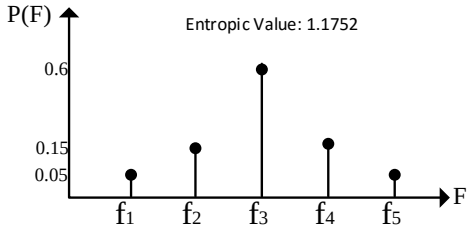

FIGURE 3.1: Example of PMF with probability spread out among the elements $f_1 - f_5$, and associated entropy

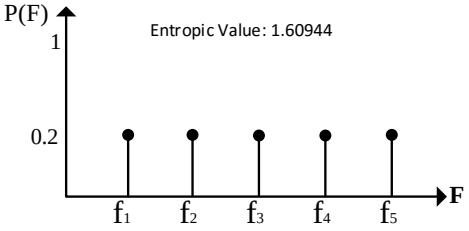

FIGURE 3.2: Example of more a spread out PMF, spread among the elements $f_1 - f_5$ with higher entropy

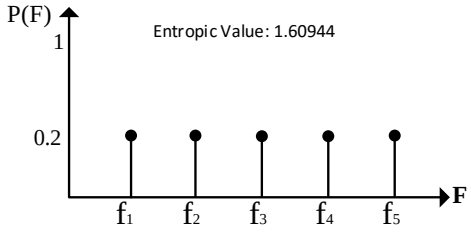

FIGURE 3.3: Example of PMF with probability evenly spread among the elements $f_1 - f_5$

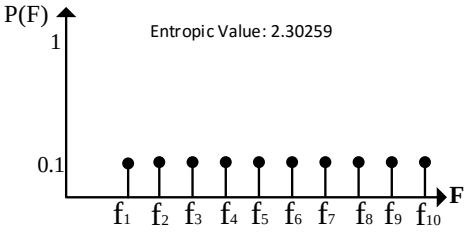

FIGURE 3.4: Example of PMF with more spreading when more elements are added ($f_1 - f_{10}$)

If the number of elements in the pool increases, then entropy can also increase due to probability maintaining the normalisation condition. This is demonstrated by Figure 3.3 and 3.4. Therefore, the more distributed or the more spread out the distribution of probability, the higher its entropy. The less spread out, then the lower the entropy.

Singh [55] summarises different interpretations of entropy, one of which was that entropy can be perceived as an inverse measure of concentration, or in other words, spreading. In a similar manner, entropy in this dissertation is interpreted as a measure of 'spreading out' of probability.

3.2.3 Maximising Spreading

Recalling that one of the main goals is to maximally spread out the PSD of a random PWM signal, then the Method of Maximum Entropy is applicable if there is an increasing monotonic relation between the spreading out of probability and spreading out of harmonic power in the PSD. If this is true, then it can be said that maximum spreading in the distribution of probability, when used in RPWM, results in what can be considered to be a maximally spread out PSD. This is under the assumption that PMFs are the only means of manipulating the PSD.

Now it becomes readily apparent that if the probability is constrained, for example by reducing the number of allowable elements in a pool, then the 'degrees' of freedom for randomisation are limited. This constrains the spreading out of probability. However, if a maximally spread PMF that still satisfies these constraints is found, then a corresponding PSD - which will also be maximally spread out - is the result.

In that regard, the optimality condition is to maximise the spreading, which is entropy, in the distribution of probability – while obeying the constraints. This is the main idea behind maximum entropy probability distributions [46, 57].

3.3 Maximum Entropy and Constraints

In the Method of Maximum Entropy (MaxEnt), constraints represent the amount of additional information that is known about the random variable. For example, suppose the required average outcome of sampling a random variable is defined, but the distribution of probability of the random variable is not known. Then this average outcome becomes a constraint that the PMF must satisfy if random samples are generated from it. This known information can be represented in a form of probability constraints and can be in a form of moments (or expectations) [58].

The probabilities p_i, are the free parameters to be optimized. The objective function is entropy (spreading out) of probability.

3.3.1 Computing Maximum Entropy PMFs

This derivation is adapted from Caticha [57]. The MaxEnt probability distribution p_i^*, is formulated as

$$p_i^* = \arg\max_{p_i} +H[\Pr(x_i)], \tag{3.2}$$

such that the expectation of some function $f_q(x_i)$,(where $q = 1, 2, \ldots, m$) is known to have the numerical values F_q:

$$E\Big[f_q(x)\Big] = \sum_i^N p_i f_q(x_i) = F_q, \quad q = 1, 2, \ldots, m, \tag{3.3}$$

where $E[\cdot]$ is the expectation operator that represents the constraints that must be obeyed.

And the obvious constraint is the normalisation constraint

$$\sum_{i}^{N} p_i = 1, \quad p_i \geq 0. \tag{3.4}$$

From the method of Lagrange [59], the Lagrangian that incorporates the constraints is

$$L = H[\Pr(x_i)] - \alpha \sum_{i}^{N} p_i - \sum_{q=1}^{m} \lambda_q E\Big[f_q(x_i)\Big], \tag{3.5}$$

where α and λ_q are Lagrange multipliers that handle the normalisation and the expectation constraints respectively.

Now taking the first variation of L with respect to p_i and equating it to zero results in

$$\delta\Big(H[\Pr(x_i)] - \alpha \sum_{i}^{N} p_i - \sum_{q=1}^{m} \lambda_q E\Big[f_q(x_i)\Big]\Big) = 0, \tag{3.6}$$

where δ here represents the first variation. The above can be rewritten as

$$\delta\Big(-\sum_{i}^{N} p_i \log p_i - \alpha \sum_{i}^{N} p_i - \sum_{q=1}^{m} \lambda_q \sum_{i}^{N} f_q(x_i) p_i\Big) = 0, \tag{3.7a}$$

$$\therefore \quad -\sum_{i}^{N} \Big(\log p_i + 1 + \alpha + \sum_{q=1}^{m} \lambda_q f_q(x_i)\Big)\delta p_i = 0. \tag{3.7b}$$

Solving Equation 3.7 yields the canonical probability distribution [60].

$$p_i^* = e^{-(\lambda_0 + \lambda_1 f_1(x_i) + \lambda_2 f_2(x_i) + \ldots + \lambda_m f_m(x_i))}, \tag{3.8}$$

where $\lambda_0 = 1 + \alpha$. λ_0 is computed by imposing the normalisation constraint. The Lagrange multipliers λ_q are determined from the expectation constraints in Equation 3.3. The resulting PMF when applying some constraints is considered next.

3.3.1.1 MaxEnt Probability With Minimal Constraints

Minimal constraints means there are no constraints imposed on the MaxEnt probabilities, except for the normalisation constraint. This can be perceived as the 'weakest' constraints due to randomisation having all available degrees of freedom. An alternative view is that no information is known except for Equation 3.4. Therefore $\lambda_q = 0$, and the MaxEnt probability distribution is reduced to $p_i^* = e^{-\lambda_0}$. From the normalisation

constraint

$$\sum_{i}^{N} e^{-\lambda_0} = 1, \tag{3.9}$$

$$\therefore e^{-\lambda_0} = \frac{1}{N}. \tag{3.10}$$

The result is

$$p_i^* = \frac{1}{N}. \tag{3.11}$$

The resulting MaxEnt PMF – given that there are minimal constraints, is a uniform distribution $p_i^* = \frac{1}{N}$ for all i.

3.3.1.2 MaxEnt Probability With Deterministic Constraints

The 'strongest' constraints possible are where no randomisation is allowed. In that case, the probability distribution is deterministic, making $N = 1$. Therefore $p_{i=a}^* = 1$ where a is some arbitrary outcome. This is still the maximum entropy PMF that satisfies the given constraints.

3.3.2 Maximum Entropy for Joint Probability Distributions

The entropy of a joint probability for a multivariate system is easy to compute. The entropy for a joint probability distribution of two random parameters X and Y, with joint probability $\Pr(x_i, y_j)$ is

$$H[\Pr(x_i, y_j)] \leq H[\Pr(x_i)] + H[\Pr(y_j)], \tag{3.12}$$

with equality if and only if x and y are independent. After computing the MaxEnt joint probability distribution, then the marginals can be found as:

$$\sum_{i} \Pr(x_i, y_j) = \Pr(y_j), \tag{3.13}$$

$$\sum_{j} \Pr(x_i, y_j) = \Pr(x_i). \tag{3.14}$$

If the variables are not independent, then the joint distribution is made up of conditional distributions. Therefore, if $\Pr(x_i, y_j)$ is the MaxEnt probability distribution subject to

constraints, then Bayes theorem can be used to find the conditional distributions

$$\Pr(x_i|y_j) = \frac{\Pr(x_i, y_j)}{\Pr(y_j)}, \tag{3.15}$$

or

$$\Pr(y_j|x_i) = \frac{\Pr(x_i, y_j)}{\Pr(x_i)}. \tag{3.16}$$

3.4 Conclusion

The concept of entropy and the Method of Maximum Entropy was introduced. Entropy is interpreted as spreading out of probability. Under the hypothesis that spreading out of probability leads to a spectral spreading in the PSD, the significance of maximum entropy was discussed, where maximum entropy provides maximally spread out probability distributions while obeying constraints placed on it. In this way, spreading out of probability while maintaining constraints becomes the objective of optimisation, so that these probability distributions may be used in random PWM for spectral spreading.

Chapter 4

Spectral Analysis of a Random PWM Signal

4.1 Introduction

The derivation of the formula for calculating the PSD of a RPWM signal is given. The importance of the PSD formula lies in the ability to analyse how probability affects the harmonic power in the PSD of a RPWM signal. The formula has been derived before, but in this case is derived specifically for DC-DC converter application, for randomising pulse width, pulse period and pulse position of the RPWM. More importantly, the PSD formula is later used extensively for analytically showing the relationship between increasing the entropy of the probability and the spreading in the PSD.

4.2 Related Work

Some of the earliest research on the subject of analytically obtaining the PSD of a RPWM signal is by Stanković [22, 45], where the PSD formula is derived, accounting for random Δ, random W and random T. However, Bech [17] argued that, although the work of Stanković has had a huge impact on the framework for the analysis of random PWM signals, the derivation on random pulse period (or random carrier frequency) is rudimentary and lacks supporting measurements. Although Bechs thesis [17], along with his publications [15] do not address random W, his work provided a more comprehensive and general derivation of the PSD formula, supported by verification measurements.

Other significant works that pursued this subject are the publications of Kirlin *et al.* [24, 61, 62], which are only focussed on random pulse position. More recent work published in *IEEE Transactions on Power Electronics* [5, 30, 63] was tailored towards inverters and space-vector random modulation [64].

The work reported in this dissertation follows the comprehensive framework of Bech, but is in this case tailored towards RPWM meant for DC-DC converters (i.e. with constant average switching duties) and addresses all three RPWM parameters. The focus on DC-DC also allows for a less sophisticated derivation. The work highlights some details that require careful attention when investigating the impact of PMFs of random Δ, random W and random T, on the PSD.

4.3 Derivation of the PSD Formula for a DC-DC RPWM

This derivation is adapted from Bech's work [17].

4.3.1 Power Spectral Density of a Signal

The PSD of a signal can be calculated by using the Wiener-Kinchin theorem [65], where the autocorrelation of the time-domain signal and the Fourier transform of the autocorrelation are Fourier transform pairs. The same process applies for a stationary random signal.

4.3.1.1 PSD of a Periodic Signal

For a deterministic signal $y(t)$ the power spectral density $S(f)$ is calculated as

$$S(f) = \int_{-\infty}^{\infty} R(\tau) e^{-j2\pi f\tau} d\tau, \tag{4.1}$$

where $R(\tau)$ is the time autocorrelation function of the signal $y(t)$ calculated as

$$R(\tau) = \lim_{T\to\infty} \frac{1}{2T} \int_{-T}^{T} y(t)y(t-\tau)dt. \tag{4.2}$$

T can be the period (it need not be) of the signal $y(t)$. And $R(\tau)$ and $S(f)$ are Fourier transform pairs

$$R(\tau) = \int_{-\infty}^{\infty} S(f) e^{j2\pi f\tau} df. \tag{4.3}$$

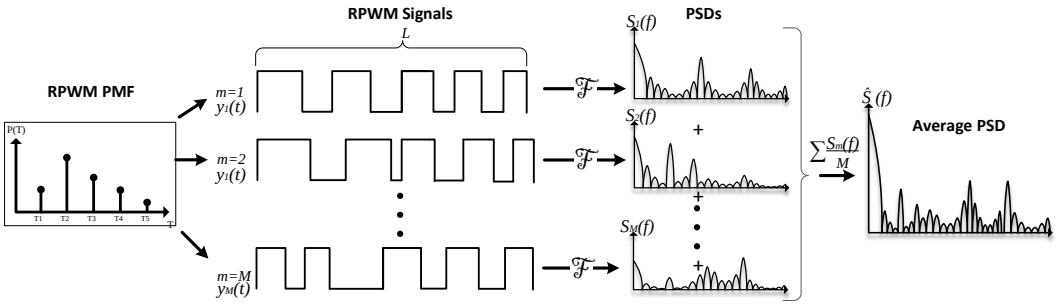

FIGURE 4.1: An illustration of estimating the PSD of a RPWM signal in simulation. Estimation procedure is based on Welch's Periodogram

4.3.1.2 PSD of a Random Signal

The PSD of a random signal $y(t, X)$ where X is the random variable, also takes the form of Equation 4.1, except now the autocorrelation is taken over the ensemble average of the signal as

$$R(\tau) = \lim_{T\to\infty} \frac{1}{2T} \int_{-T}^{T} E\big[y(t, X)y(t-\tau, X)\big]dt, \tag{4.4}$$

where $E[\cdot]$ is an average taken over the whole ensemble of $y(t, X)$ [45].

4.3.2 Estimating the PSD of a Signal in Simulation

For simulations to estimate a PSD, the signal $y(t)$ is sampled into I discrete-time samples $y(t_i)$ $(i = 1, 2, ..., I)$. The PSD can then be estimated using Welch's Periodogram [66]. This is done by splitting the I samples of $y(t_i)$ into M segments, each of length L (so that $LM = I$). The Discrete Fourier Transform (DFT) of each segment is then calculated to obtain the segment's PSD

$$S_m(f_i) = |Y_m(f_i)|^2, \tag{4.5}$$

where $Y_m(f_i)$ $(m = 1, 2..., M)$ is the DFT of the m^{th} segment $y_m(t_i)$ of length L. The M segments are then averaged to obtain the final estimate of the PSD as

$$\hat{S}(f_i) = \frac{1}{M} \sum_{m} S_m(f_i). \tag{4.6}$$

For RPWM the segments can be generated separately, each segment following a predefined PMF as shown in Figure 4.1. Equation 4.6 is reported to provide a good estimate of the spectral content of the signal $y(t)$ [16] .

4.3.3 PSD Formula of a RPWM Signal

Deriving the PSD formula follows three steps. First the RPWM signal is parameterised in the time-domain. Equation 4.4 is then used to obtain the autocorrelation, and finally Equation 4.1 is used to obtain the PSD.

4.3.3.1 Parameterisation of the Switching Function

The switching function was already parameterised earlier in Equation1.1.2.1. It is now expanded to include the random variables as

$$x(t, T, \Delta, W) = \sum_{k=-\infty}^{\infty} u(t - (t_k + \Delta_k), W_k), \tag{4.7}$$

where $\xi_k = t_k + \Delta_k$. The switching cycle time t_k is computed by summing up all the preceding pulse periods as

$$t_k = ... + T_1 + T_2 + ... + T_{k-1}. \tag{4.8}$$

Thus t_k is a function of the random variable T. In that way the switching function x in Equation 4.7 is a function of all three random variables.

4.3.3.2 The Autocorrelation of the Random PWM signal

For notation, the switching function will be reduced to $x(t, X)$ where X is a vector containing the random variables Δ, T and W.

The autocorrelation of the switching function is therefore

$$R_x(\tau) = \lim_{T\to\infty} \frac{1}{2T} \int_{-T}^{T} E\big[x(t, X)x(t - \tau, X)\big]dt. \tag{4.9}$$

Now, consider a truncated version $x_N(t, X)$ of $x(t, X)$ existing between the switching cycles $(-N, N)$ given as

$$x_N(t, X) = \sum_{k=-N}^{N} u(t - \xi_k, W_k). \tag{4.10}$$

Since $u(t)$ is a single pulse, it means Equation 4.10 above consists of a total number of $2N + 1$ pulses. If the signal has an average period of $\overline{T}$, then its autocorrelation function

can be rewritten as

$$R_{x_N}(\tau) = \lim_{N\to\infty} \frac{1}{(2N+1)\overline{T}} \int_{-N\overline{T}}^{N\overline{T}} E\big[x_N(t,X)x_N(t-\tau,X)\big]dt. \tag{4.11}$$

The switching function x_N in the expectation brackets can be written in terms of the right hand side of Equation 4.10. The integration limits can also be extended to $(-\infty,\infty)$ since this does not affect the integration results due to x_N being bounded [only exists between $(-N,N)$],

$$R_{x_N}(\tau) = \lim_{N\to\infty} \frac{1}{(2N+1)\overline{T}} \int_{-\infty}^{\infty} E\big[\sum_{k=-N}^{N}\sum_{\tilde{k}=-N}^{N} u(t-\xi_k,W_k)u(t-\tau-\xi_{\tilde{k}},W_{\tilde{k}})\big]dt. \tag{4.12}$$

The functions u can each be represented as their inverse Fourier Transforms,

$$u(t-\xi_k,W_k) = \int_{-\infty}^{\infty} U(f_1,T_k,W_k,\Delta_k)e^{-j2\pi f_1\xi_k}e^{j2\pi f_1 t}df_1, \tag{4.13a}$$

$$u(t-(\tau+\xi_{\tilde{k}}),W_{\tilde{k}}) = \int_{-\infty}^{\infty} U(f_2,T_{\tilde{k}},W_{\tilde{k}},\Delta_{\tilde{k}})e^{-j2\pi f_2(\tau+\xi_{\tilde{k}})}e^{j2\pi f_2 t}df_2. \tag{4.13b}$$

The Fourier transform $U(f,T_k,W_k,\Delta_k)$ will be represented as $U(f,X_k)$ for convenience. Variables f_1 and f_2 are used to distinguish the frequencies of the associated functions.

Inserting Equation 4.13a and 4.13b into the autocorrelation function results in

$$R_{x_N}(\tau) = \lim_{N\to\infty} \frac{1}{(2N+1)\overline{T}} \int_{-\infty}^{\infty} E\big[\iint_{-\infty}^{\infty}\sum_{k=-N}^{N}\sum_{\tilde{k}=-N}^{N} U(f_1,X_k)e^{-j2\pi f_1\xi_k}e^{j2\pi f_1 t}$$
$$U(f_2,X_{\tilde{k}})e^{-j2\pi f_2(\tau+\xi_{\tilde{k}})}e^{j2\pi f_2 t}\big]df_2df_1dt. \tag{4.14}$$

The expectation can be moved outside the integration since its a linear operator. The order of integration is also changed to yield

$$R_{x_N}(\tau) = \lim_{N\to\infty} \frac{1}{(2N+1)\overline{T}} E\big[\iiint_{-\infty}^{\infty}\sum_{k=-N}^{N}\sum_{\tilde{k}=-N}^{N} U(f_1,X_k)e^{-j2\pi f_1\xi_k}$$
$$U(f_2,X_{\tilde{k}})e^{-j2\pi f_2(\tau+\xi_{\tilde{k}})}e^{j2\pi(f_2+f_1)t}dtdf_2df_1\big], \tag{4.15}$$

so that the integral is taken over t first. The Poisson identity [67] is now used to simplify the t integral as

$$\int_{-\infty}^{\infty} e^{j2\pi(f_2+f_1)t}dt = \delta(f_1+f_2), \tag{4.16}$$

where δ in this case is an impulse function. So Equation 4.15 becomes

$$R_{x_N}(\tau) = \lim_{N\to\infty} \frac{1}{(2N+1)\overline{T}} E\big[\iint_{-\infty}^{\infty} \sum_{k=-N}^{N} \sum_{\tilde{k}=-N}^{N} U(f_1, X_k) e^{-j2\pi f_1 \xi_k} \\ U(f_2, X_{\tilde{k}}) e^{-j2\pi f_2(\tau+\xi_{\tilde{k}})} \delta(f_1+f_2) df_2 df_1 \big]. \tag{4.17}$$

The sifting property of the impulse function stated as

$$\int_{-\infty}^{\infty} g(f_2)\delta(f_2-(-f_1))df_2 = g(-f_1), \tag{4.18}$$

can now be applied to yield

$$R_{x_N}(\tau) = \lim_{N\to\infty} \frac{1}{(2N+1)\overline{T}} E\big[\int_{-\infty}^{\infty} \sum_{k=-N}^{N} \sum_{\tilde{k}=-N}^{N} U(f_1, X_k) e^{-j2\pi f_1 \xi_k} \\ U(-f_1, X_{\tilde{k}}) e^{j2\pi f_1(\tau+\xi_{\tilde{k}})} df_1 \big]. \tag{4.19}$$

The variable f_1 can now be changed back to f. Notice that the function $U(-f, X_k)$ is a complex conjugate of $U(f, X_{\tilde{k}})$ therefore $U(-f, X_k) = \overset{*}{U}(f, X_{\tilde{k}})$ and the result is

$$R_{x_N}(\tau) = \lim_{N\to\infty} \frac{1}{(2N+1)\overline{T}} E\big[\int_{-\infty}^{\infty} \sum_{k=-N}^{N} \sum_{\tilde{k}=-N}^{N} U(f, X_k) \\ \overset{*}{U}(f, X_{\tilde{k}}) e^{-j2\pi f(\xi_k-\xi_{\tilde{k}})} e^{j2\pi f\tau} df \big]. \tag{4.20}$$

The final step is to simplify the above equation. Let $l = \tilde{k} - k$. This allows for rewriting the above equation in terms of l and k which will later allow for further simplification of $R_{x_N}(\tau)$. Therefore

$$R_{x_N}(\tau) = \lim_{N\to\infty} \frac{1}{(2N+1)\overline{T}} E\big[\int_{-\infty}^{\infty} \sum_{k=-N}^{N} \sum_{l+k=-N}^{l+k=N} U(f, X_k) \\ \overset{*}{U}(f, X_{l+k}) e^{-j2\pi f(\xi_k-\xi_{l+k})} e^{j2\pi f\tau} df \big]. \tag{4.21}$$

Now it is required that the expectation operator only be a function of l. For this, a multiplier is introduced, defined as

$$y_{k+l} = \begin{cases} 1, & -N \le (k+l) \le N, \\ 0 & else. \end{cases} \tag{4.22}$$

The y_{k+l} is now inserted to multiply the summation over $l+k$ in Equation 4.21. In this

way the summation over $l+k$ can be extended from $-\infty$ to ∞ without affecting the overall summation result. This makes

$$R_{x_N}(\tau) = \lim_{N\to\infty} \frac{1}{(2N+1)\overline{T}} E\Big[\int_{-\infty}^{\infty} \sum_{k=-N}^{N} \sum_{l=-\infty}^{\infty} y_{k+l} U(f, X_k) \overset{*}{U}(f, X_{l+k}) e^{-j2\pi f(\xi_k - \xi_{l+k})} e^{j2\pi f\tau} df \Big]. \tag{4.23}$$

From this, the expectation operator can be taken into the integrand. This yields

$$R_{x_N}(\tau) = \lim_{N\to\infty} \frac{1}{(2N+1)\overline{T}} \int_{-\infty}^{\infty} \sum_{k=-N}^{N} \sum_{l=-\infty}^{\infty} E\big[y_{k+l} U(f, X_k) \overset{*}{U}(f, X_{l+k}) e^{-j2\pi f(\xi_k - \xi_{l+k})} e^{j2\pi f\tau} df \big]. \tag{4.24}$$

Recall that the expectation is taken over the ensemble of the three random variables, and that this is a stationary random process. Consider a similar stationary random PWM signal $\sum_{k=-N}^{N} q_k$, where k is the switching cycle, the expectation over the ensemble is

$$E[\sum_{k=-N}^{N} q_k]. \tag{4.25}$$

The expectation can be taken into the summation, and since the signal is stationary, the summation over k can be changed as follows

$$E[\sum_{k=-N}^{N} q_k] = \sum_{k=-N}^{N} E[q_k] = (2N+1)E[q_0]. \tag{4.26}$$

In other words, the expectation over the ensemble can be taken on the $k=0$ switching cycle only (because its ensemble expectation is similar to the $k = 1, 2.., N$ cycles) and multiplied by the number of terms in the summation.

The same principle is applied to Equation 4.24. This cancels out the $\frac{1}{2N+1}$ factor in Equation 4.24. The result is

$$R_{x_N}(\tau) = \lim_{N\to\infty} \frac{1}{\overline{T}} E\Big[\int_{-\infty}^{\infty} \sum_{l=-\infty}^{\infty} y_{0+l} U(f, X_0) \overset{*}{U}(f, X_{l+0}) e^{-j2\pi f(\xi_0 - \xi_{l+0})} e^{j2\pi f\tau} df \Big]. \tag{4.27}$$

The random variables T, Δ and W are now returned to replace X

$$R_{x_N}(\tau) = \lim_{N\to\infty} \frac{1}{\overline{T}} E\big[\int_{-\infty}^{\infty} \sum_{l=-\infty}^{\infty} y_{0+l} U(f, T_0, W_0, \Delta_0) \overset{*}{U}(f, T_l, W_l, \Delta_l) e^{-j2\pi f(\xi_0 - \xi_l)} e^{j2\pi f\tau} df \big]. \tag{4.28}$$

Now the limit of the above function as $N \to \infty$ can be applied. Applying this limit also means that R_{x_N} becomes the untruncated version. This only affects the function y as it was only defined as equal to 1 within $(-N, N)$, and zero everywhere else. Applying this means $y_{0+l} = 1$ for all $|N| \to \infty$. The autocorrelation may be written finally as

$$R_x(\tau) = \frac{1}{\overline{T}} E\big[\int_{-\infty}^{\infty} \sum_{l=-\infty}^{\infty} U(f, T_0, W_0, \Delta_0) \overset{*}{U}(f, T_l, W_l, \Delta_l) e^{-j2\pi f(\xi_0 - \xi_l)} e^{j2\pi f\tau} df \big]. \tag{4.29}$$

4.3.3.3 The General Power Spectral Density Formula

The final step is to take the Fourier transform of the autocorrelation function. The autocorrelation function is already an inverse Fourier transform. The final equation is

$$S_x(f) = \frac{1}{\overline{T}} \sum_{l=-\infty}^{\infty} E\big[U(f, T_0, W_0, \Delta_0) \overset{*}{U}(f, T_l, W_l, \Delta_l) e^{-j2\pi f(\xi_0 - \xi_l)} \big], \tag{4.30}$$

which is the same result obtained and verified by Bech and Stanković [17, 45]. Now this equation can be expanded to finally indicate the probability dependence,

$$S_x(f) = \frac{1}{\overline{T}} \sum_{l=-\infty}^{\infty} \sum_{T_0, W_0, \Delta_0} \sum_{T_l, W_l, \Delta_l} U(f, T_0, W_0, \Delta_0) \overset{*}{U}(f, T_l, W_l, \Delta_l) e^{-j2\pi f(\xi_0 - \xi_l)} \Pr(T_0, W_0, \Delta_0 | D) \Pr(T_l, W_l, \Delta_l | D). \tag{4.31}$$

The impact of the joint probability distribution in Equation 4.31 is the main interest in this dissertation. The succeeding chapters focus on how this joint probability impacts $S_x(f)$. Once this relationship has been established, it will be used to maximally spread out the PSD. However, Equation 4.30 will be the starting point of this process.

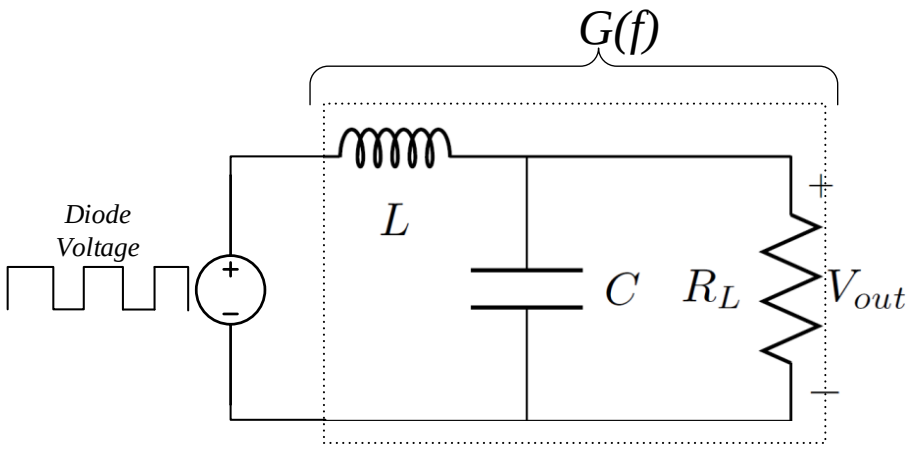

FIGURE 4.2: Equivalent Buck converter circuit, with $G(f)$ as a LTI filter

4.3.3.4 PSD in a DC-DC Converter

Studies by Stanković [45] and later reiterated by Bech [17] and Tse *et al.* [21] argue that if the random signal is stationary, and the converter can be generalised as a linear time-invariant filter, then the output spectrum of the converter can be related to the input using the fundamental theorem of linear time-invariant systems [68]. Therefore, if the random process $x(t, X)$ is stationary, and its spectrum is $S_x(f)$, then the converter output spectrum is given by

$$S_{out}(f) = |G(f)|^2 S_x(f), \tag{4.32}$$

where $G(f)$ in this case is the transfer characteristic of the filter. For the case of a single-switch buck converter, $G(f)$ would be as shown in Figure 4.2, and the *DiodeVoltage* is equivalently the random input switching signal $x(t, X)$ [21]. This assumes that the buck is operating in continuous conduction mode and that $G(f)$ is stable. In this way, the output PSD can be calculated. Given this, the output spectrum does not form part of the main focuses of this research. Only the input spectrum is analysed as the worst case of the source of harmonics that cause conducted EMI in converters. The output voltage of the buck converter will, however, be analysed in later chapters in order to determine the extent to which the probability distributions can maintain the time-domain constraints (or design constraints) while spreading out the PSD.

4.4 Conclusion

This chapter was focussed on deriving the PSD formula for the purpose of further analysis of the impact of probability on the PSD of a random PWM signal. The chapter also presents a technique for estimating the PSD for the purpose of simulated illustrations that will follow. The derivation process overlaps with other researchers that derived the formula, however the process presented here was tailored towards a DC-DC converter with a stationary random PWM switching function. In this way, the derivation is less complex and more comprehensive, and allows for highlighting the dependence of the PSD on the probability of the three random variables T, Δ and W, or equivalently the joint probability distribution.

Chapter 5

Impact of Probability on Spectral Spreading

5.1 Introduction

One of the major contributions of this dissertation is finding the impact of spreading probability on the spectral characteristics of a RPWM. There are two main concepts that underpin these considerations. Firstly, it is important to note that the alterations made to the PMF (as the independent variable) of the random PWM are measurable. Secondly, the impact of this alteration on the PSD (dependent variable) must also be measurable. This will allow one to analyse and quantify the changes being made to the PMF, and also quantify the impact of those changes on the PSD.

In the case of this work, the spreading out of probability is the independent variable, and it has already been indicated that this spreading out of probability in the PMF is quantifiable as entropy. The spreading out of harmonic power in the PSD is the dependent variable. This chapter will, therefore, propose a measure of spreading in the PSD before establishing the impact of spreading probability on the harmonic power of the PSD referred to as spectral spreading. Therefore, the difference between probability spreading and spectral spreading must be noted.

Based on this, the relationship between entropy of PMF and spectral spreading is then argued for. The focus is to prove the hypothesis - using a structured argument

and accompanying evidence - that increasing spreading in RPWM PMFs leads to increased spreading in the PSD, and that in general there exists an increasing monotonic relationship between the two.

5.2 Related Work

5.2.1 Quantifying PDF Impact on Spectral Spreading

In 1994 Andrzej Trzynadlowski, Frede Blaabjerg *et al.* published a review of RPWM modulation techniques for converter-fed drives [7], where they highlighted that the impact of probability distribution had not been thoroughly investigated. This may be partly due to the absence of a method of truly quantifying this impact.

A number of publications have explored the idea of measuring the impact of probability on the spectral characteristics of random PWM signals. One of the publications closest to the aims in this dissertation is presented by Tse *et al.* [21, 29, 33, 69], where the effectiveness of the random PWM probabilities on spreading harmonic power is investigated through a randomness level $\Re$ defined for each random variable

for random Δ:

$$\Re_{\Delta} = \frac{\Delta_{min} - \Delta_{max}}{\overline{T}}, \tag{5.1}$$

for random Δ:

$$\Re_{W} = \frac{W_{min} - W_{max}}{\overline{T}}, \tag{5.2}$$

for random T:

$$\Re_{T} = \frac{T_{min} - T_{max}}{\overline{T}}, \tag{5.3}$$

where the subscripts min and max are the minimum and maximum allowable values for the respective PWM parameters, and $\overline{T}$ is the average switching period. The investigation found that in general, the harmonic components gradually spread over as $\Re$ is increased from 0 to 0.2. This method shows the effectiveness of the degree of randomness on the PSD, but it ignores the rest of the values between the min and max allowable values. In addition, this measure relies on $\overline{T}$ to be constant for a valid comparison

reference point. As such it does not address the possibility of having different nominal switching pulse periods. Furthermore, the impact on the PSD is only analysed through visual observation of the spectrum.

Another publication investigated the impact of the size of the randomisation pool on the spread spectrum effects [51]. The work showed that when using a pool of five carrier frequencies or more, the spread spectrum effects are almost identical to using a continuous PDF for randomisation. Such an investigation offers insight into how the size of the pool can be used to spread the spectrum. Unfortunately, it does not take into account the probabilities of the elements in the pool as this also affects spectral spreading. In addition, the degree to which this affects the PSD is similarly visually observed.

As opposed to the above discussed methods, when investigating the impact of random PWM, entropy of probability already takes into account the size of the pool, as well as the probabilities of the elements in the pool (this has been shown in Chapter 3). In that respect, it is better suited to measuring the impact of probability.

To the best of the author's knowledge, a spectral performance measure proposed by Huo *et al.* and known as the Harmonic Spread Factor (HSF) is the most used in publications [9, 31, 44, 49]. The HSF is reported to quantify the spread spectrum effects of random PWM. As such it may be useful for investigating the impact of probability on spectral spreading. The HSF is, however, not preferred as a measure of spectral spreading, as it is also of interest in this dissertation, to explore an alternative method of quantifying spectral spreading as opposed to the HSF. More importantly, the HSF has a major disadvantage compared to entropy which is discussed in detail next.

5.2.2 Harmonic Spread Factor versus Entropy

The HSF is another proposed measure for quantifying harmonic power spread. This concept was first introduced by Bin Huo [44], which is a statistical deviation measure for evaluating random PWM techniques. The HSF is defined as

$$HSF = E\Big[(\sum_{i>1}^{N} S_i - S_0)^2\Big], \tag{5.4}$$

where N is the total number of harmonics considered, S_i is the magnitude of the i^{th} harmonic and S_0 is the harmonic average calculated as

$$S_0 = \frac{1}{N} \sum_{i>1}^{N} S_j. \tag{5.5}$$

Then for a widely spread spectrum such as white noise, the HSF would be zero [44].

Note that Equation 5.4 is essentially computing the statistical variance of harmonics in the PSD. Given this, it would be of great benefit to compare the relation between entropy and variance to obtain a better measure of the spread of harmonic power. Mukherjee and Ratnaparkhi [70] and as cited by Singh [55], compared the relationship between entropy and variance and found that these two quantities are – to some extent – closely related. However, another important finding was that even though these are closely related, the affinity (or closeness) of different probability distributions belonging to the same family with a common variance, can be an entropy – based measure [70].

This comparison points out that it is possible for two distributions to possess the same variance (or HSF) but different entropies. For example, if the distributions are unimodal with a common variance, then the difference in their entropies may point to the longer tail of one of the distributions [55], wherein a longer tail implies 'more spread out'.

A better parallel between spectral entropy and probability entropy is drawn later. But at this point it can be said that the idea of 'tail' differences also applies when it comes to spectral entropy since a PSD also posses 'tails' composed of side-lobes. Given these properties, entropy can be viewed as a more sensitive measure of spreading than the HSF.

5.2.3 Existing Use of Spectral Entropy

The concept of spectral entropy is not new. There are some publications that have shown its use in signal processing [71–74].

Spectral entropy can be tracked to the year 2004 when it was first introduced by Misra *et al.* [71], where they showed that a PSD can be viewed as a probability mass function, when normalised. They apply this for automatic speech recognition (ASR), where a spectrum with lower entropy is an indication of voiced sounds and one with a higher entropy (or flatter spectrum) corresponds to a spectrum with no speech.

Other applications of spectral entropy that followed include robust online music detection [74], classification of speech from speakers to predict depression [72] and for classification of brain signals, to identify right hand and left hand movements [73].

The similarity between the properties of a PMF and a normalised PSD is what allows for using entropy to quantify spectral spreading. The main difference between the discussed applications and the one proposed here is the interpretation of spectral entropy and its application to random PWM. In this case, spectral entropy is viewed as a quantity measuring the spreading out of harmonic power, and thus is later used to infer the extent to which a PSD of a RPWM signal is spread out when the spreading out of probability in the PMF is altered.

5.3 Quantifying Spectral Spreading Using Entropy

If the PSD can possess the same characteristics that probability possesses, particularly a distribution of a density as well as normalisation (sum to 1) of the density, then spreading out in the PSD can be quantified by using Shannons entropy. The phenomenon of spreading of harmonic power in the PSD is first clarified.

5.3.1 Definition of Spectral Spreading

The general notion of spreading is that the harmonic power, which exists in high amplitudes, moves to other frequencies in such a way that the original harmonic would have lost its power to other frequencies. Many authors adopt this notion [5, 7, 34–43].

Investigation by Stone *et al.*[75] show that random PWM, particularly random carrier frequency, smears out the narrow-band power associated with non-random PWM, without significantly affecting the total power emitted. In other words, the idea of 'smearing' out points to the fact that no new power is being added or removed, but the total power - before and after randomisation - remains unchanged [7]. If the total power is significantly changed, then it cannot be called a spreading or 'smearing'.

Research by Bech and Stanković [17, 45] uses the PSD formula to analytically show that, when randomising the PWM, the PSD acquires a continuous component, as compared to the PSD of a non-random modulation, which only has a discrete component. Figure 5.1 is an illustration of a PSD with a discrete and continuous component. The amplitude of the discrete components is reduced due to the randomisation. From this

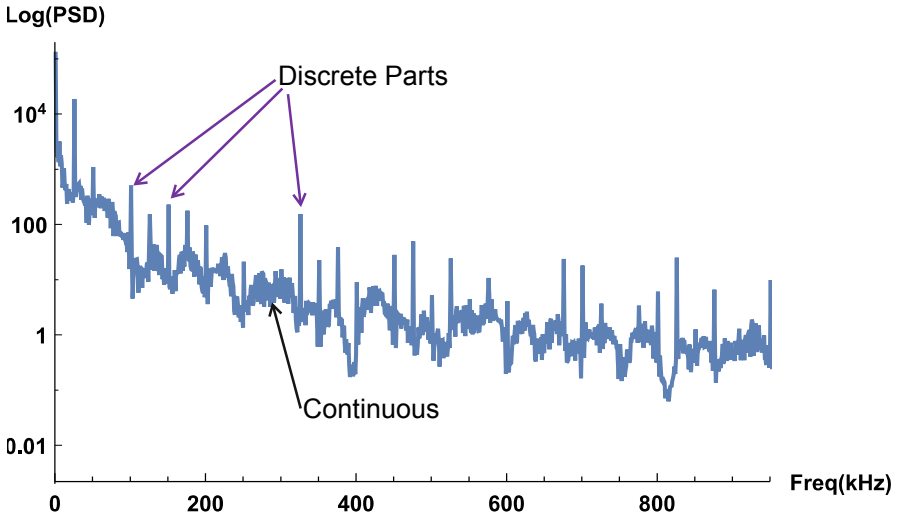

FIGURE 5.1: An illustration of a PSD with discrete and continuous components.

perspective, 'spreading out' of harmonic power means that the power that existed in harmonics of the non-random PSD has been redistributed to other frequencies, so that the discrete part (the harmonics) has a reduced amplitude. In this way, it can be accepted that spreading out implies a reduction of the high amplitude harmonics. If that is the case, then a PSD can be normalised by the total power.

It is important to note, however, that spreading out does not explicitly and always imply a reduction in the harmonic amplitudes, as it may be possible in some cases that a spreading out in one area leads to a concentration in another area, even though there occurred, on average, a spreading out in the observed frequency band.

5.3.2 Discrete PSD Spreading

Given that the PSD can be sampled to obtain N discrete samples (using Equation 4.5 and 4.6), the PSD can be normalised as

$$\tilde{S}_i = \frac{\hat{S}_x(f_i)}{\sum_i \hat{S}_x(f_i)}. \tag{5.6}$$

For random PWM, the amplitudes of the harmonic power changes, yet the total average power, $\sum_i \hat{S}_x(f_i)$ must remain unchanged [7] (Note that since the PSD of the random PWM is estimated in Monte Carlo simulations, the total *average* power is considered).

In this way, the PSD behaves like discrete probability density as it is normalised i.e. the way spreading occurs in a PMF is the same way it occurs in a normalised discrete PSD.

The Shannon entropy of the normalised PSD can therefore be calculated as

$$H[\tilde{S}_i] = -\sum_{i=0}^{N} \tilde{S}_i \log(\tilde{S}_i), \tag{5.7}$$

which is referred to as *spectral entropy*. Thus the higher the entropy, the more spread out the harmonic power density, and the opposite holds also.

It should be noted that from this point on, spectral entropy refers to Equation 5.7 which quantifies spreading out of harmonic power in the PSD, while probability entropy is spreading of probability in the PMF (Equation 3.1).

5.3.3 Valid Spectral Entropy Comparison

According to Equations 5.7 and 5.6, spectral entropy is inversely proportional to the average total power $\sum_i^N \hat{S}(f_i)$. For a valid comparison of spectral entropies from different PSDs, the average total powers of each PSD must not vary – at least not significantly for the random PWM case. Else if, for example, the average total power decreases while harmonic power is being spread out more and more, then it might appear as if the spectral entropy $H[\tilde{S}_i]$ is increasing due to increased harmonic power spread, while in actual fact the average total power is the one responsible for the increase in $H[\tilde{S}_i]$ and not the actual spreading out of harmonic power. Thus if the average total power remains unchanged while randomising the PWM, then the relationship between PMF entropy and spectral entropy can be investigated without confounding effect.

5.3.4 Continuous PSD Spreading

It would be ideal to be able to analytically obtain a continuous measure of the entropy of the PSD and probability distribution. Caticha and Marsh [57, 76], extend the concept of entropy for continuous distributions as a quantity known as continuous, or differential entropy, where it is concluded that the relative entropy (or the Kullback-Leibler divergence) has more value for continuous entropy [57]. However, this depth and complexity exceed the intended scope of this research, especially considering that the intention is to extend the concept of entropy to quantifying spreading in the PSD.

In any case, a discrete entropy has the benefit of having a more intuitive interpretation and analysis, which allows for its extensibility to spectral entropy.

5.4 Relationship between PSD Entropy and Probability Entropy

The relationship between entropy of a probability and spectral entropy is now investigated. The assertion that seeks to be proven in this section is stated again as: 'When the entropy of probability is increased, so will the spectral entropy monotonically increase'. From these statements, a final conclusion is drawn.

It is emphasised that the work presented in this section adapts the work of Bech [17] and Stanković [45]. But more importantly, their work is further extended on in order to investigate the relationship between PSD spreading and probability spreading. This accounts for one of the major contributions of this dissertation.

5.4.1 Proof Approach

A direct proof, or any purely analytical proof, requires that the concept of continuous entropy be applied for analysing the PSD formula (which may be purely continuous) and the probability (which in this case is discrete). However, this approach will not be used due, to its complexity, as previously justified in Section 5.3.4. Such an exercise is left for future research. Instead, the statement will be proven from an argumentative approach, where a set of supporting points are given from both an analytical and supporting evidence-driven perspective.

In the analytical argument case, the PSD formula in Equation 4.30 of Chapter 4 is used. The PSD of randomising each parameter is considered. In each case the PSD formula is analysed to observe the results when the probability approaches maximum spreading (or maximum entropy), which is a uniform PMF, and when probability approaches minimum spreading, which is a deterministic PMF with minimum entropy.

From the case with simulated illustrations, the entropy of probability is varied in an increasing manner, and the spectral entropy is observed.

Argument Assumptions and Objectives

The following assumptions are highlighted:

- The three random parameters are randomised independently.
- The PMFs of the three parameters are the only means of altering the PSD.
- The PSD formula is an accurate representation of the PSD of a RPWM signal.

The objectives of this section are:

- to provide a high degree of confidence that the statement is true under the stated assumptions, and
- to prepare the use of maximum entropy probabilities for finding maximum spreading in the PSD.

The relationship does not need to be linear – monotonicity is the important factor. If this can be shown, then there is sufficient reason to believe that maximum spreading in the PDF leads to a maximum spreading in the PSD.

5.4.2 Argument for Spectral Spreading in PSD Formula due to PMF Spreading

This argument section is separated into three random PWM cases, the case for random W, random Δ and random T. The PSD formula in Equation 4.30 is the key point for this argument. It relies heavily on the procedures presented by Stanković [45] and Bech [17] for simplifying the PSD formula for each random parameter. However, in this work, a further step is taken to show how the PSD formula changes when the PMFs of Δ, T and W approach maximum and minimum spreading/entropy.

5.4.2.1 Random Pulse Width

For random W only, at each switching cycle l the pulse width has a total of N_W possible outcomes. For convenience, the random W is represented as a random variable that is a function of the index r in the pool and l as $W_{l,r}$, where $r = 1, 2, .., N_W$. The subscript

l is the switching cycle (same as k), that resulted during the derivation. l is used here for consistence with the PSD formula.

The PSD formula (Equation 4.30) is thus rewritten as.

$$S_x(f) = \frac{1}{T}\sum_{l=-\infty}^{\infty} E\big[U(f,W_{0,r})\overset{*}{U}(f,W_{l,r})e^{-j2\pi f(\xi_0-\xi_l)}\big] \tag{5.8}$$

The expectation is taken over N_W members of the ensemble. Since the pulse period and width are constant, they shall be represented as $T = T_c$ and $\Delta = \Delta_c$ respectively. The switching cycle period is $t_l = lT_c$. Thus, for $l = 0$

$$\xi_0 = t_0 + \Delta_c = \Delta_c, \tag{5.9}$$

$$\xi_0 - \xi_l = \Delta_c - (lT_c + \Delta_c) = -lT_c. \tag{5.10}$$

Equation 5.8 can be rewritten as

$$S_x(f) = \frac{1}{T}\sum_{l=-\infty}^{\infty} E\big[U(f,W_{0,r})\overset{*}{U}(f,W_{l,r})e^{j2\pi flT_c}\big]. \tag{5.11}$$

Since the randomisation at every switching cycle is independent of the preceding switching cycles, then the expectation of the product can be rewritten as the product of expectations,

$$S_x(f) = \frac{1}{T_c}\sum_{l=-\infty}^{\infty} E\big[U(f,W_{0,r})\big]E\big[\overset{*}{U}(f,W_{l,r})e^{j2\pi flT_c}\big]. \tag{5.12}$$

However, the above would be incorrect because at $l = 0$, the product of expectations is not applicable. This can be seen in the middle term below when expanding the summation of Equation 5.11, and showing only the terms at $l = -1, 0, 1$

$$\begin{aligned} S_x(f) = \ldots &+ E\big[U(f,W_{0,r})\overset{*}{U}(f,W_{-1,r})e^{j2\pi f(-1)T_c}\big] \\ &+ E\big[U(f,W_{0,r})\overset{*}{U}(f,W_{0,r})e^{j2\pi f0T_c}\big] \\ &+ E\big[U(f,W_{0,r})\overset{*}{U}(f,W_{1,r})e^{j2\pi f1T_c}\big] + \ldots \end{aligned} \tag{5.13}$$

In other words, if all the terms are rewritten as products of expectations, all the terms would be correct, except the term:

$$\ldots + E\big[U(f,W_{0,r})\big]E\big[\overset{*}{U}(f,W_{0,r})\big] + \ldots$$

To eliminate this issue, the expectation bracket in Equation 5.11 can be rewritten as a product of expectations, but now the incorrect term must be subtracted from the sum, and the correct one added,

$$\begin{aligned} S_x(f) = \frac{1}{T_c}\Big[\sum_{l=-\infty}^{\infty} & E\big[U(f,W_{0,r})\big] E\big[\overset{*}{U}(f,W_{l,r}) e^{j2\pi f l T_c}\big] \\ & - E\big[U(f,W_{0,r})\big] E\big[\overset{*}{U}(f,W_{0,r})\big] \\ & + E\big[U(f,W_{0,r})\overset{*}{U}(f,W_{0,r})\big]\Big]. \end{aligned} \tag{5.14}$$

Now the simplification process can proceed. Note that the value of $U(...)$ is not directly affected by the switching cycle variable l – i.e. randomisation outcome of W, does not depend on l. Therefore $U(...)$ can be placed outside the summation and l will be omitted. Therefore, $U(f,W_r)$ will be used. Furthermore, $U(f,W_r)\overset{*}{U}(f,W_r) = |U(f,W_r)|^2$ since $U(f,W_r)$ is real. The result is

$$S_x(f) = \frac{1}{T_c}\Big[E|U(f,W_r)|^2 - \Big|E\big[U(f,W_r)\big]\Big|^2 + E\big|U(f,W_r)\big|^2 \sum_{l=-\infty}^{\infty} E\big[e^{j2\pi f l T_c}\big]\Big]. \tag{5.15}$$

Only the exponential function remains in the summation.

The exponential is not a function of W. It can, therefore, be removed from the expectation brackets. Next, the Poisson Identity that represents a Dirac comb as a Fourier series [45, 77] is

$$\sum_{k=-\infty}^{\infty} \delta(f - \frac{k}{T_c}) = T_c \sum_{l=-\infty}^{\infty} e^{j2\pi l T_c} \tag{5.16}$$

After imposing this identity, the following is obtained

$$S_x(f) = \underbrace{\frac{1}{T_c}\Big[E\big[|U(f,W_r)|^2\big] - \Big|E\big[U(f,W_r)\big]\Big|^2\Big]}_{\textbf{Continuous spectral component}} + \underbrace{E\big[|U(f,W_r)|^2\big]\frac{1}{T_c^2}\sum_{k=-\infty}^{\infty}\delta(f-\frac{k}{T_c})}_{\textbf{Discrete spectral component}}. \tag{5.17}$$

Equation 5.17 is also found in the work of Stanković [45]. It can be seen that it is composed of a discrete part (due to the Dirac delta function) and a continuous part. This marks the final stage of the simplification.

Recalling that when spreading out of probability is increased, the entropy of the

PMF approaches maximum entropy and so probability approaches a uniform distribution. If there are a total of N_W possible outcomes, then $\Pr(W_r) \to \frac{1}{N_W}$ (with minimal constraints).

On the other hand, the PMF approaches a deterministic probability as the spreading is decreased. Therefore, if one of the outcomes is w_c then $\Pr(W_{r=c}) \to 1$. Alternatively, this can be represented as $\Pr(W_r) \to \delta(W - w_c)$.

The impact of spreading out probability on the PSD formula can now be investigated. For this, two cases are considered governed by the following questions.

- **Case A**: What happens to the PSD formula, when the spreading out of probability in the PMF of W is increased?
- **Case B**: What happens to the PSD formula when the spreading out of probability is decreased?

Case A: Increasing Entropy of Probability

The first two terms in Equation 5.17 are essentially a variance. The variance of a random variable X holds the equality

$$E[(X - E[X])^2] = E[X^2] - E[X]^2. \tag{5.18}$$

Applying this result to Equation 5.17 results in

$$S_x(f) = \frac{1}{T_c}\Big[E\big[(|U(f,W_r)| - E[|U(f,W_r)|])^2\big] + E\big[|U(f,W_r)|\big]^2 \frac{1}{T_c}\sum_{k=-\infty}^{\infty}\delta(f - \frac{k}{T_c})\Big]. \tag{5.19}$$

After expanding the expectation operators and leaving out the outer most-expectation, the result is

$$S_x(f) = \frac{1}{T_c}\Big[E\big[\Big(|U(f,W_r)| - \underbrace{\sum_{r=1}^{N_W}|U(f,W_r)|\Pr(W_r)}_{\mathbf{a}}\Big)^2\big] + \underbrace{\sum_{r=1}^{N_W}|U(f,W_r)|^2\Pr(W_r)}_{\mathbf{b}} \frac{1}{T_c}\sum_{k=-\infty}^{\infty}\delta(f - \frac{k}{T_c})\Big]. \tag{5.20}$$

Now consider term **a** and term **b**. The PMF $\Pr(W_r)$ in both the terms contributes to the magnitude of each term.

Term **a** is isolated and simplified below. It is known that the PMF approaches $\frac{1}{N_W}$ for all r, therefore

$$\sum_{r=1}^{N_W} |U(f,W_r)|\Pr(W_r) \rightarrow \frac{\sum_{r=1}^{N_W} |U(f,W_r)|}{N_W}, \tag{5.21}$$

and $U(f,W_r)$ is essentially a Fourier Transform of a rectangular function, $U(f,W_r) = W_r \operatorname{sinc}(\pi f W_r)$,

$$\sum_{r=1}^{N_W} |U(f,W_r)|\Pr(W_r) \rightarrow \frac{\sum_{r=1}^{N_W} |W_r \operatorname{sinc}(\pi f W_r)|}{N_W}. \tag{5.22}$$

Equation 5.22 above shows that as probability approaches uniform distribution, the overall magnitude of the expression decreases due to the $\frac{1}{N_W}$ factor that gets introduced. This is also easier to see if probability spreading is increased by increasing N_W. However, notice that the values of the elements in W_r will also affect the overall magnitude. If most of the elements in the pool of W are large in magnitude, then so will be the numerator of Equation 5.22. In other words, if the average magnitude of W is increased, then this will result in an increase in the overall magnitude of Equation 5.22, and vice-versa.

Therefore, in order to limit the effect of W, so that probability alone can be investigated, assume that the average of all the elements in W remains constant (alternatively that the difference between the elements in W is very small) as the spreading of probability $\Pr(W_r)$ is increased. Inserting this term back into Equation 5.20

$$S_x(f) \rightarrow \frac{1}{T_c}\Big[\underbrace{E\Big[\Big(|U(f,W_r)| - \underbrace{\frac{\sum_{r=1}^{N_W} |W_r \operatorname{sinc}(\pi f W_r)|}{N_W}}_{\mathbf{a}}\Big)^2\Big]}_{\textbf{Continuous spectral component}} + \underbrace{\underbrace{\frac{\sum_{r=1}^{N_W} |W_r \operatorname{sinc}(\pi f W_r)|^2}{N_W T_c}}_{\mathbf{b}} \sum_{k=-\infty}^{\infty} \delta(f - \frac{k}{T_c})}_{\textbf{Discrete spectral component}}\Big]. \tag{5.23}$$

From Equation 5.23, it can be inferred that if probability approaches $\frac{1}{N_W}$, then term **a** decreases. The overall continuous part thus increases because $|U(f,W_r)|$ subtracts term **a** which is growing smaller and smaller. In the limit as N_W increases, the term

a approaches zero, at which point the continuous part is essentially the expectation of $|U(f, W_r)| - 0$.

On the other hand, the magnitude of the discrete part decreases (due to the magnitude of the factor **b**) as probability distribution approaches uniform distribution. In the limit as N_W increases, factor **b** approaches zero, and the discrete part essentially disappears. Therefore, the overall effect of increasing the spreading in probability is that it leads to an increase in the continuous part, while decreasing the discrete part.

The effect of the magnitude of the elements in W will be discussed further in later sections, where it will be shown how the magnitudes in W affect the spectral spreading. Therefore, it should be noted that the above conclusion applies under the assumption that the effect of W is constrained as probability is spread.

Case B: Decreasing Entropy of Probability

For this case, Equation 5.23 can be used to infer what happens when probability entropy (or spreading) decreases. The probability distribution approaches certainty. Therefore $N_W \to 1$. As a result the magnitude of term **a** increases, causing the continuous part to decrease and the magnitude of the discrete part to increase. The PSD therefore approaches

$$S_x(f) \to \frac{1}{T_c}\Big[E\big[\Big(|U(f)| - |U(f)|\Big)^2\big] + \frac{1}{T_c}|U(f)|^2 \sum_{k=-\infty}^{\infty} \delta(f - \frac{k}{T_c})\Big], \tag{5.24}$$

wherein the continuous term disappears, and only the discrete part remains,

$$S_x(f) \to \frac{1}{T_c^2}|U(f)|^2 \sum_{k=-\infty}^{\infty} \delta(f - \frac{k}{T_c}), \tag{5.25}$$

which is essentially the PSD for a deterministic PWM. In this sense, all the continuous power went to the discrete part, and as such spectral spreading has been reduced.

5.4.2.2 Random Pulse Position

The procedure for simplifying the PSD formula for random Δ is the same as in random W.

The variable for Δ is represented as $\Delta_{l,j}$, where $j = 1, 2, 3..., N_\Delta$ is the index of the elements in the pool,

$$S_x(f) = \frac{1}{T}\sum_{l=-\infty}^{\infty} E\big[U(f,\Delta_{0,j})\overset{*}{U}(f,\Delta_{l,j})e^{-j2\pi f(\xi_0-\xi_l)}\big]. \tag{5.26}$$

The pulse period and width are constant at $T = T_c$ and $W = W_c$ respectively. Therefore,

$$\xi_0 - \xi_l = \Delta_{0,j} - (lT_c + \Delta_{l,j}). \tag{5.27}$$

Similar to random W, randomisation is independent of the switching cycle l. The expectation of products can be rewritten as a product of expectations. And again the $l = 0$ term is corrected. The result is

$$\begin{aligned} S_x(f) = \frac{1}{T_c}\Big[&\sum_{l=-\infty}^{\infty} E\big[U(f,\Delta_{0,j})e^{-j2\pi f\Delta_{0,j}}\big]E\big[\overset{*}{U}(f,\Delta_{l,j}))e^{-j2\pi f(-(lT_c+\Delta_{l,j}))}\big] \\ &- E\big[U(f,\Delta_{0,j})e^{-j2\pi f\Delta_{0,j}}\big]E\big[\overset{*}{U}(f,\Delta_{0,j})e^{j2\pi f\Delta_{0,j}}\big] \\ &+ E\big[U(f,\Delta_{0,j})\overset{*}{U}(f,\Delta_{0,j})\big]\Big]. \end{aligned} \tag{5.28}$$

The outcome of the randomisation of Δ is not affected by the switching cycle l. The subscript l can therefore be omitted, and the associated factors can be pulled out of the summation,

$$\begin{aligned} S_x(f) = \frac{1}{T_c}\Big[&E\big[U(f,\Delta_j)e^{-j2\pi f\Delta_j}\big]E\big[\overset{*}{U}(f,\Delta_j)e^{j2\pi f\Delta_j}\big]\sum_{l=-\infty}^{\infty} e^{j2\pi flT_c} \\ &- E\big[U(f,\Delta_j)e^{-j2\pi f\Delta_j}\big]E\big[\overset{*}{U}(f,\Delta_j)e^{j2\pi f\Delta_j}\big] \\ &+ E\big[U(f,\Delta_j)\overset{*}{U}(f,\Delta_j)\big]\Big]. \end{aligned} \tag{5.29}$$

Now the complex conjugate pairs are simplified and the Poisson identity applied to the infinite summation of the exponential. Furthermore, the Fourier transform function $U(...)$ is $W_r sinc(\pi f W_r)$, therefore, unlike the pulse width, U is not a function of the pulse position. Therefore, all the $U(...)$ functions can be moved outside of the respective expectation operators. The result is

$$S_x(f) = \frac{1}{T_c}|U(f)|^2\Big[\big[1 - |E\big[e^{-j2\pi f\Delta_j}\big]|^2\big] + \frac{|E\big[e^{-j2\pi f\Delta_j}\big]|^2}{T_c}\sum_{k=-\infty}^{\infty}\delta(f - \frac{k}{T_c})\quad\Big]. \tag{5.30}$$

which is consistent with Bech's work [17]. Next the two cases are considered.

- **Case A**: What happens to the PSD formula, when the spreading out of probability in the PMF of Δ is increased?
- **Case B**: What happens to the PSD formula when the spreading out of probability is decreased?

Case A: Increasing Entropy of Probability

The probability approaches uniform probability $\frac{1}{N_\Delta}$, for all j.

Therefore Equation 5.30 approaches

$$S_x(f) \rightarrow \frac{1}{T_c}|U(f)|^2\Big[\underbrace{\big[1-\frac{1}{N_\Delta^2}\Big|\sum_{j=1}^{N_\Delta} e^{-j2\pi f\Delta_j}\Big|^2\big]}_{\textbf{Continuous}}+ \underbrace{\frac{1}{N_\Delta^2 T_c}\Big|\sum_{j=1}^{N_\Delta} e^{-j2\pi f\Delta_j}\Big|^2\sum_{k=-\infty}^{\infty}\delta(f-\frac{k}{T_c})\Big]}_{\textbf{Discrete}} \tag{5.31}$$

From here it is clear that, when probability approaches a uniform distribution, the factor $\frac{1}{N_\Delta^2}$ is introduced. The factor by which the continuous part increases is the same factor by which the magnitude of the discrete part decreases. This is a clear indication of discrete power being transferred to make up the continuous power, which is essentially a spreading out of harmonic power.

Case B: Decreasing Entropy of Probability

When decreasing probability entropy, probability becomes more concentrated to one possible outcome in random Δ. From Equation 5.31, it follows that $N_\Delta \rightarrow 1$. It is easy to see that this results in the discrete part only, the same as in Equation 5.25. All the power has now been concentrated into the discrete part, and this is an indication of the opposite of spectral spreading (or spectral concentration).

5.4.2.3 Random Pulse Period

For random T, the non-random parameters are constant at $W = W_c$ and $\Delta = \Delta_c$ respectively. The random variable is represented as $T_{l,i}$, where $i = 1, 2, 3, ..., N_T$,

$$\xi_0 - \xi_l = t_0 + \Delta_0 - (t_l + \Delta_l), \tag{5.32}$$

and since $\Delta_0 = \Delta_l = \Delta_c$ for all l, therefore

$$\xi_0 - \xi_l = t_0 - t_l. \tag{5.33}$$

Therefore, the following can be said [17]

$$t_l - t_0 = \begin{cases} -\sum_{n=l}^{-1} T_n, & \text{for} \quad l \leq -1, \\ 0, & \text{for} \quad l = 0, \\ \sum_{n=0}^{l-1} T_n, & \text{for} \quad l \geq 1. \end{cases} \tag{5.34}$$

This is easily determined from Equation 4.8, where t_l is calculated by adding up the preceding pulse periods.

Let the average period be $\overline{T}$. Inserting the above equation into the general PSD formula (Equation 4.30) and expanding the l summation (only showing the summation terms in the range $-3 \leq l \leq 3$), the following is obtained

$$\begin{aligned} S_x(f) = \frac{1}{\overline{T}} \Big[... &+ E\big[U(f, T_{0,i}) \overset{*}{U}(f, T_{-3,i}) e^{-j2\pi f(T_{-3,i}+T_{-2,i}+T_{-1,i})}\big] \\ &+ E\big[U(f, T_{0,i}) \overset{*}{U}(f, T_{-2,i}) e^{-j2\pi f(T_{-2,i}+T_{-1,i})}\big] \\ &+ E\big[U(f, T_{0,i}) \overset{*}{U}(f, T_{-1,i}) e^{-j2\pi f(T_{-1,i})}\big] \\ &+ E\big[U(f, T_{0,i}) \overset{*}{U}(f, T_{0,i})\big] \\ &+ E\big[U(f, T_{0,i}) \overset{*}{U}(f, T_{1,i}) e^{-j2\pi f(T_{0,i})}\big] \\ &+ E\big[U(f, T_{0,i}) \overset{*}{U}(f, T_{2,i}) e^{-j2\pi f(T_{0,i}+T_{1,i})}\big] \\ &+ E\big[U(f, T_{0,i}) \overset{*}{U}(f, T_{3,i}) e^{-j2\pi f(T_{0,i}+T_{1,i}+T_{2,i})}\big] + ... \\ &\Big]. \end{aligned} \tag{5.35}$$

The above equation can be rewritten as a sum of the product of expectations for the factors that do not have a common switching cycle l,

$$\begin{aligned}
S_x(f) = \frac{1}{\overline{\overline{T}}}\Big[&... + E\big[U(f,T_{0,i})\big]E\big[\overset{*}{U}(f,T_{-3,i})e^{-j2\pi f(T_{-3,i})}\big]E\big[e^{-j2\pi fT_{-2,i}}\big]E\big[e^{-j2\pi f(T_{-1,i})}\big] \\
&+ E\big[U(f,T_{0,i})\big]E\big[\overset{*}{U}(f,T_{-2,i})e^{-j2\pi f(T_{-2,i})}\big]E\big[e^{-j2\pi f(T_{-1,i})}\big] \\
&+ E\big[U(f,T_{0,i})\big]E\big[\overset{*}{U}(f,T_{-1,i})e^{-j2\pi fT_{-1,i}}\big] \\
&+ E\big[U(f,T_{0,i})\overset{*}{U}(f,T_{0,i})\big] \\
&+ E\big[U(f,T_{0,i})e^{-j2\pi fT_{0,i}}\big]E\big[\overset{*}{U}(f,T_{1,i})\big] \\
&+ E\big[U(f,T_{0,i})e^{-j2\pi fT_{0,i}}\big]E\big[\overset{*}{U}(f,T_{2,i})\big]E\big[e^{-j2\pi fT_{1,i}}\big] \\
&+ E\big[U(f,T_{0,i})e^{-j2\pi fT_{0,i}}\big]E\big[\overset{*}{U}(f,T_{3,i})\big]E\big[e^{-j2\pi fT_{1,i}}\big]E\big[e^{-j2\pi fT_{2,i}}\big] + ... \\
&\Big].
\end{aligned} \tag{5.36}$$

Now the common factors can be factored out. These are the factors at $l = 0$

$$\begin{aligned}
S_x(f) = \frac{1}{\overline{\overline{T}}}\Big[&E\big[U(f,T_{0,i})\big]\Big\{... + E\big[\overset{*}{U}(f,T_{-3,i})e^{-j2\pi f(T_{-3,i})}\big]E\big[e^{-j2\pi fT_{-2,i}}\big]E\big[e^{-j2\pi f(T_{-1,i})}\big] \\
&+ E\big[\overset{*}{U}(f,T_{-2,i})e^{-j2\pi f(T_{-2,i})}\big]E\big[e^{-j2\pi f(T_{-1,i})}\big] \\
&+ E\big[\overset{*}{U}(f,T_{-1,i})e^{-j2\pi fT_{-1,i}}\big]\Big\} \\
&+ E\big[U(f,T_{0,i})\overset{*}{U}(f,T_{0,i})\big] \\
&+ E\big[U(f,T_{0,i})e^{-j2\pi fT_{0,i}}\big]\Big\{E\big[\overset{*}{U}(f,T_{1,i})\big] \\
&+ E\big[\overset{*}{U}(f,T_{2,i})\big]E\big[e^{-j2\pi fT_{1,i}}\big] \\
&+ E\big[\overset{*}{U}(f,T_{3,i})\big]E\big[e^{-j2\pi fT_{1,i}}\big]E\big[e^{-j2\pi fT_{2,i}}\big] + ...\Big\} \\
&\Big]
\end{aligned} \tag{5.37}$$

The switching cycle l has no effect on the random selection of T. Therefore the subscripts l in $T_{l,i}$ can be omitted; i.e. $E[e^{-j2\pi fT_i}] \equiv E[e^{-j2\pi fT_{l,i}}]$ for all l,

$$\begin{aligned} S_x(f) = \frac{1}{\overline{T}}\Big[& \\ E\big[U(f,T_i)\big]\Big\{ & \ldots + E\big[\overset{*}{U}(f,T_i)e^{-j2\pi fT_i}\big]E\big[e^{-j2\pi fT_i}\big]E\big[e^{-j2\pi fT_i}\big] \\ & + E\big[\overset{*}{U}(f,T_i)e^{-j2\pi fT_i}\big]E\big[e^{-j2\pi fT_i}\big] \\ & + E\big[\overset{*}{U}(f,T_i)e^{-j2\pi fT_i}\big]\Big\} \\ & + E\big[U(f,T_i)\overset{*}{U}(f,T_i)\big] \\ & + E\big[U(f,T_i)e^{j2\pi fT_i}\big]\Big\{E\big[\overset{*}{U}(f,T_i)\big] \\ & + E\big[\overset{*}{U}(f,T_i)\big]E\big[e^{j2\pi fT_i}\big] \\ & + E\big[\overset{*}{U}(f,T_i)\big]E\big[e^{j2\pi fT_i}\big]E\big[e^{j2\pi fT_i}\big] + \ldots\Big\} \\ & \Big]. \end{aligned} \tag{5.38}$$

Again, a common factor can be factored out in each group of summations. The sequence in each group is essentially an infinite geometric series,

$$\begin{aligned} S_x(f) = \frac{1}{\overline{T}}\Big[& E\big[U(f,T_i)\big]E\big[\overset{*}{U}(f,T_i)e^{-j2\pi fT_i}\big]\sum_{l=0}^{\infty}E\big[e^{-j2\pi fT_i}\big]^l \\ & + E\big[|U(f,T_i)|^2\big] \\ & + E\big[U(f,T_i)e^{j2\pi fT_i}\big]E\big[\overset{*}{U}(f,T_i)\big]\sum_{l=0}^{\infty}E\big[e^{j2\pi fT_i}\big]^l\Big]. \end{aligned} \tag{5.39}$$

The geometric series is convergent if $|E[e^{j2\pi fT_i}]| < 1$,

$$\sum_{l=0}^{\infty}E[e^{j2\pi fT_i}]^l = \frac{1}{1-E[e^{j2\pi fT_i}]}. \tag{5.40}$$

Also note that the first term and the last term in Equation 5.39 are complex conjugates. This produces the final result

$$S_x(f) = \frac{1}{\overline{T}}\Big[E\big[|U(f,T_i)|^2\big] + 2\Re\Big(\frac{E\big[U(f,T_i)\big]E\big[\overset{*}{U}(f,T_i)e^{j2\pi fT_i}\big]}{1-E[e^{j2\pi fT_i}]}\Big)\Big]. \tag{5.41}$$

This marks the final stage of simplification of the PSD formula for random T, and is consistent with Bech's work [17]. As opposed to random Δ and W, the PSD does not have a discrete part. A further step is now taken to investigate the impact of probability on Equation 5.41.

Case A: Increasing Entropy of Probability

Equation 5.41 is first expanded to include the PMF $\Pr(T_i)$.

$$S_x(f) = \frac{1}{\overline{T}}\Big[\underbrace{\sum_{i=1}^{N_T}|U(f,T_i)|^2\Pr(T_i)}_{\mathbf{a}} + \underbrace{2\Re\Big(\frac{\sum_{i=1}^{N_T}|U(f,T_i)|^2 e^{j2\pi fT_i}\Pr(T_i)^2}{1-\sum_{i=1}^{N_T}e^{j2\pi fT_i}\Pr(T_i)}\Big)}_{\mathbf{b}}\Big]. \tag{5.42}$$

For this case, it is difficult to infer how the PSD formula changes when the probability approaches maximum entropy. One way around this is to consider a few special cases that will provide insight. Consider cases where the exponential $e^{j2\pi fT_i} = e^{j2\pi\frac{n}{2}}$ where n is (1) an odd integer, and (2) an even integer.

(1) For $fT_i = \frac{n}{2}$ and n is odd. The exponential is $e^{j2\pi fT_i} = e^{j2\pi\frac{n}{2}} = (-1)$:

$$S_x(f) = \frac{1}{\overline{T}}\Big[\sum_{i=1}^{N_T}|U(f,T_i)|^2\Pr(T_i) + 2\Big(\frac{\sum_{i=1}^{N_T}|U(f,T_i)|^2(-1)\Pr(T_i)^2}{1-\sum_{i=1}^{N_T}(-1)\Pr(T_i)}\Big)\Big]. \tag{5.43}$$

As probability $\Pr(T_i)$ approaches $\frac{1}{N_T}$,

$$S_x(f) \to \frac{1}{\overline{T}}\Big[\frac{1}{N_T}\sum_{i=1}^{N_T}|U(f,T_i)|^2 + 2\Big(\frac{\frac{1}{N_T^2}\sum_{i=1}^{N_T}|U(f,T_i)|^2(-1)}{1-\frac{1}{N_T}\sum_{i=1}^{N_T}(-1)}\Big)\Big]. \tag{5.44}$$

Simplifying the above gives

$$S_x(f) \to \frac{1}{\overline{T}}\Big[\frac{1}{N_T}\sum_{i=1}^{N_T}|U(f,T_i)|^2 - 2\Big(\frac{\frac{1}{N_T^2}\sum_{i=1}^{N_T}|U(f,T_i)|^2}{2}\Big)\Big], \tag{5.45}$$

which results in

$$S_x(f) \to \frac{1}{\overline{T}}\Big[\sum_{i=1}^{N_T}|U(f,T_i)|^2\underbrace{(\frac{1}{N_T}-\frac{1}{N_T^2})}_{\mathbf{a}}\Big]. \tag{5.46}$$

From the above perspective, as PMF approaches $1/N_T$, term **a** increases. Or more easily, if the pool is not fixed, as PMF is spread out more by increasing N_T, the overall magnitude of term **a** in Equation 5.46 increases ($\frac{1}{N_T^2}$ decreases faster than $\frac{1}{N_T}$), which leads to an overall increase in the magnitude of continuous $S_x(f)$.

(2) For $fT_i = \frac{n}{2}$ and n is even, $e^{j2\pi fT_i} = e^{j2\pi\frac{n}{2}} = (1)$:

$$S_x(f) \rightarrow \frac{1}{\overline{T}}\Big[\frac{1}{N_T}\sum_{i=1}^{N_T}|U(f,T_i)|^2 + 2\underbrace{\Big(\frac{\frac{1}{N_T^2}\sum_{i=1}^{N_T}|U(f,T_i)|^2(1)}{1-\frac{1}{N_T}\sum_{i=1}^{N_T}(1)}\Big)}_{\mathbf{b}}\Big]. \tag{5.47}$$

From the above perspective, the denominator of term **b**, approaches zero, so that the magnitude of $S_x(f)$ grows rapidly (the spectrum might constitute some spikes) but still remains continuous.

For the cases where $e^{j2\pi fT_i} = \pm j$ the real part ($\Re$) of the expression **b** in Equation 5.42 simplifies to Equation 5.45. Thus, for these two cases, the same conclusion (increase in continuous power) applies.

From considering the above cases, it can be inferred that $S_x(f)$ remains continuous with increasing magnitude for the most part, and may have some spikes due to the cases where $e^{j2\pi fT_i} = 1$. However, the overall effect is that the more spread out the probability is, the more $S_x(f)$ experiences an increase in continuous power, and when ever power becomes continuous, it is an indication of spectral spreading.

Case B: Decreasing Entropy of Probability

When the probability approaches 1, then no randomisation occurs, so that $N_T \rightarrow 1$, and $\overline{T}$ becomes $\overline{T} = T_c$, Equation 5.42 becomes,

$$S_x(f) \rightarrow \frac{1}{T_c}\Big[|U(f,T_c)|^2 + 2\Re\Big(\frac{|U(f,T_c)|^2 e^{j2\pi fT_c}}{1-e^{j2\pi fT_c}}\Big)\Big]. \tag{5.48}$$

In a similar manner, this case is difficult to infer the effect of decreasing probability spreading. A few simplification steps are necessary and are employed. Returning the geometric series into the above equation results in

$$S_x(f) \rightarrow \frac{1}{T_c}\Big[|U(f,T_c)|^2 + \overbrace{2\Re\Big(|U(f,T_c)|^2 e^{j2\pi fT_c}\sum_{l=0}^{\infty}e^{j2\pi fT_c l}\Big)}^{a}\Big]. \tag{5.49}$$

For simplification of the above equation, consider the term labelled a only. The exponential in the summation is multiplied by 2 and divided by 2,

$$a = 2\Re\Big(|U(f,T_c)|^2 e^{j2\pi fT_c}\frac{1}{2}\sum_{l=0}^{\infty}2e^{j2\pi fT_c l}\Big). \tag{5.50}$$

The exponential outside the summation is multiplied by the exponential within the summation, so that the exponents add up, the result is

$$a = 2\Re\Big(|U(f,T_c)|^2\frac{1}{2}\sum_{l=0}^{\infty}2e^{j2\pi fT_c(l+1)}\Big). \tag{5.51}$$

Since the exponential is multiplied by 2, it can be split into two exponential functions,

$$a = 2\Re\Big(|U(f,T_c)|^2\frac{1}{2}\Big\{\sum_{l=0}^{\infty}e^{j2\pi fT_c(l+1)} + \sum_{l=0}^{\infty}e^{j2\pi fT_c(l+1)}\Big\}\Big). \tag{5.52}$$

Now let $l+1=q$, therefore

$$a = 2\Re\Big(|U(f,T_c)|^2\frac{1}{2}\Big\{\sum_{q=1}^{\infty}e^{j2\pi fT_cq} + \sum_{q=1}^{\infty}e^{j2\pi fT_cq}\Big\}\Big). \tag{5.53}$$

If only the real part in the summations is considered, then the following is true

$$\Re(\sum_{q=1}^{\infty}e^{j2\pi fT_cq}) = \Re(\sum_{q=1}^{\infty}e^{-j2\pi fT_cq}), \tag{5.54}$$

which means the following also holds

$$\Re(\sum_{q=1}^{\infty}e^{j2\pi fT_cq} + \sum_{q=1}^{\infty}e^{j2\pi fT_cq}) = \Re(\sum_{q=1}^{\infty}e^{j2\pi fT_cq} + \sum_{q=-\infty}^{-1}e^{j2\pi fT_cq}). \tag{5.55}$$

Therefore, one of the summations can have the limits $(-\infty,-1)$, result is

$$a = 2\Re\Big(|U(f,T_c)|^2\frac{1}{2}\Big\{\sum_{q=1}^{\infty}e^{j2\pi fT_cq} + \sum_{q=-\infty}^{-1}e^{j2\pi fT_cq}\Big\}\Big). \tag{5.56}$$

The new limits $(-\infty,-1)$ are changed to $(-\infty,0)$, which adds an extra term in the summation. That extra term is at $q=0$. The extra term can be corrected by subtracting it from the summation

$$a = 2\Re\Big(|U(f,T_c)|^2\frac{1}{2}\Big(\sum_{q=1}^{\infty}e^{j2\pi fT_cq} + \sum_{q=-\infty}^{0}e^{j2\pi fT_cq} - e^{j2\pi fT_c0}\Big)\Big). \tag{5.57}$$

The two summations can now be combined so that the new limits are $(-\infty$ to $\infty)$

$$a = 2\Re\Big(|U(f,T_c)|^2\frac{1}{2}\Big\{\sum_{q=-\infty}^{\infty}e^{j2\pi fT_cq} - 1\Big\}\Big). \tag{5.58}$$

This allows for imposing the Poisson identity,

$$a = 2\Re\Big(|U(f,T_c)|^2\frac{1}{2}\Big\{\frac{1}{T_c}\sum_{k=-\infty}^{\infty}\delta(f-\frac{k}{T_c})-1\Big\}\Big). \tag{5.59}$$

Since the above equation only consists of a real part, then the $\Re$ symbol can be omitted. The rest of the equation then becomes

$$S_x(f) \to \frac{1}{T_c}\Big[|U(f,T_c)|^2 + |U(f,T_c)|^2\Big\{\frac{1}{T_c}\sum_{k=-\infty}^{\infty}\delta(f-\frac{k}{T_c})-1\Big\}\Big]. \tag{5.60}$$

The final result is

$$S_x(f) \to \frac{1}{T_c^2}|U(f,T_c)|^2\sum_{k=-\infty}^{\infty}\delta(f-\frac{k}{T_c}), \tag{5.61}$$

which is discrete only and is a PSD formula of a non-random PWM. In this way, power density is re-concentrated to the discrete parts, and this is an indication of reduced spectral spreading.

5.4.3 Remarks on Analytical Arguments

Through considering how the PSD formula is affected when probability of each random parameter approaches minimum spreading and maximum spreading, insight as to how the PSD is affected is obtained. The PSD formula indicates that, when probability approaches a uniform PMF, the discrete part of the PSD is transferred to the continuous part of the PSD. And when probability approaches a deterministic PMF[1], the power in the continuous part moves to the discrete part, so that only the discrete part remains. This transfer of harmonic power from discrete part to the continuous part is an indication of the spreading in the PMF *causing* a spreading out of power in the PSD formula.

5.4.4 Argument for Spectral Spreading in Monte Carlo Simulations

To further support the arguments posed in the previous section, three simulations were performed where each simulation focuses on randomising T, Δ and W. The simulations were run to match the arguments related to increasing the entropy of probability from minimum to maximum, and observing the impact on the spreading out of power in the

[1] A deterministic PMF consists of an outcome with a probability of 1.

PSD – as quantified by spectral entropy. The probability is varied from non-random to uniformly random.

5.4.4.1 Aspects of Simulation

The simulation procedure follows the parameter selection process as described in Section 2.4.2 in Chapter 2 for the univariate case. Where a pulse train is created based on the parameters produced by a *RandomGenerator* (see Figure 2.1). The pulse train must therefore be generated such that its statistical properties match the probability distributions given to the random generator. This means that the pulse train must be wide-sense stationary. To achieve this, Mathematica uses the function `RandomChoice` that takes two arguments: a set or a sample space of values S_{set} which represents the pool for RPWM, and their corresponding probability masses P_{mass}. This allows it to sample values for the selected PWM parameter at random, based on the probability mass given to it. The length of the pulse train must also be long enough to ensure stationarity. Once the pulse train is generated, its PSD is estimated.

When estimating the PSD, issues such as spectral leakage can affect the accuracy of the PSD estimate. For valid and accurate statistical results, a discussion on these aspects follows.

5.4.4.2 Issues on Pulse Train Sampling

In order to ensure that the generated pulse train is wide-sense stationary, the pulse train must be sufficiently long. These are characteristics of a stationary ergodic stochastic process [56]. This means that the ensemble average (or the expectation operator) can be approximated by a time average.

If M blocks of random pulse trains are generated, where each random pulse train has a total of N pulses and the m^{th} block $(m = 1, 2, .., M)$ is parametrised by $x_m(t)$, then the ensemble average is given by

$$E[x(t)] = \frac{1}{M} \sum_{m=1}^{M} x_m(t). \tag{5.62}$$

From a Monte Carlo perspective, M is the total number of simulation trials, where a pulse train is generated in each trial.

However, since obtaining the PSD is the next step, instead of averaging the time-domain signal, the PSD can be calculated on each block first, and the averaging can then follow. This essentially is Welch's periodogram formula for estimating the PSD in Equation 4.6.

5.4.4.3 Issues on PSD Estimation in Simulation

Spectral Leakage

When estimating the PSD, an undesired effect known as spectral leakage is inevitable most of the time, where the power of one frequency bin 'leaks' to other frequencies. This leakage phenomenon may interfere with the spreading effects introduced by RPWM. It is, therefore, important to minimise spectral leakage to obtain more reliable results. In practice, spectral leakage is not a major issue as it only represents a sampling problem and not a practical or physical phenomenon.

Coherent sampling and windowing are often the two main approaches used to mitigate this effect. Furthermore, careful attention must be paid to the type of window to be used, since different windows have different effects on spectral leakage. However, if the conditions of coherent sampling can be met, then there is no need for windowing to be used.

Consider an example where a deterministic pulse train is generated, and its PSD is estimated. The pulse train has a period of 0.015 s, and was sampled at 0.01/2500 s, which is a sampling frequency of 250 kHz. However, the frequency of the square wave is 66.6667 Hz. This means that the available integer bins of 1,2,3,...,250 kHz are not matched with the available frequency of 66.667 Hz, and as a result, the power 'leaks' to the adjacent frequency bins. Figure 5.2 compares the estimated PSDs with and without coherent sampling.

The condition for coherent sampling is that the sampling rate is an integer multiple of the period of the signal, or vice versa. For example, if the frequency of the square wave had been 50 Hz, then the bins would have been matched, and the PSD would be as shown in Figure 5.2A.

In the case of random modulation, the actual period of the signal is not completely known. However, if the sampling frequency is such that it is an integer multiple of all the possible frequencies that the signal will have, then coherent sampling can occur so that the effect of spectral leakage is reduced. The same principle must be applied for

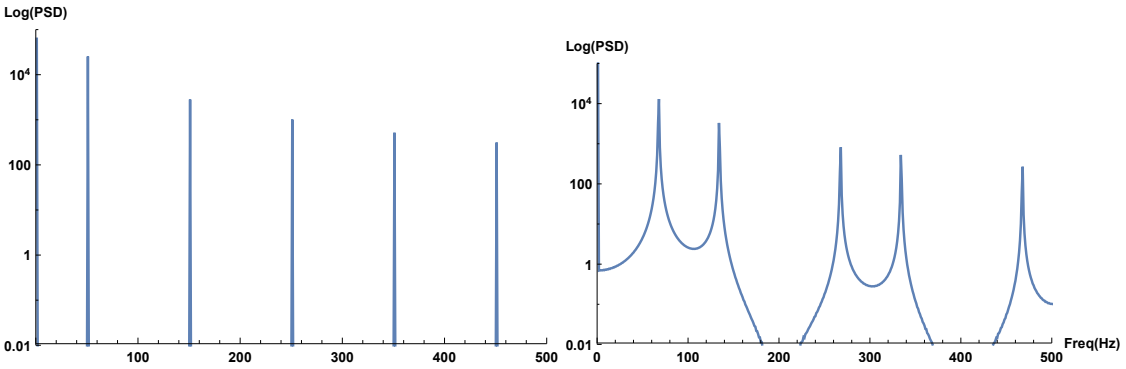

(A) Power Density Spectrum with no spectral leakage, frequency 50 Hz

(B) Power Density Spectrum with spectral leakage, frequency 66.667Hz

FIGURE 5.2: Power Density Spectrum of non-random pulse train, showing spectral leakage effect when sampling frequency and signal frequency are not coherent. Both signals sampled at 250Khz

the pulse width and pulse position. Therefore, for the RPWM case, the pool was chosen in the manner that each possible value has a frequency that meets the condition for coherent sampling.

5.4.4.4 Simulation Method

The simulations were conducted by creating a pool of 5 values for each random parameter. The probabilities p_i where adjusted so that their entropy increases from minimum to maximum entropy. This adjustment was such that the probability spreads out, while ignoring the average outcome when values are sampled from each distribution. In each case, a PWM pulse train was constructed and its spectral entropy was calculated using Equation 5.7. This was done for 30 simulation trials and an average was then taken.

The table below shows how the probabilities were spread out along with their respective entropic values.

The values in the following pool were selected in order to satisfy coherent sampling requirements as described in Section 5.4.4.3.

$$T \in \{8, 20, 25, 40, 50\}\mu s, \tag{5.63a}$$

$$\Delta \in \{8, 20, 25, 40, 50\}\mu s, \tag{5.63b}$$

$$W \in \{8, 20, 25, 40, 50\}\mu s. \tag{5.63c}$$

TABLE 5.1: Increasing entropic values of probability distributions from minimum to maximum

p_1	p_2	p_3	p_4	p_5	$H[\Pr]$ (with log base e)
0	0	1	0	0	0
0	0.05	0.9	0.05	0	0.394398
0.05	0.05	0.8	0.05	0.05	0.77
0.05	0.1	0.7	0.1	0.05	1.00976
0.05	0.15	0.6	0.15	0.05	1.11752
0.05	0.2	0.5	0.2	0.05	1.28992
0.1	0.2	0.4	0.2	0.1	1.47081
0.15	0.2	0.3	0.2	0.15	1.5741
0.2	0.2	0.2	0.2	0.2	1.60944

The sampling frequency was increased to 500kHz for finer frequency resolution. This also contributes to minimising spectral leakage.

One parameter was randomise d at a time, whiles the others were fixed. For each randomisation, the fixed parameters were adjusted to obey the primary constraints. Figure 5.3 summarises the flow of the Monte Carlo simulation performed in Mathematica.

Remarks on the choices of some values

The size of the pool was kept at 5 as this was seen as sufficient to demonstrate the impact of probability entropy on spectral entropy. These simulations focus only demonstrating entropy itself. Thirty simulations where seen as sufficient to capture the overall pattern, although a higher number of simulations and probabilities should only affect the smoothing of the overall pattern.

5.4.5 Entropy Simulation Results

The following results are an indication of the simulated relationship between probability entropy and spectral entropy of the PSD.

5.4.5.1 Random Pulse Period

In Figure 5.4, the figure on the left (Figure 5.4A) shows the result for 30 simulated trials for random T indicated by different colours, and on the right (Figure 5.4B), the average of those 30 trials is plotted.

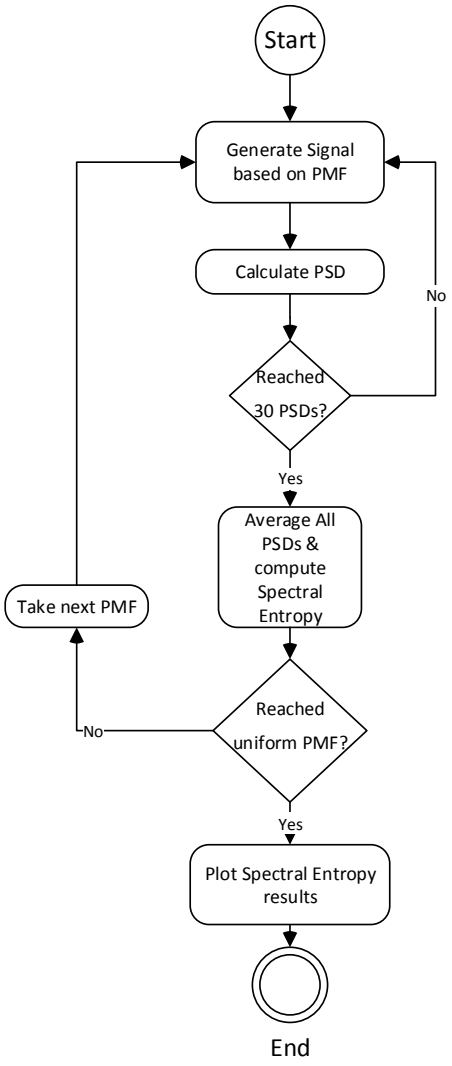

FIGURE 5.3: Showing flow of Monte Carlo simulation. This simulation was done for random T, Δ and W.

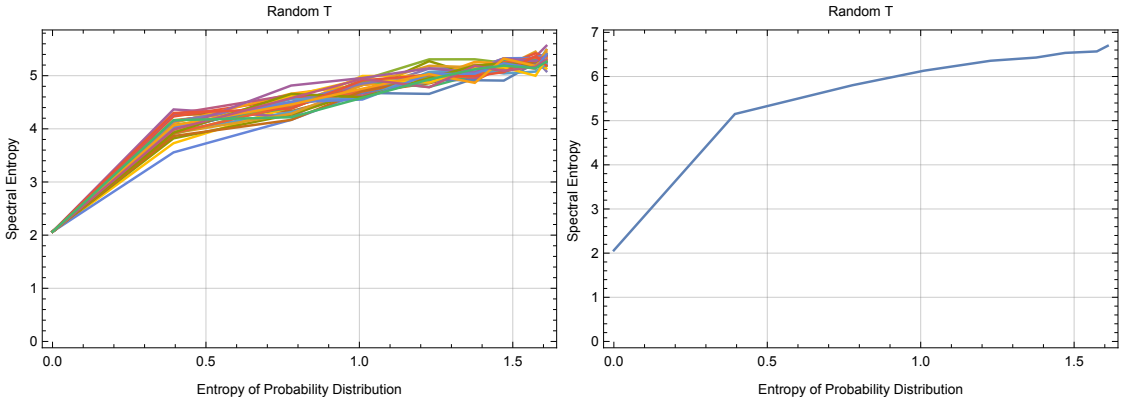

(A) Relationship for 30 simulated curves (B) Average pattern of the 30 curves

FIGURE 5.4: Showing relationship between probability entropy and spectral entropy for random T

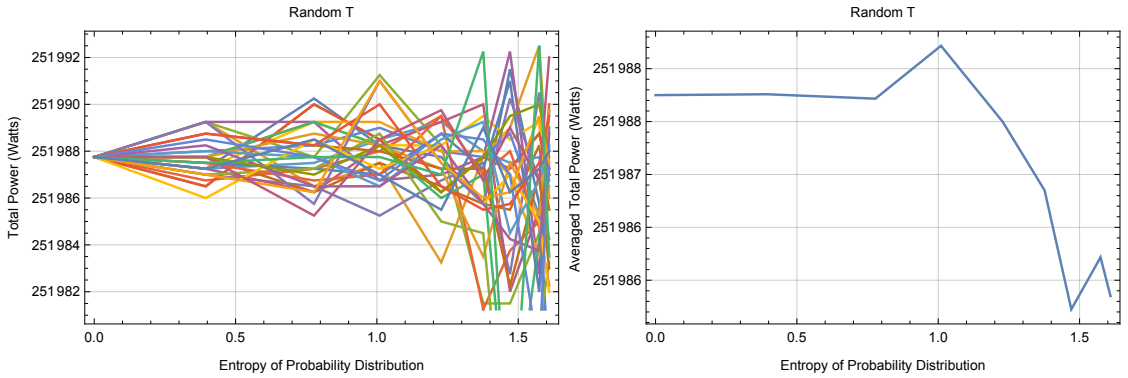

(A) Relationship for 30 simulated curves (B) Average power of the 30 curves

FIGURE 5.5: Showing relationship between probability entropy and total power for random T

The first observation to note in the average case (Figure 5.4B) is the following: as the entropy of probability is increased, from non-random to the most random (uniform distribution), the spectral entropy also increases. This implies that the PSD is spreading out. This agrees with the theoretical arguments discussed in Section 5.4.2.3.

The second observation is that, from the averaged case, there exists a monotonic relationship between probability entropy and PSD entropy. The non-averaged case (Figure 5.4A) highlights that this relationship only exists on an average basis, and it further highlights the degree to which the spectral entropy fluctuates due to the random nature.

The average total power allows for verifying the validity of the spectral entropy relation to probability entropy. Figure 5.5 shows how the total power varies for each of the 30 trials and how it varies on average . It is clear that there exists some variation in the average total power. However, the magnitude of the variation is significantly small as seen from the numerical values on the y-axis. In addition, the overall pattern does not correlate to the overall pattern in the entropy curves. Therefore, it is extremely unlikely that the total power is the reason behind the monotonic relationship observed.

5.4.5.2 Random Pulse Position

Similar to the previous case, Figure 5.6B shows an increase in the average spectral entropy as the probability entropy increases from minimum to maximum for random Δ.

Monotonicity between probability entropy and spectral entropy is also observed for this random case. The total power curves are shown in Figure 5.7. From the averaged

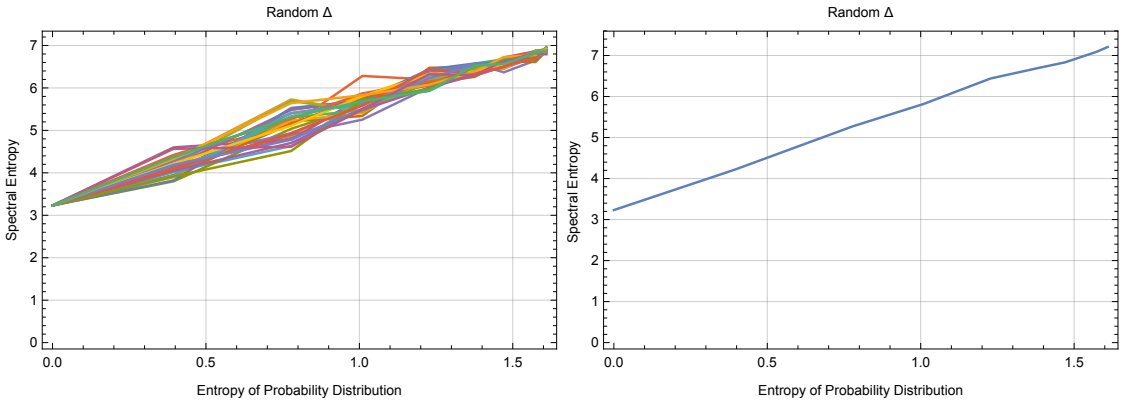

(A) Relationship for 30 simulated curves (B) Average pattern of the 30 curves

FIGURE 5.6: Showing relationship between probability entropy and spectral entropy for random Δ

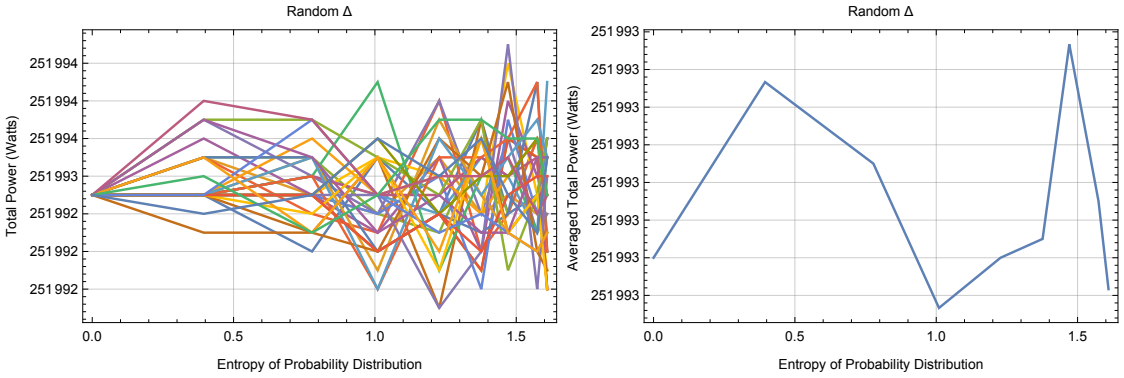

(A) Relationship for 30 simulated curves (B) Average power of the 30 curves

FIGURE 5.7: Showing relationship between probability entropy and total average power for random Δ

total power, there exist some fluctuations, which however, do not correlate to the relationship shown in the entropy curves of Figure 5.6. In addition, as viewed from the Total Power axis, the fluctuations in the averaged total power are also relatively small. Therefore, similar to random T, it is highly unlikely that the total power is responsible for the monotonic relationship that has been shown.

5.4.5.3 Random Pulse Width

The results for the random pulse width also show a monotonic relationship of spectral entropy and probability entropy in Figure 5.8B. Unlike the previous cases however, the average total power shown in Figure 5.9B, increases significantly and this increase is monotonic.

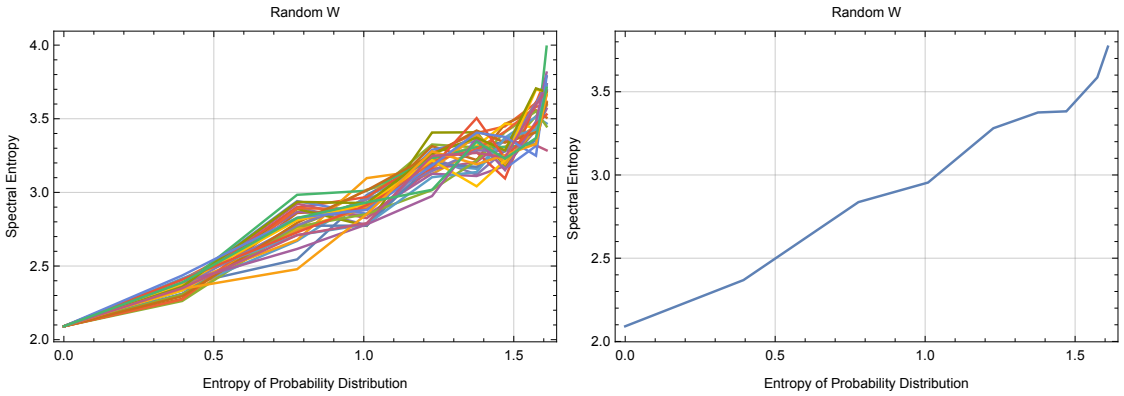

(A) Relationship for 30 simulated curves (B) Average pattern of the 30 curves

FIGURE 5.8: Showing relationship between probability entropy and spectral entropy for random W

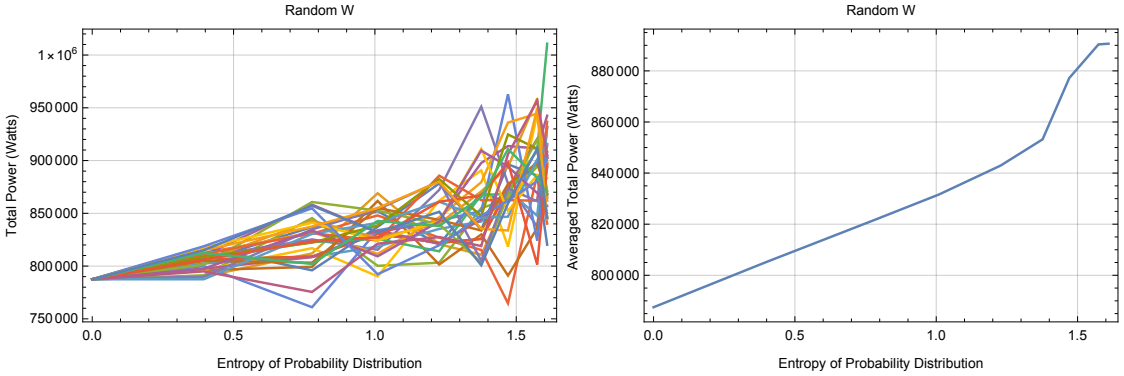

(A) Relationship for 30 simulated curves (B) Average pattern of the 30 curves

FIGURE 5.9: Showing relationship between probability entropy and total average power for random W

The reason behind this is that randomising W, also randomises the total power contained by each pulse (the total power of a pulse directly depends on the pulse width), as opposed to random T or random Δ. The steady increase in average total power is due to the average pulse width of the entire RPWM signal growing due to increased spreading in the PMF. The manner in which the probability distribution changes has resulted in an increase in the average pulse width. This is consistent with the theoretical arguments made in Section 5.4.2.1.

One could argue therefore that the computed spectral entropy for random W is compromised since the average total power increases monotonically. However, with respect to the very same argument, the overall pattern of spectral entropy should be monotonically decreasing because of the inverse relationship. Because this is not the case, it means that the spreading out of probability counteracted the impact of the average total power, thereby resulting in an overall increasing spectral entropy. This implies

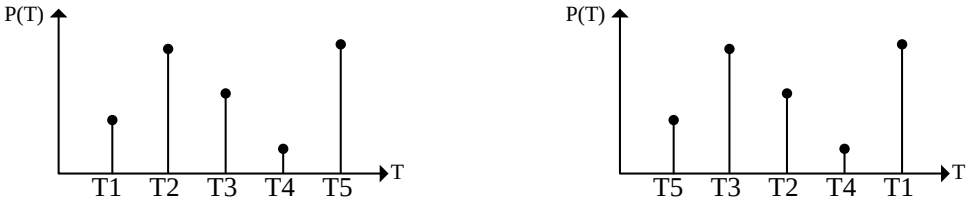

(A) Original PMF (B) Rearranged PMF

FIGURE 5.10: Showing rearranging order of probability, without changing PMF shape

that, if the change in the average total power is sufficiently large, spectral entropy will be significantly affected.

5.4.5.4 Spectral Entropy with Fixed Probability Entropy

It is possible to investigate spectral entropy without increasing probability entropy. This can be done by rearranging the position of the elements in the pool, without changing the shape of probability. For example, the pool is rearranged from Figure 5.10A to Figure 5.10B and the shape remains the same.

However, rearranging the positions is the same as changing the average outcome, without changing the shape of the PMF. Changing the average outcome essentially means a specific value will occur more frequently than other values. Therefore, there may be several ways of increasing spectral entropy using probability, but the focus here is on spreading of probability only. The investigation of the impact of the average outcome of Δ, W and T on spectral entropy is reserved for Chapter 6.

5.4.5.5 Random Pulse Width Entropy Dilemma

It has been shown that when randomising T, the increasing entropy of probability increases the average spectral entropy, and that this relationship is monotonic. The same holds for random Δ. Sufficient reason for the same relationship to exist for random W has also been given, even though the average total power has some influence on this relationship due to its significant change. However, this change can be significantly reduced by ensuring that when randomising W, the average pulse width remains constant. This is the same constraint that had to be applied in the analytical argument section in Section 5.4.2.1. In other words, the randomisation must be constrained to reduce

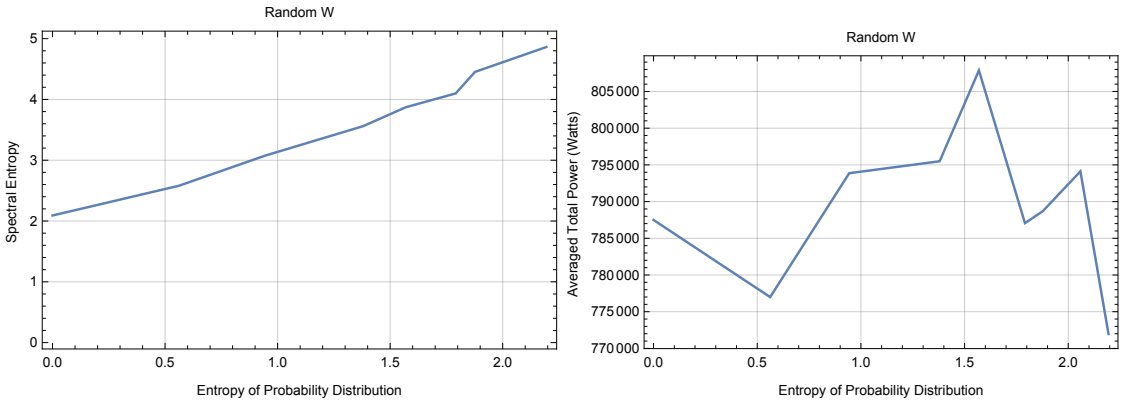

(A) Spectral Entropy and probability entropy (B) Average total power for random W

FIGURE 5.11: Showing spectral entropy versus probability entropy for random W, and average total power versus probability entropy. Probability entropy increased by increasing pool size for W

variation in total power. But the dilemma is that probability entropy must be gradually increased in order to show the relationship between probability entropy and spectral entropy.

Recalling that entropy of probability can also be increasing by increasing the pool size. Then the way around this issue is by allowing the pool size to change as well while ensuring that the average outcome of random W is prevented from varying. The result of this is shown in Figure 5.11. The figure shows that the average total power does not monotonically increase as before, and it can be said that the changes (difference) in the average total power is reduced.

Thus spectral entropy increases monotonically with probability entropy.

5.4.5.6 Remarks on Simulation Arguments

The Monte Carlo simulation results showed that, when the probability is spread out from minimum to maximum spreading, the PSD also spreads out accordingly, and this spreading out is quantifiable by spectral entropy. Thus spectral entropy sufficiently captures the monotonic relationship between probability spreading and spectral spreading.

5.5 Argument Summary

The arguments presented in this chapter are now consolidated. An argument structure that summarises all the important points and associated evidence is presented.

5.5.1 Argument Proposition

The Argument proposes the following conclusion:
"A maximum spreading in probability distribution leads to a maximum spreading in the power density spectrum"
Two important factors are included in the proposed conclusion, causality and correlation. This conclusion can be rendered true given that there is a causal and increasing monotonic relationship between probability entropy and spectral entropy.

5.5.2 Argument Structure

A good argument is one that is supported by sufficient evidence. Its aim was to provide the reader with a high degree of confidence in the proposed conclusion. The argument structure and summery is provided in Figure 5.12

5.5.2.1 Remarks on Given Argument

Sufficient reason now exists to believe that an increase in the entropy of probability leads to an increase in the spreading/entropy of the PSD. It can, therefore, be concluded that, given that probability is the only means of spreading the power density spectrum, and there is a monotonicity relationship between the two, maximum entropy probabilities lead to maximum spreading in the PSD.

One may argue that the provided argument lacks a closed-form solution, or a lack of an analytical expression describing increasing monotonicity between probability entropy and spectral entropy. However, the given argument still remains plausible due to the supporting evidence as well as the repeatability of the evidence. In that sense, the presented conclusions can be used for further analysis. A closed-form solution is left for future research.

Furthermore, and most importantly, the presented evidence qualifies the use of the Method of Maximum Entropy for maximally spreading the PSD using PMFs.

5.6 Conclusion

This chapter had one main focus point, which was to investigate the impact of spreading out the probability that governs random PWM process, on spreading out of harmonic

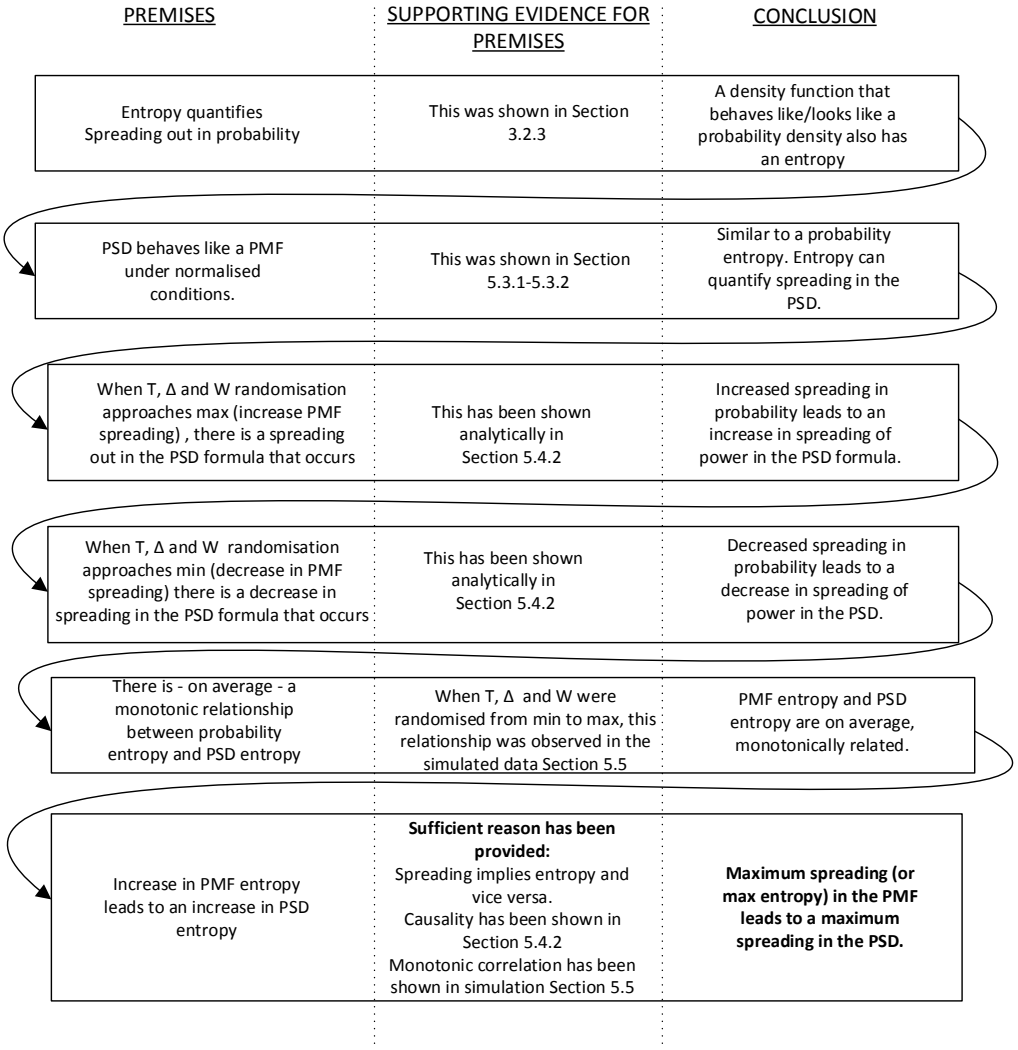

FIGURE 5.12: Overall argument structure and argument summery for why maximum spreading in the PDF leads to a maximum spreading in the PSD

power in the PSD. However, this focus point depended on first showing that the impact of probability spreading on spectral spreading is quantifiable as spectral entropy. The concept of spectral entropy was introduced and the manner in which it quantifies spectral spreading was then discussed. This then allowed for discussing how spreading out of probability affects spectral spreading - an argument that provided sufficient reason to accept the conclusion that, when probability spreads out (from minimum to maximum spreading), so does the spectral spreading. This conclusion allows for the use of the Method of Maximum Entropy (in probability) for maximising spreading in the PSD.

Chapter 6

Spectral Shaping using Maximum Entropy Probability Distributions

6.1 Introduction

Spectral shaping in RPWM is commonly approached from an optimisation perspective, where given a probability distribution and a random modulation pool of possible values, a probability distribution must be found, such that the high amplitude harmonics of the power density spectrum of a PWM signal are reduced. This criterion is useful for applications where harmonics that are particularly harmful, or cause interference problems, are mitigated. Since the relationship between probability spreading and spectral spreading has been established, this optimisation perspective is justified.

The random pool and the probabilities have different levels of impact on the spectral characteristics of a PWM. If the pool of randomisation is large, then there are more degrees of freedom of randomisation. From what has been shown so far, a large RPWM pool constitutes a probability distribution with higher entropy. A high entropy PMF results in a more spread out spectrum. However, there are practical limitations when it comes to large pools. For example, certain microprocessors might have a minimum and a maximum possible switching frequency that they can generate. There is also a finite number of possible switching frequencies that a microprocessor can have. Generally, there will always be a limited pool when it comes to practical implementation.

Give this limitation, an alternative way of spreading the spectrum can be the use of PMF of the random PWM signal itself.

It has been plausibly shown in previous chapters that a spreading out of probability distributions monotonically results in a spreading out in the PSD. Because this is true, then by maximally spreading out the probability distribution, the PSD can also be maximally spread out, given time-domain constraints. This is where maximum entropy probability distributions come in.

This chapter derives a set of formulas based on the Method of Maximum Entropy, that produce a PMF that will maximally spread the PSD, while obeying the time-domain randomisation constraints. Additionally, this approach allows for later identifying limitations to spectral spreading when using probability. The objective is, therefore, to show how MaxEnt probabilities result in maximally spread out PSDs, under the time-domain constraints.

Four randomisation cases are considered, starting with three univariate cases: random T, random W, random Δ and lastly a joint randomisation of the three (trivariate randomisation). The PSD generated based on MaxEnt probabilities of each random case is illustrated, and the spectral performance (spectral entropy) is calculated. The extent to which the random PWM obeys the constraints is analysed by implementing the random PWM in a DC-DC converter circuit and observing the average output voltage of the converter as well as the random PWM signal itself.

The second part of this chapter investigates the impact of altering the secondary constraints (magnitude of the average outcomes $\overline{T}$, $\overline{W}$ and $\overline{\Delta}$) on the spreading out capabilities of the PSD, given a limited pool. As will be seen, this will provide what can be viewed as a region of time-domain constraints (from 'strongest' to 'weakest') in which spectral spreading can be maximised, as well as the trade-offs involved between the level of secondary constraints and maximally spreading the spectrum.

6.2 Related Work in Spectral Shaping from RPWM optimisation

Given that there is always a limited number of elements in a pool, it is possible to optimize for the 'best pool' that will reduce the high amplitude harmonics.

An optimisation of carrier frequencies in a limited pool is presented by Trzynadlowski *et al.* [25]. The pool is selected such that the possible frequencies are far from the least common multiple of all the frequencies. This mitigates the harmonics that are introduced

by common multiples frequencies. This effect can also be reduced by using relatively prime numbers in the values of the pool of carrier frequencies.

The papers by Kirlin *et al.* [19, 26], focuse on equally spaced carrier frequencies, and the probabilities of those frequencies are optimised. The optimisation criterion, however, is slightly different in that it does not focus on the discrete part of the spectrum, but on maximising the power contained by the continuous noise spectrum. Stanković [45] presents an approach where the Fourier transform of the time-domain probabilities is the characteristic function and the probability masses are the parameters to be optimised. And the optimisation aim is to minimise the signal power in a frequency range (wide band minimisation) and the minimisation of one or more multiple discrete harmonics (narrow band optimisation). All these optimisations are done such that the time-domain constraints are obeyed.

The approach presented in this chapter is similar to the techniques in the cited literature that optimise for the probability distribution, given a limited pool. However, the novelty lies in the objective function which leads to a novel optimisation application. The objective is to spread out the harmonic power in the PSD as much as allowably possible, while maintaining constraints. This allows for the use of maximum entropy probabilities as well as an investigation into the extent to which spectral spreading can occur, thus uncovering some limiting factors.

6.3 Maximum Entropy RPWM Probability Distributions

The process for finding the probabilities applied here is as described in Chapter 3. However, in this case it is generalised for randomising the pulse width, pulse period and position. An added benefit is that a designer desiring to use RPWM to minimise harmonics, given specified DC-DC converter constraints, can apply the methods presented here.

6.3.1 Derivation of MaxEnt PMFs for RPWM

Given a pool for each random parameter as given in Equation 2.1 of Chapter 2. The general random PWM joint probability distribution is represented in general as

$$\Pr(T_i, W_r, \Delta_j) = p_{i,r,j}. \tag{6.1}$$

A MaxEnt joint probability distribution $p^*_{i,r,j}$ is required,

$$p^*_{i,r,j} = \arg\max_{p_{i,r,j}} +H[\Pr(T_i, W_r, \Delta_j)], \tag{6.2}$$

such that the following constraints are obeyed

$$\sum_{i,r,j} p_{i,r,j} f_q(x_i, x_r, x_j) = F_q, \quad q = 1, 2, ..., m, \tag{6.3}$$

$$\sum_{i,r,j} p_{i,r,j} = 1, \quad p_{i,r,j} \geq 0, \quad \forall(i, l, j). \tag{6.4}$$

The general solution is therefore

$$p^*_{i,r,j} = e^{-(\lambda_0 + \lambda_1 f_1(x_i, x_r, x_j) + \lambda_2 f_2(x_i, x_r, x_j) + ... + \lambda_m f_m(x_i, x_r, x_j))}. \tag{6.5}$$

6.3.2 Conditional Maximum Entropy RPWM Probabilities

It was previously discussed that the conditional relationship between T, W and Δ depends on the order of the random selection process. This highlights the importance of conditional PMFs in order to obey primary constraints. However, a more general approach independent of the order of selection will be later introduced as a more general case, especially for the trivariate (joint) randomisation.

6.3.2.1 RPWM MaxEnt Constraints for Conditional Probabilities

The primary constraints are stated again for convenience

$$0 \leq \Delta_k < T_k \tag{6.6a}$$

$$0 \leq W_k < T_k \tag{6.6b}$$

$$\Delta_k + W_k < T_k \tag{6.6c}$$

An important constraint for RPWM in DC-DC converters is that the duty cycle, on average, must remain constant. For this, the average pulse period and the average pulse width must be constant. Each random parameter must have its own expected average based on the probability that it is sampled from. Thus, if the random PWM parameters

had been randomised independently, the secondary constraints would be defined as

$$\sum_i p_i T_i = \overline{T} = \zeta, \tag{6.7a}$$

$$\sum_r p_r W_r = \overline{W} = \gamma, \tag{6.7b}$$

$$\sum_j p_j \Delta_j = \overline{\Delta} = \alpha, \tag{6.7c}$$

where the symbols ζ, γ and α are the constant parameters for the pulse width, period and position respectively. These are the parameters that would be specified for deterministic PWM.

However, it is known that the random parameters are not independent of one another. Therefore, the marginal probabilities in Equation 6.7 are not correct since they do not encompass the conditionality that the parameters hold in order to obey the primary constraints (see Section 2.4.2.2). Therefore, the relationship between the parameters must be described for both the univariate and the trivariate cases.

6.3.3 Univariate MaxEnt PMFs

For this case, the PMF of each random parameter is conditional on the fixed one. If the joint probability is described as $p_{i,r,j}$, the indicices for the non-random parameters are fixed at some value.

6.3.3.1 Constraints

The secondary constraints for each univariate randomisation are

$$\sum_i p_{i|j,r} T_i = \overline{T} = \zeta, \quad \text{for random} \quad T, \quad \text{fixed} \quad W \quad \& \quad \Delta, \tag{6.8a}$$

$$\sum_r p_{r|i,j} W_r = \overline{W} = \gamma, \quad \text{for random} \quad W, \quad \text{fixed} \quad T \quad \& \quad \Delta, \tag{6.8b}$$

$$\sum_j p_{j|i,r} \Delta_j = \overline{\Delta} = \alpha, \quad \text{for random} \quad \Delta, \quad \text{fixed} \quad T \quad \& \quad W, \tag{6.8c}$$

where the conditional PMF $p_{i|j,r}$ represents $\Pr(T_i|W_r, \Delta_j)$, $p_{r|i,j}$ is $\Pr(W_r|T_i, \Delta_j)$ and $p_{j|i,r}$ is $\Pr(\Delta_j|T_i, W_r)$. Each of the above therefore has its own MaxEnt PMF.

Similarly, the MaxEnt joint PMF $p^*_{i,j,r}$ that describes the random PWM signal will be one of the following

$$p^*_{i|j,r} = e^{-(\lambda_0+\lambda_1 T_i)}, \quad \text{for random} \quad T, \quad \text{fixed} \quad W \quad \& \quad \Delta, \tag{6.9}$$

$$p^*_{r|i,j} = e^{-(\lambda_0\lambda_1 W_r)}, \quad \text{for random} \quad W, \quad \text{fixed} \quad T \quad \& \quad \Delta, \tag{6.10}$$

$$p^*_{j|i,r} = e^{-(\lambda_0+\lambda_1 \Delta_j)}, \quad \text{for random} \quad \Delta, \quad \text{fixed} \quad T \quad \& \quad W. \tag{6.11}$$

Each random strategy has its own λ_1 that is solved from using its own secondary constraint. Using random T only for the rest of the derivation, the next step involves solving for the two Lagrange multipliers λ_0 and λ_1.

6.3.4 Solving for Lagrange Multipliers

The normalisation $\sum_{i,j,r} p^*_{i,j,r} = 1$ determines the first Lagrange multiplier. For random T only, the normalisation constraint becomes

$$\sum_i p^*_{i|j,r} = 1. \tag{6.12}$$

Applying this to Equation 6.9 results in

$$p^*_{i|j,r} = \frac{e^{-\lambda_1 T_i}}{\sum_i e^{-\lambda_1 T_i}}. \tag{6.13}$$

Now if random values are sampled from the above distribution, there are values in T_i that may be greater than the fixed W and Δ, which may cause the primary constraints to be disobeyed. Therefore, in order for the conditionality to be contained in the MaxEnt PMF, the values in T_i must be updated such that the values that may lead to violating the primary constraints have a probability of zero, or are just removed from the pool. Then the Lagrange multiplier λ_1 must be solved with the new updated pool in place. Thus, let the new updated pool be T'_i such that $\Delta_c + W_c < T'_i$ is satisfied (Δ_c and W_c are the fixed values). This ensures that the primary constraint is not violated.

Once this is fulfilled, the MaxEnt PMF is rewritten in-terms of the updated pool T'_i

$$p^*_{i|j,r} = \frac{e^{-\lambda_1 T'_i}}{\sum_i e^{-\lambda_1 T'_i}}. \tag{6.14}$$

Next, the secondary constraint is used to solve for λ_1. Substituting Equation 6.14 into Equation 6.8a results in

$$\frac{\sum_i e^{-\lambda_1 T_i'} T_i'}{\sum_i e^{-\lambda_1 T_i'}} = \zeta \tag{6.15}$$

Equation 6.15 marks the final step for finding the MaxEnt PMF. Once the numerical value of λ_1 is found, it can be inserted back into Equation 6.14.

The same must be applied for the other univariate cases. For random W, fixed T and Δ, the MaxEnt PMF is

$$p^*_{r|i,j} = \frac{e^{-\lambda_1 W_r'}}{\sum_r e^{-\lambda_1 W_r'}}, \tag{6.16}$$

and the Lagrange multiplier is obtained from

$$\frac{\sum_r e^{-\lambda_1 W_r'} W_r'}{\sum_r e^{-\lambda_1 W_r'}} = \gamma. \tag{6.17}$$

For random Δ, fixed T and W, the MaxEnt PMF is

$$p^*_{j|i,r} = \frac{e^{-\lambda_1 \Delta_j'}}{\sum_j e^{-\lambda_1 \Delta_j'}}, \tag{6.18}$$

and the Lagrange multiplier is obtained from

$$\frac{\sum_j e^{-\lambda_1 \Delta_j'} \Delta_j'}{\sum_j e^{-\lambda_1 \Delta_j'}} = \alpha. \tag{6.19}$$

6.3.5 Trivariate MaxEnt PMF

6.3.5.1 Constraints

For this illustration, assume that the order of randomisation is $T \to W \to \Delta$. The correct secondary constraints, based on this Markov model is

$$\sum_i p_i T_i = \zeta, \tag{6.20a}$$

$$\sum_r p_{r|i} W_r = \gamma, \tag{6.20b}$$

$$\sum_j p_{j|i,r} \Delta_j = \alpha, \tag{6.20c}$$

where the marginal probability of each parameter is conditional on the previously randomised parameter. There are a total of three constraints, therefore $m = 3$. Following

Equation 6.3 implies $f_1 = T_i$, $f_2 = W_r$ and $f_3 = \Delta_j$. The joint MaxEnt probability is therefore given as

$$p^*_{i,r,j} = e^{-(\lambda_0+\lambda_1 T_i+\lambda_2 W_r+\lambda_3 \Delta_j)}. \tag{6.21}$$

The above equation is then used to calculate the marginal conditional PMFs. From the product rule, a joint probability $\Pr(T_i, W_r, \Delta_j)$ is expanded as

$$\Pr(T_i, W_r, \Delta_j) = \Pr(T_i)\Pr(W_r|T_i)\Pr(\Delta_j|W_r, T_i). \tag{6.22}$$

Using the short notation

$$p^*_{i,r,j} = (p_i) \cdot (p_{r|i}) \cdot (p_{j|r,i}). \tag{6.23}$$

From Bayes, the marginal conditional PMFs are computed as

$$\Pr(T_i) = \sum_{W,\Delta} \Pr(T_i, W_r, \Delta_j), \tag{6.24}$$

$$\Pr(W_r|T_i) = \frac{\sum_\Delta \Pr(T_i, W_r, \Delta_j)}{\Pr(T_i)}, \tag{6.25}$$

$$\Pr(\Delta_j|W_r, T_i) = \frac{\Pr(T_i, W_r, \Delta_j)}{\sum_\Delta \Pr(T_i, W_r, \Delta_j)}. \tag{6.26}$$

Using the short notation, the MaxEnt conditional PMFs are

$$p^*_i = \sum_{r,j} p^*_{i,r,j} \tag{6.27}$$

$$p^*_{r|i} = \frac{\sum_j p^*_{i,r,j}}{p_i} \tag{6.28}$$

$$p^*_{j|i,r} = \frac{p^*_{i,r,j}}{\sum_j p^*_{i,r,j}} \tag{6.29}$$

The secondary constraints, if required, can be rewritten in terms of the MaxEnt joint probability $p^*_{i,r,j}$ as

$$\sum_i \sum_{j,r} p^*_{i,r,j} T_i = \zeta, \tag{6.30a}$$

$$\frac{\sum_r \sum_j p^*_{i,r,j} W_r}{\sum_{j,r} p^*_{i,r,j}} = \gamma, \tag{6.30b}$$

$$\frac{\sum_j p^*_{i,r,j} \Delta_j}{\sum_j p^*_{i,r,j}} = \alpha. \tag{6.30c}$$

6.3.5.2 Solving for Lagrange Multipliers

Imposing the normalisation constraint $\sum_{i,j,r} p^*_{i,j,r} = 1$ onto Equation 6.21 result in

$$p^*_{i,j,r} = \frac{e^{-(\lambda_1 T_i + \lambda_2 W_r + \lambda_3 \Delta_j)}}{\sum_{i,j,r} e^{-(\lambda_1 T_i + \lambda_2 W_r + \lambda_3 \Delta_j)}}. \tag{6.31}$$

Substituting the above into Equation 6.30a results in

$$\frac{\sum_{i,r,j} T_i e^{-(\lambda_1 T_i + \lambda_2 W_r + \lambda_3 \Delta_j)}}{\sum_{i,j,r} e^{-(\lambda_1 T_i + \lambda_2 W_r + \lambda_3 \Delta_j)}} = \zeta. \tag{6.32}$$

Substituting Equation 6.31 into Equation 6.30b

$$\frac{\sum_{r,j} W_r e^{-(\lambda_1 T_i + \lambda_2 W_r + \lambda_3 \Delta_j)}}{\sum_{j,r} e^{-(\lambda_1 T_i + \lambda_2 W_r + \lambda_3 \Delta_j)}} = \gamma. \tag{6.33}$$

Substituting Equation 6.31 into Equation 6.30c

$$\frac{\sum_{j} \Delta_j e^{-(\lambda_1 T_i + \lambda_2 W_r + \lambda_3 \Delta_j)}}{\sum_{j} e^{-(\lambda_1 T_i + \lambda_2 W_r + \lambda_3 \Delta_j)}} = \alpha. \tag{6.34}$$

The summations can be simplified for each of the three equations above, to give the three equations respectively

$$\frac{\sum_i e^{-\lambda_1 T_i} T_i}{\sum_i e^{-\lambda_1 T_i}} = \zeta, \tag{6.35}$$

$$\frac{\sum_r e^{-\lambda_2 W_r} W_r}{\sum_r e^{-\lambda_2 W_r}} = \gamma, \tag{6.36}$$

$$\frac{\sum_j e^{-\lambda_3 \Delta_j} \Delta_j}{\sum_j e^{-\lambda_3 \Delta_j}} = \alpha. \tag{6.37}$$

Furthermore, inserting Equation 6.31 into Equation 6.27-6.29 and simplifying, results in

$$p^*_i = \frac{e^{-\lambda_1 T_i}}{\sum_i e^{-\lambda_1 T_i}} \tag{6.38}$$

$$p^*_{r|i} = \frac{e^{-\lambda_2 W_r}}{\sum_r e^{-\lambda_2 W_r}} \tag{6.39}$$

$$p^*_{j|i,r} = \frac{e^{-\lambda_3 \Delta_j}}{\sum_j e^{-\lambda_3 \Delta_j}} \tag{6.40}$$

At this stage, it is easy to infer what the conditional MaxEnt PMFs would be if the selection order or the Markov model had been different.

The three equations above essentially imply that if one requires to randomise a PWM

and obey both the primary and secondary constraints while maximizing the spreading out of probability, then the random variables T, W and Δ have to be consecutively sampled from the three respective equations above. This is similar to the example of rolling the three dice such that some constraints are met (see Section 2.4.2.2). Thus if one chooses to sample T first, then certain elements in W that may result in the primary constraints being disobeyed must have a zero probability of being chosen.

To impose this zero probability, the random pool of the parameter can be updated before solving for its MaxEnt PMF to exclude the outcomes that would result in the constraints being disobeyed.

To further clarify this, consider this example

1. The Lagrange multiplier λ_1 in Equation 6.35 is solved first. This will determine the MaxEnt PMF for random T in Equation 6.38. The PMF is then used to sample T. The outcome of sampling T is T_k, and T_k will determine what the new elements in the pool of W_r should be, so that all elements obey the primary constraints (i.e. $W_k < T_k$). Let the updated pool be $W_r^{'}$.

2. Once these values are determined, the Lagrange multiplier λ_2 can be solved using Equation 6.36 with the new updated pool. This will determine the conditional MaxEnt PMF $p^*_{r|i}$ in Equation 6.39. Next is to randomise new W' based on the computed PMF. The outcome of this randomisation W_k determines the updated pool $\Delta_j^{'}$ such that primary constraints are not violated (i.e. $\Delta_k + W_k < T_k$).

3. In the same manner, the Lagrange multiplier λ_3 is solved in light of the new pool $\Delta_j^{'}$. And finally, this constitutes the conditional MaxEnt PMF $p^*_{j|i,r}$ and Equation 6.40 can be found.

Conditional MaxEnt probabilities are now rewritten to include the updated pools which carry the interdependence between the parameters

$$p_i^* = \frac{e^{-\lambda_1 T_i}}{\sum_i e^{-\lambda_1 T_i}} \tag{6.41}$$

$$p^*_{r|i} = \frac{e^{-\lambda_2 W_r^{'}}}{\sum_r e^{-\lambda_2 W_r^{'}}} \tag{6.42}$$

$$p^*_{j|i,r} = \frac{e^{-\lambda_3 \Delta_j^{'}}}{\sum_j e^{-\lambda_3 \Delta_j^{'}}} \tag{6.43}$$

This approach sufficiently handles the primary constraints. For single parameter randomisation, it simplifies to a 'non-Markov model' based randomisation.

6.3.5.3 Issues with Markov Model Based Randomisation

This approach highlights the importance of MaxEnt PMF maintaining primary constraints, which also helps describe how conditional probabilities can achieve this. Unfortunately, this process is not perfect and has some major issues that arise, especially when all parameters are randomised. There are cases where the Lagrange multipliers have no solution. This occurs if the elements in the new pool ($W_r^{'}$ and $\Delta_j^{'}$) are outside the allowable range, which is when the average outcomes (secondary constraints) are either bigger or smaller than all the elements in the updated pools. Therefore, an algorithm that deals with this would have to be developed. Even though each switching cycle has its own MaxEnt PMFs, there is no assurance that the long RPWM signal will obey the secondary constraints since the PMF of each parameter changes at every cycle.

Alternatively, one might consider some sampling algorithms, such as the Metropolis or Metropolis-Hastings algorithm [78], or the accept-reject algorithm [79], which deal with sampling from a pre-defined distribution, and outcomes that are not allowed, or disobey constraints, are rejected. However, these also introduce problems where rejecting an outcome simply introduces a zero probability of *that* outcome and the rest of the shape of the distribution remains the same, which effectively alters the mean (average outcome) of the distribution.

In light of such challenges, a new general approach has been developed and is described next.

6.4 A More General Solution of Conditional MaxEnt PMF

It has become evident that the difficulty lies in ensuring that the PMF obeys the primary constraints at all switching cycles. The main idea is to solve for a more general stationary joint MaxEnt PMF that ensures this. This process will be split into three main subsections described in the following manner:

- Firstly, a new joint random PWM pool from which to sample is recreated. The new joint pool is a function that takes in an index and puts out a 3 dimensional vector of T, W and Δ values.

- The new pool is then updated to obey the primary constraints, and the secondary constraints are rewritten in vector form.
- The Lagrange multipliers are lastly redefined to be in vector form as well, and the joint MaxEnt PMF is thus found.

Since this new method requires vectors representing the joint combination of T, W and Δ, the MaxEnt PMF will be derived again later to show consistency with the original derivation in Chapter 3.

6.4.1 New Joint Random PWM Pool

Since the random PWM parameters are discrete and thus finite, there is always a finite combination of the values of the parameters.

If each of the random PWM parameter pools are

$$T \in \{T_1, T_2, ..., T_i, ..., T_{N_T}\}, \tag{6.44a}$$

$$\Delta \in \{\Delta_1, \Delta_2, ..., \Delta_j, ..., \Delta_{N_\Delta}\}, \tag{6.44b}$$

$$W \in \{W_1, W_2, ..., W_r, ..., W_{N_W}\}, \tag{6.44c}$$

then consider all possible combinations of triplets of values in $\{T_i, W_r, \Delta_j\}$ that define a single pulse. All the possible combinations of triplets are

$$
\begin{aligned}
&T = T_1 : \\
&\qquad \{T_1, W_1, \Delta_1\}, \{T_1, W_1, \Delta_2\}, \ldots, \{T_1, W_1, \Delta_{N_\Delta}\}, \\
&\qquad \{T_1, W_2, \Delta_1\}, \{T_1, W_2, \Delta_2\}, \ldots, \{T_1, W_2, \Delta_{N_\Delta}\}, \\
&\qquad\quad \vdots \qquad\quad \vdots \qquad \ddots \qquad \vdots \\
&\qquad \{T_1, W_{N_W}, \Delta_1\}, \{T_1, W_{N_W}, \Delta_2\}, \ldots, \{T_1, W_{N_W}, \Delta_{N_\Delta}\}, \\
&T = T_2 : \\
&\qquad \{T_2, W_1, \Delta_1\}, \{T_2, W_1, \Delta_2\}, \ldots, \{T_2, W_1, \Delta_{N_\Delta}\}, \\
&\qquad \{T_2, W_2, \Delta_1\}, \{T_2, W_2, \Delta_2\}, \ldots, \{T_2, W_2, \Delta_{N_\Delta}\}, \\
&\qquad\quad \vdots \qquad\quad \vdots \qquad \ddots \qquad \vdots \\
&\qquad \{T_2, W_{N_W}, \Delta_1\}, \{T_2, W_{N_W}, \Delta_2\}, \ldots, \{T_2, W_{N_W}, \Delta_{N_\Delta}\}, \\
&\quad \vdots \\
&T = T_{N_T} : \\
&\qquad \{T_{N_T}, W_1, \Delta_1\}, \{T_2, W_1, \Delta_2\}, \ldots, \{T_2, W_1, \Delta_{N_\Delta}\}, \\
&\qquad \{T_{N_T}, W_2, \Delta_1\}, \{T_{N_T}, W_2, \Delta_2\}, \ldots, \{T_{N_T}, W_2, \Delta_{N_\Delta}\}, \\
&\qquad\quad \vdots \qquad\quad \vdots \qquad \ddots \qquad \vdots \\
&\qquad \{T_{N_T}, W_{N_W}, \Delta_1\}, \{T_{N_T}, W_{N_W}, \Delta_2\}, \ldots, \{T_{N_T}, W_{N_W}, \Delta_{N_\Delta}\}.
\end{aligned}
$$

Then the total combinatorial number of triplets is $N_T \times N_W \times N_\Delta$. The triplets make up a new random PWM joint pool J, consisting of all the possible triplets as its elements.

$$
\begin{aligned}
J = \Big[& \{T_1, W_1, \Delta_1\}, \{T_1, W_1, \Delta_2\}, \ldots, \{T_1, W_1, \Delta_{N_\Delta}\}, \\
& \{T_1, W_2, \Delta_1\}, \{T_1, W_2, \Delta_2\}, \ldots, \{T_1, W_2, \Delta_{N_\Delta}\}, \\
& \quad \vdots \qquad\quad \vdots \qquad \ddots \qquad \vdots \\
& \{T_1, W_{N_W}, \Delta_1\}, \{T_1, W_{N_W}, \Delta_2\}, \ldots, \{T_1, W_{N_W}, \Delta_{N_\Delta}\}, \\
& \{T_2, W_1, \Delta_1\}, \{T_2, W_1, \Delta_2\}, \ldots, \{T_2, W_1, \Delta_{N_\Delta}\}, \\
& \{T_2, W_2, \Delta_1\}, \{T_2, W_2, \Delta_2\}, \ldots, \{T_2, W_2, \Delta_{N_\Delta}\}, \\
& \quad \vdots \qquad\quad \vdots \qquad \ddots \qquad \vdots \\
& \{T_2, W_{N_W}, \Delta_1\}, \{T_2, W_{N_W}, \Delta_2\}, \ldots, \{T_2, W_{N_W}, \Delta_{N_\Delta}\}, \\
& \vdots \\
& \{T_{N_T}, W_1, \Delta_1\}, \{T_2, W_1, \Delta_2\}, \ldots, \{T_2, W_1, \Delta_{N_\Delta}\}, \\
& \{T_{N_T}, W_2, \Delta_1\}, \{T_{N_T}, W_2, \Delta_2\}, \ldots, \{T_{N_T}, W_2, \Delta_{N_\Delta}\}, \\
& \quad \vdots \qquad\quad \vdots \qquad \ddots \qquad \vdots \\
& \{T_{N_T}, W_{N_W}, \Delta_1\}, \{T_{N_T}, W_{N_W}, \Delta_2\}, \ldots, \{T_{N_T}, W_{N_W}, \Delta_{N_\Delta}\} \Big].
\end{aligned} \tag{6.45}
$$

The variable J can be viewed as a non-linear function that takes an index n as an input and produces a 3 dimensional vector $\mathbf{V}$ as

$$J_n = \mathbf{V}_{i,r,j}, \quad n = 1, 2, ..., N_J, \tag{6.46}$$

where

$$\mathbf{V}_{i,r,j} = \begin{bmatrix} T_i \\ W_r \\ \Delta_j \end{bmatrix}, \tag{6.47}$$

and $N_J = N_T \times N_W \times N_\Delta$. The index n corresponds to some combination of i, r, j. Note that by considering J only, the joint random PWM has been reduced from a four-dimensional problem (three inputs, one output) to a two-dimensional problem. Thus the associated PMF will also be a two-dimensional PMF.

6.4.2 Primary and Secondary Constraints

In this case, the triplets that are valid for RPWM are those that obey the primary constraints. The pool J can therefore be modified or updated based on the conditions that each triplet is suited for RPWM. The new pool will only contain triplets that obey the primary constraints. The triplet that does not satisfy the primary constraint inequality

$$\Delta_j + W_r < T_i, \tag{6.48}$$

is eliminated from the old pool. This process forms a new updated pool denoted J'. The total number of elements it possesses will be less than the original $N_T \times N_W \times N_\Delta$.

Based on the primary constraints, some combinations of i, r, j will not exist in the new updated pool. The new pool will have the triplet combinations

$$J'_n = \mathbf{V}'_{i,r,j} = \begin{bmatrix} T_i \\ W_r \\ \Delta_j \end{bmatrix}, \quad for \quad \Delta_j + W_r < T_i. \tag{6.49}$$

where n is now made to represent the index in the new pool $n = 1, 2, ..., N_{J'}$.

Next are the secondary constraints. These can be restated as

$$\sum_{n}^{N_{J'}} p^*_n J'_n = \mathbf{C}, \tag{6.50}$$

where p^*_n is the new joint MaxEnt PMF and $\mathbf{C} = [\zeta \quad \gamma \quad \alpha]^T$, a vector containing the expected average outcomes for T,W and Δ (the superscript T here represent vector transpose). Note that p^*_n is a scaler, which ensures that the vector dimensions in Equation 6.50 are consistent.

6.4.3 Solution of Lagrange Multiplier and MaxEnt PMF

Following the pattern of MaxEnt PMFs as has been previously derived, the joint MaxEnt PMF for the new pool is now stated. But a few alterations are made to accommodate J'_n that produces a 3D vector

$$p^*_n = \frac{e^{\boldsymbol{\lambda}^T J'_n}}{\sum_n^{N_{J'}} e^{\boldsymbol{\lambda}^T J'_n}}, \tag{6.51}$$

where $\boldsymbol{\lambda}^T$ is the transpose of a 3D column vector of Lagrange multipliers

$$\boldsymbol{\lambda} = \begin{bmatrix} \lambda_1 \\ \lambda_2 \\ \lambda_3 \end{bmatrix}. \tag{6.52}$$

The joint MaxEnt PMF in Equation 6.51 has been stated without assurance that it is consistent with the original derivations. The derivation follows in the next subsection. However, at this stage, a few things are worth noting from Equation 6.51. The MaxEnt PMF remains a scaler, so that the likelihood of selecting a certain triplet $\{T_i, W_r, \Delta_j\}$, identifiable by n, only has a single probability, which invariably is the idea behind a multivariate joint probability distribution. Additionally, by reducing the multivariate case to a univariate solution, obeying the primary constraints was simplified.

This approach is more generalised and, as a result, if required, it can be applied to single parameter randomisations.

6.4.4 Derivation of the New Joint MaxEnt PMF Formula

The entropy of probability is

$$H[p_n] = \sum_{n}^{N_{J'}} p_n \log p_n. \tag{6.53}$$

A MaxEnt probability distribution is required such that the following is satisfied

$$\sum_{n}^{N_{J'}} p_n J'_n = \mathbf{C}, \tag{6.54}$$

and the normalisation condition

$$\sum_{n}^{N_{J'}} p_n = 1. \tag{6.55}$$

Similar to Chapter 3 the method of Lagrange is applied, except in this case, the first Lagrange multiplier is introduced as a column vector $\boldsymbol{\lambda}$ with the same dimensions as $\mathbf{V}'$, but inserted as the transpose $\boldsymbol{\lambda}^T$,

$$L = -\sum_{n}^{N_{J'}} p_n \log p_n - \alpha \sum_{n}^{N_{J'}} p_n - \sum_{n}^{N_{J'}} p_n \boldsymbol{\lambda}^T J'_n \tag{6.56}$$

Since J'_n produces the vector $\mathbf{V}'_{i,r,j}$, the product of $\boldsymbol{\lambda}^T$ and the vector $\mathbf{V}'_{i,r,j}$ results in a scaler, and thus the dimensions for Equation 6.56 are consistent. Lastly, the canonical distribution is found in the exact same procedure as previously discussed in Chapter 3.

$$\delta L = -\sum_{n}^{N_{J'}} \Big(\log p_n + 1 + \alpha + \boldsymbol{\lambda}^T J'_n \Big) \partial p_n = 0. \tag{6.57}$$

Solving the above equation results in the MaxEnt probability distribution

$$p_n^* = e^{-(\lambda_0 + \boldsymbol{\lambda}^T J'_n)}, \tag{6.58}$$

where $\lambda_0 = 1 + \alpha$. Solving for the λ_0 from the normalisation constraint results in Equation 6.51.

6.5 Maximum Entropy Numerical Example

A numerical example to demonstrate the impact of these maximum entropy probability distributions on spectral spreading, is now considered. A comparison between a joint randomisation of all three versus univariate randomisation is given. The case used is as follows

Use a PWM that is meant for a 12 to 6V buck converter, with a switching frequency of 25kHz. The required duty ratio is 50%. *The secondary constraints are therefore:* $\zeta = 40\mu s$, $\gamma = 20\mu s$, *and for this example, the pulse position can be half the size of the pulse width as* $\alpha = 10\mu s$ *(For convenience, if* Δ *is not random, it can be kept at* 0[1]).

The available limited pool is

$$T \in \{8, 20, 25, 40, 50\}\mu s, \tag{6.59a}$$

$$\Delta \in \{8, 20, 25, 40, 50\}\mu s, \tag{6.59b}$$

$$W \in \{8, 20, 25, 40, 50\}\mu s. \tag{6.59c}$$

Similar to Chapter 5, these values were carefully picked to minimise the effect of spectral leakage for the purpose of this analysis. In addition, since randomisation of T and W also varies the duty ratio, it implies that the duty ratio will 'jump' from one value to

[1]The pulse position does not have any impact on the duty cycle (if it does not overlap into other pulses), thus designers will most likely not specify this. It does, however, affect the spreading out capabilities in the PSD provided it is randomised as has been shown in previous chapters.

another. The magnitudes of the intervals between each value in the pools of T and W were thus selected to exaggerate the effect of randomisation on the duty ratio. As will be seen, this exaggeration will be reflected by the ripple voltage in the output of the simulated DC-DC converter.

First the univariate cases (random T, given W & Δ; random W, given T & Δ; random Δ given T & W) are presented, and the trivariate randomisation of all three follows last. In each case, the random PWM signal is generated, the PSD and the constraints of each random modulation technique are analysed. This is done by observing the PWM signal plot, for primary constraints (overlapping pulses), and the DC-DC converter average output voltage for the secondary constraints. (The average output voltage is used in order to present an application perspective, the actual average values of the random parameters can be easily computed from the average output voltage and the corresponding non-random parameter).

6.5.1 Random Pulse Period

For random T only, W and Δ are fixed at $20\mu s$ and 0μ respectively. These can be used as pools with indices of 1 each.

Using Equation 6.14 as the MaxEnt PMF means the pool T must be modified to ensure primary constraints are obeyed. Therefore T' is $\{25, 40, 50\}\mu s$. All the Lagrange multiplier in this numerical example were solved using Wolfram Mathematica's `"Solve"` function. Solving the Lagrange multiplier λ_1 from Equation 6.15 replacing $T_i = T_i'$ results in $\lambda_1 = -16.2186$. The conditional MaxEnt PMF for random T is therefore

$$p^*_{i|r=1,j=1} = \frac{e^{16.2186T_i'}}{\sum_{i=1}^{3} e^{16.2186T_i'}}. \tag{6.60}$$

This distribution is plotted in Figure 6.1A. The random PWM was then generated using the MaxEnt PMF Equation 6.60, and the estimated PSD spectrum was plotted. The resulting PSD is illustrated in Figure 6.1B and Figure 6.1C. On all PSD plots, the y-axis Log(PSD)= $\log \hat{S}(f_i)$.

Evidently, the PSD has been widely spread out in comparison to the deterministic (non-random) PSD. Observe that the harmonic power has spread out, to form a continuous spectrum, consisting of some sharp 'kinks'. This illustration matches the descriptions of the PSD for a PWM with random T, described earlier in Chapter 5. It can be said that this is the maximally spread out PSD when randomising T. In other

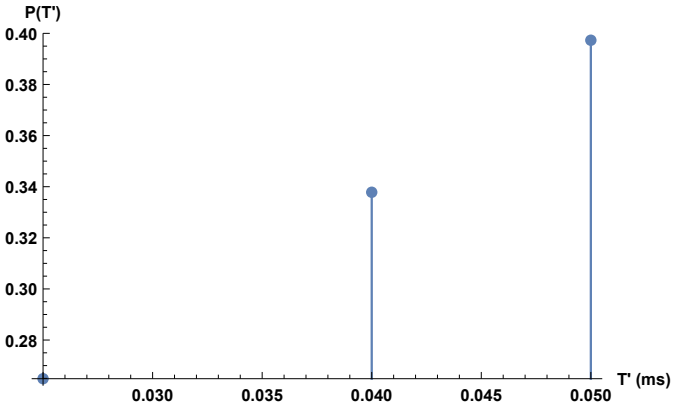

(A) MaxEnt Probabability Distribution for random T' Modulation

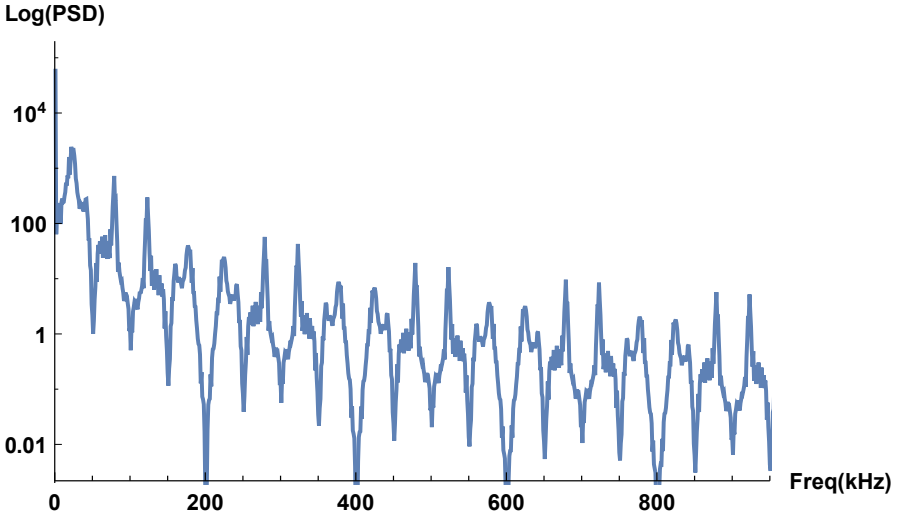

(B) PSD from conditional MaxEnt random T' Modulation

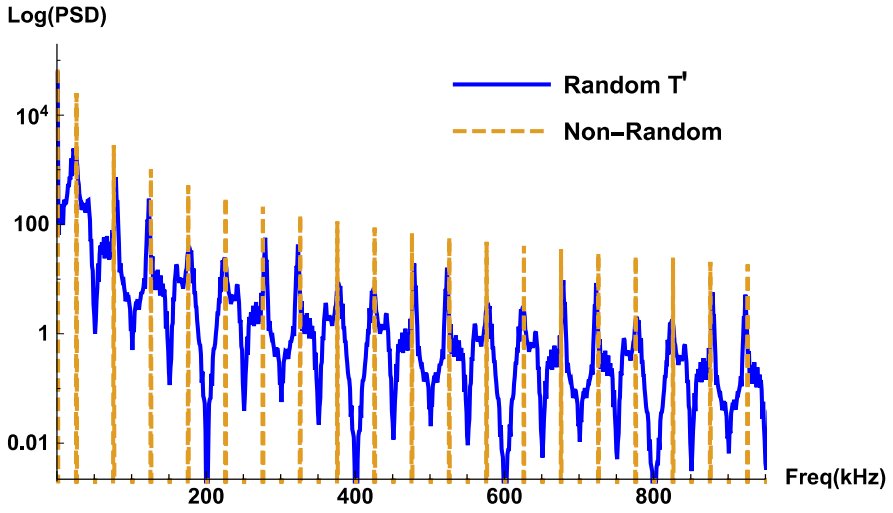

(C) PSD from conditional MaxEnt PMF random T' modulation compared to deterministic PSD

FIGURE 6.1: Showing conditional MaxEnt PMF with associated PSD for random T'

words, no other probability distribution, given the same pool and the same constraints, can spread the spectrum more than the presented one. This is loosely stated, however, since the extent to which the constraints are obeyed is still to be shown.

6.5.2 Random Pulse Width

For random W only, T and Δ are fixed at $40\mu s$ and 0μ respectively. Therefore, the updated pool W' is $\{8, 20, 25\}\mu s$. Solving the Lagrange multiplier λ_2 from Equation 6.17 results in $\lambda_2 = -51.498$. The conditional MaxEnt PMF for random W is therefore

$$p^*_{r|i=1,j=1} = \frac{e^{51.498W'_i}}{\sum_{r=1}^{3} e^{51.498W'_r}}. \tag{6.61}$$

This distribution is plotted in Figure 6.2A. The PSD resulting from the conditional MaxEnt PMF is illustrated in Figure 6.2B and Figure 6.2C.

From visual observation, the PSD is more spread out than the deterministic PSD. This case also contains the PSD features previously described in Chapter 5 where the spectrum contains both a continuous component and discrete component.

6.5.3 Random Pulse Position

For random Δ, the updated pool Δ' is $\{8, 20\}\mu s$. In this case, λ_3 results in $\lambda_3 = 134.12$. The conditional MaxEnt PMF for random Δ is therefore

$$p^*_{j|i=1,r=1} = \frac{e^{-134.12\Delta'_j}}{\sum_{j=1}^{2} e^{-134.12\Delta'_j}}. \tag{6.62}$$

This distribution is plotted in Figure 6.3A. The PSD resulting from the conditional MaxEnt PMF is illustrated in Figure 6.3B and Figure 6.3C for comparison to the deterministic case.

Again, it is evident that the PSD has been widely spread out, while containing a continuous and a discrete component.

6.5.4 All Random (Trivariate)

Following the discussed method in Section 6.4, a new pool containing a combination of all the possible triplets for $\{T, W, \Delta\}$ that characterise a pulse, must be found. This is

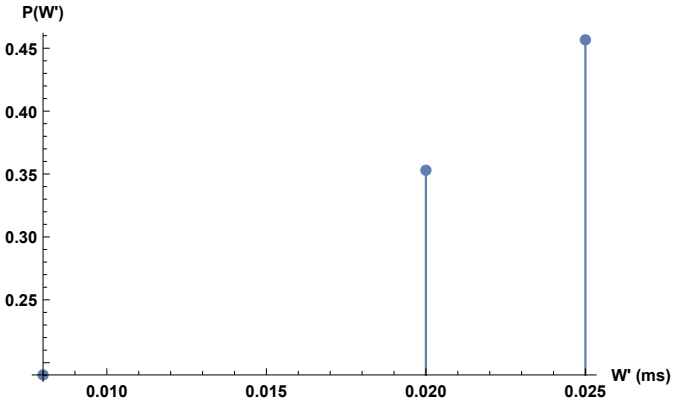

(A) Conditional MaxEnt Probability Distribution for random W'

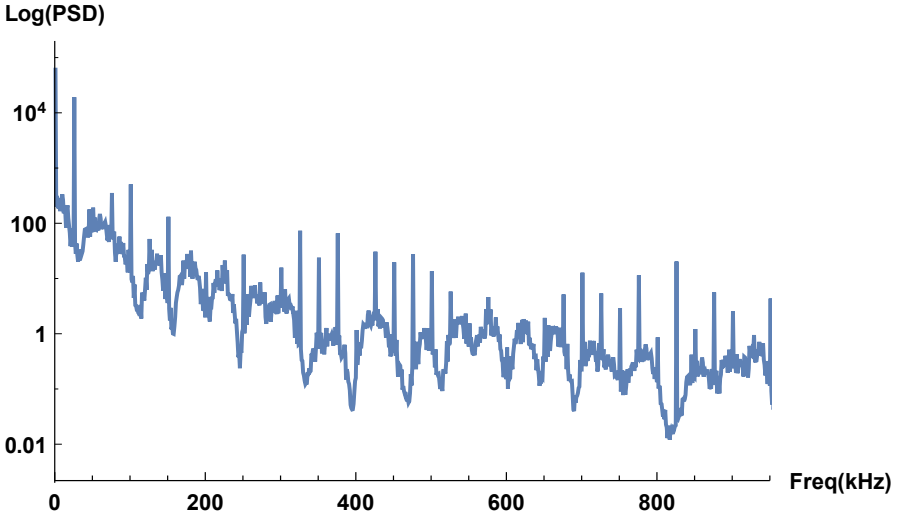

(B) PSD from conditional MaxEnt Random random W' Modulation

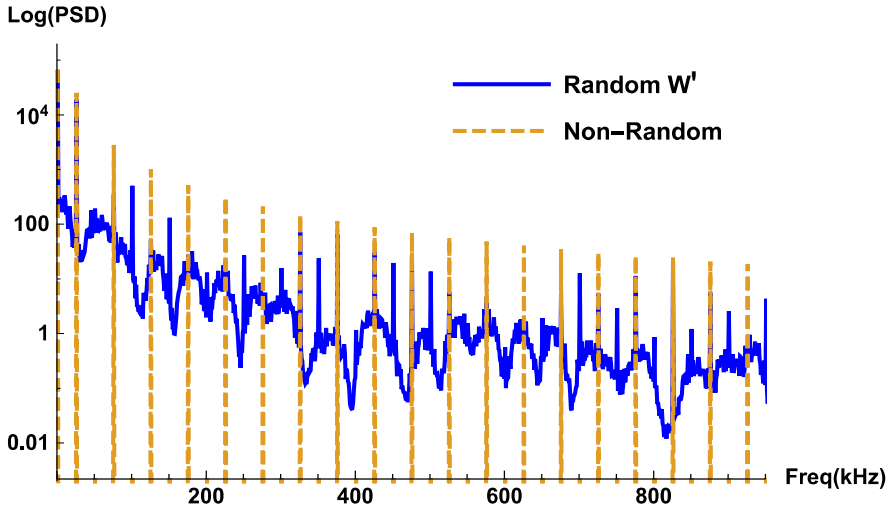

(C) PSD from MaxEnt random W' Modulation compared to deterministic PSD

FIGURE 6.2: Showing conditional MaxEnt PMF with associated PSD from random W' compared to deterministic PSD

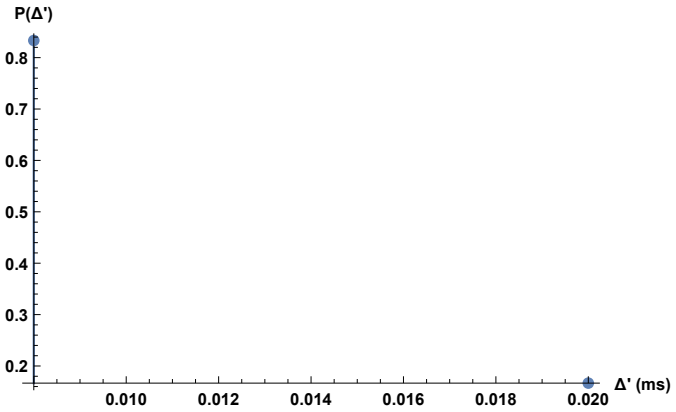

(A) Conditional MaxEnt Probability Distribution for random Δ'

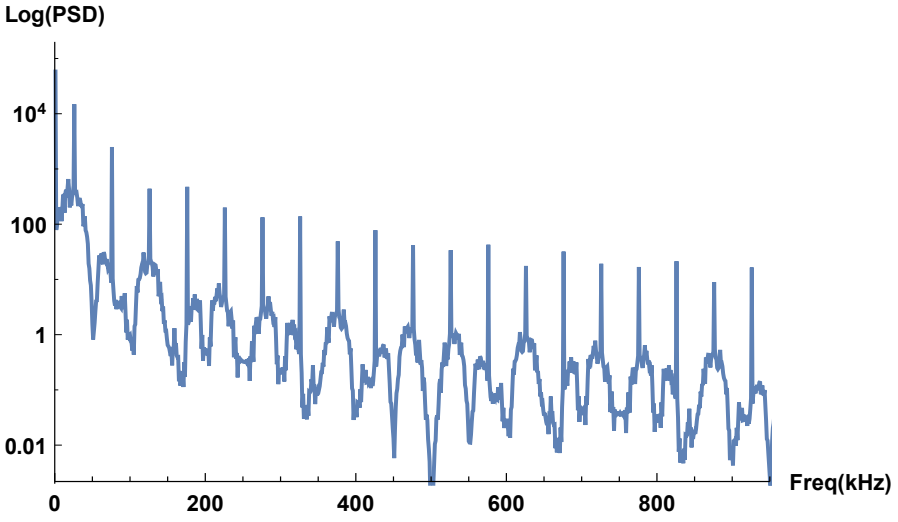

(B) PSD for conditional MaxEnt probability random Δ'.

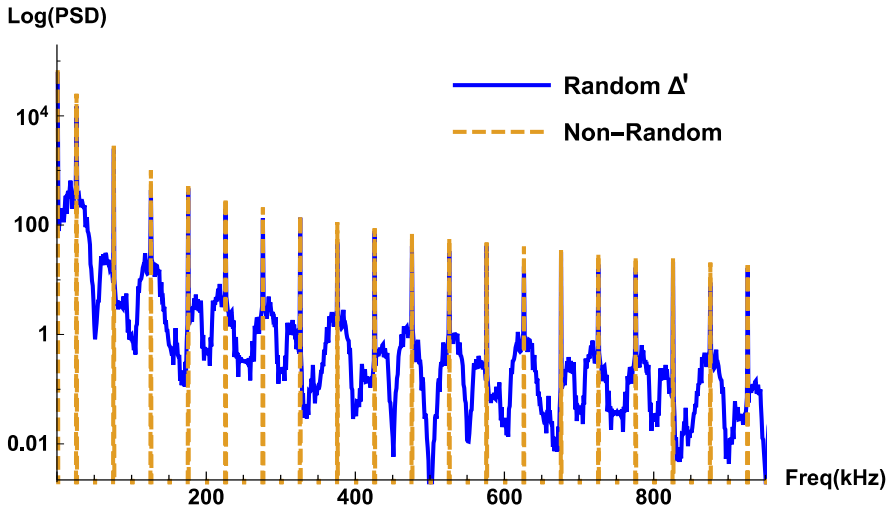

(C) PSD for MaxEnt random Δ' modulation compared to deterministic PSD.

FIGURE 6.3: Showing conditional MaxEnt PMF with associated PSD for random Δ'

computed from the entire modulation pool for each random parameter

$$T \in \{8, 20, 25, 40, 50\}\mu s, \tag{6.63a}$$

$$\Delta \in \{8, 20, 25, 40, 50\}\mu s, \tag{6.63b}$$

$$W \in \{8, 20, 25, 40, 50\}\mu s, \tag{6.63c}$$

Therefore, the pool J has $N_J = 125$, total elements of $\{T, W, \Delta\}$ triplets. These are easily computed from Matlab or Mathematica. The same applies for computing the updated pool J' that contains triplets of values that obey the primary constraints.

Due to the large size of J, only the updated pool J' is shown,

$$\begin{aligned} J' = \big[&\{20, 8, 8\}, \{25, 8, 8\}, \{40, 8, 8\}, \{40, 8, 20\}, \\ &\{40, 8, 25\}, \{40, 20, 8\}, \{40, 25, 8\}, \{50, 8, 8\}, \\ &\{50, 8, 20\}, \{50, 8, 25\}, \{50, 8, 40\}, \{50, 20, 8\}, \\ &\{50, 20, 20\}, \{50, 20, 25\}, \{50, 25, 8\}, \{50, 25, 20\}, \\ &\{50, 40, 8\}\big]. \end{aligned} \tag{6.64}$$

The total number of triplets has been reduced to $N_{J'} = 17$ elements. The joint MaxEnt PMF is,

$$p_n^* = \frac{e^{\boldsymbol{\lambda}^T J'_n}}{\sum_{n=1}^{17} e^{\boldsymbol{\lambda}^T J'_n}}. \tag{6.65}$$

The Lagrange multiplier must be solved such that the MaxEnt PMF satisfies

$$\sum_{n=1}^{17} p_n^* J'_n = \begin{bmatrix} 40 \\ 20 \\ 10 \end{bmatrix} \mu s \tag{6.66}$$

Inserting Equation 6.65 into 6.66 results in

$$\sum_{n=1}^{17} \frac{e^{\boldsymbol{\lambda}^T \mathbf{V}'_n} J'_n}{\sum_{n=1}^{17} e^{\boldsymbol{\lambda}^T \mathbf{V}'_n}} = \begin{bmatrix} 40 \\ 20 \\ 10 \end{bmatrix} \mu s. \tag{6.67}$$

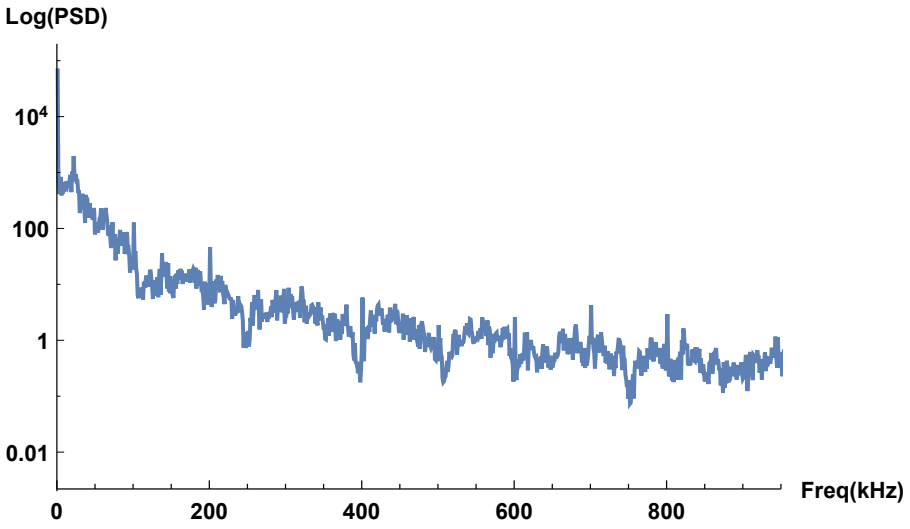

(A) PSD when randomising all three parameters

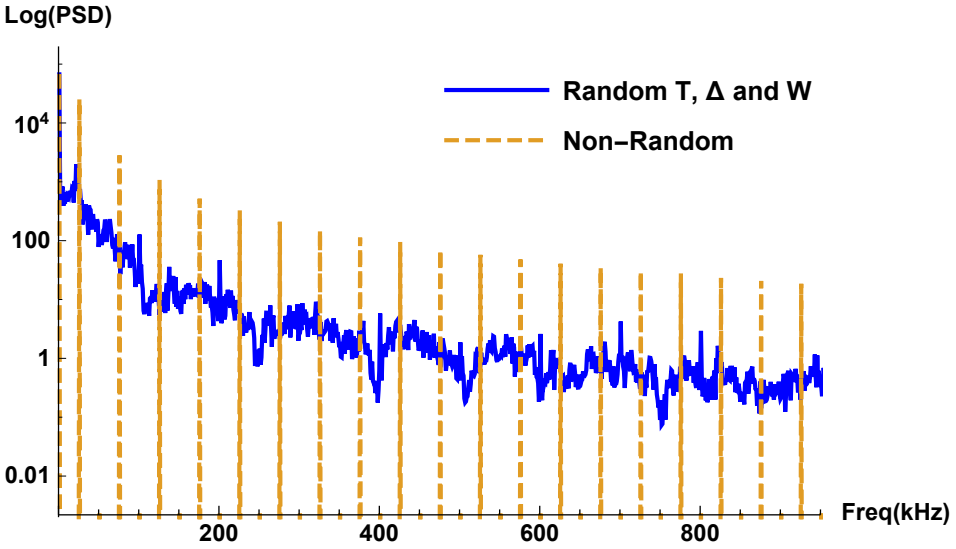

(B) PSD when randomising all three parameters compared to deterministic PSD

FIGURE 6.4: Showing conditional MaxEnt Joint Probability Distribution with associated PSD randomising pulse width, pulse period and pulse position

The above system of non-linear equations can be solved with an optimization solver in Mathematica or Matlab. The result that satisfies the equations was computed to be

$$\boldsymbol{\lambda} = \begin{bmatrix} 59.2089 \\ -57.2833 \\ 70.1512 \end{bmatrix} \tag{6.68}$$

which concludes the computation of the joint MaxEnt PMF that obeys the constraints. The PSD resulting from this PMF is plotted in Figure 6.4A and Figure 6.4B.

From visual observation, it is clear that the spectrum has been spread out more than

the spectra of the univariate cases. This is expected given that the trivariate case has more degrees of freedom, and thus higher entropy, than any of the univariate cases.

6.5.4.1 PSD Spreading Comparison

In all random cases, the spectra clearly showed an indication of spectral spreading. Next, the spectral performances are quantified and compared. These are quantified using the spectral entropy equation (Equation 5.7) from Chapter 5.

TABLE 6.1: Comparison of Spectral Entropy for random Δ, W, T and joint modulations

	Non-Random	randΔ	rand W	rand$T$	rand Δ, T, W
Spectral Ent	1.53	2.6588	2.57	4.24145	4.769

TABLE 6.2: Comparison of total average powers for Δ, W, T and joint modulations (in Watts), and difference from deterministic total power of 627427 W.

Random Strategy	Average total power	% Error
Random Δ	625024	0.40
Random W	626427	0.17
Random T	625024	0.40
Joint rand Δ, T, W	607656	3.15

From Table 6.1, the spectral entropy in the trivariate case is more than in any univariate spectral entropy. This matches with the visually observable comparison of the PSD, where the trivariate PSD appears to have been more spread out.

Since random T only possesses a continuous part, it is expected that it would be more spread out than random Δ and W. This is true when comparing the PSD plots and the spectral entropies.

Comparing the PSDs of random W and random Δ, random W appears more spread out than random Δ. However, the spectral entropies do not represent this. It is highly likely that the average total power plays a role in estimating the spectral entropy of each PSD. The Table 6.2 shows how the average total powers compare, relative to the average total power of the non-deterministic case. Given that the average total power of random W is less than that of random Δ, it is likely that this is the reason why the spectral entropy of random W is less than Δ. It is seen that even though spectral entropy agrees with what is visually observable, for a true spectral spreading measure, there needs to be a common reference point, which is the average total power. Random T and random

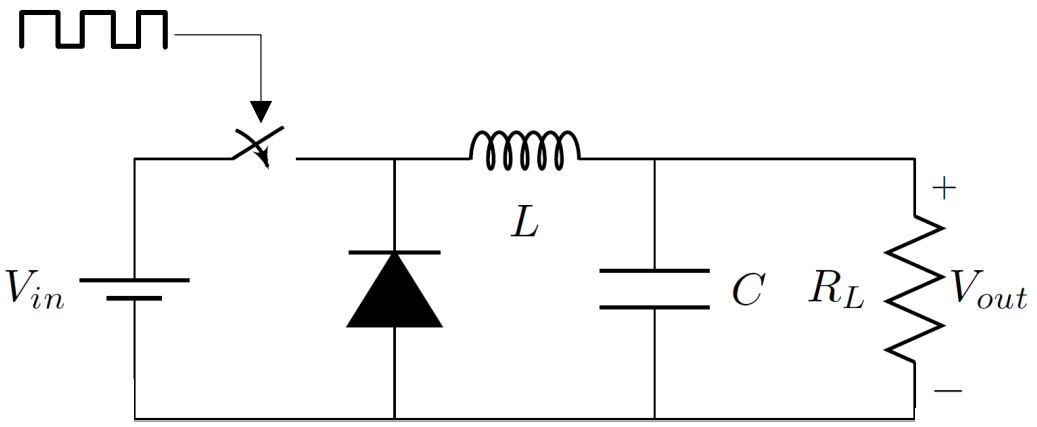

FIGURE 6.5: Buck converter model circuit

Δ both have the exam same average total power, which makes the spectral entropy comparison more credible and better reflects the true measure of spreading.

6.5.5 Impact of Conditional RPWM on DC-DC Converter

The extent to which the conditional distributions maintain the constraints is now illustrated. The three univariate random strategies are presented first, followed by the joint randomisation (trivariate) of the three. Figure 6.5 represents the model circuit used for this simulation. The output voltage of each randomisation is compared to the output voltage of 5.91 V in the deterministic case. Note that in the computation for the average output voltage, the transient part is not included.

6.5.5.1 Random Pulse Period

Figure 6.6A shows the resulting random PWM signal for conditional random modulation with the conditional pool of random T'. Needless to say that the conditional MaxEnt PMF acceptably maintains the primary constraints as indicated by the absence of overlapping or coinciding pulses. The conditional MaxEnt probabilities also acceptably obeys the secondary constraints as indicated by the average output voltage of 5.84 V. (tabulated in Table 6.3).

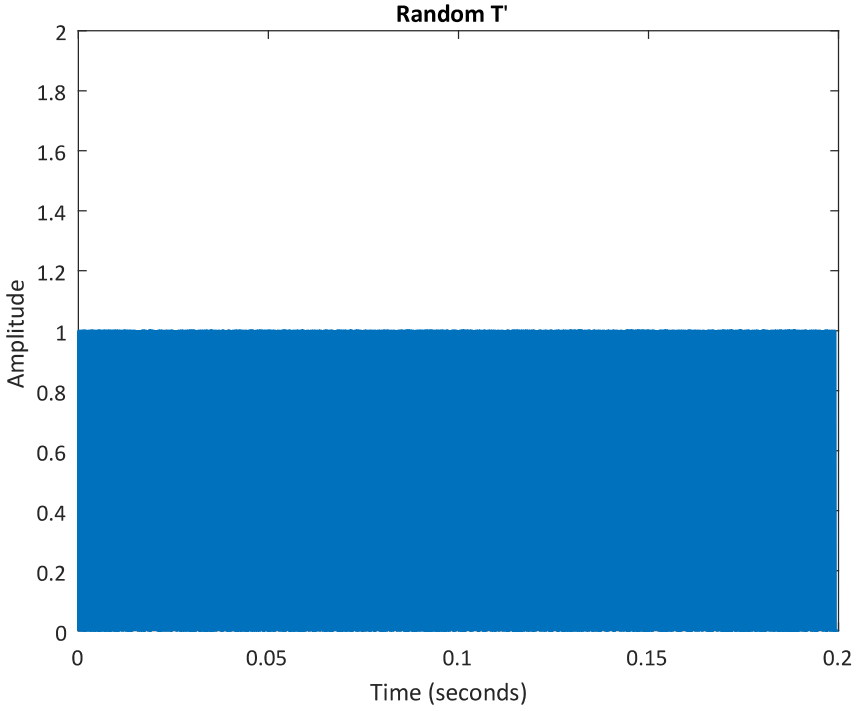

(A) PWM for conditional random T'

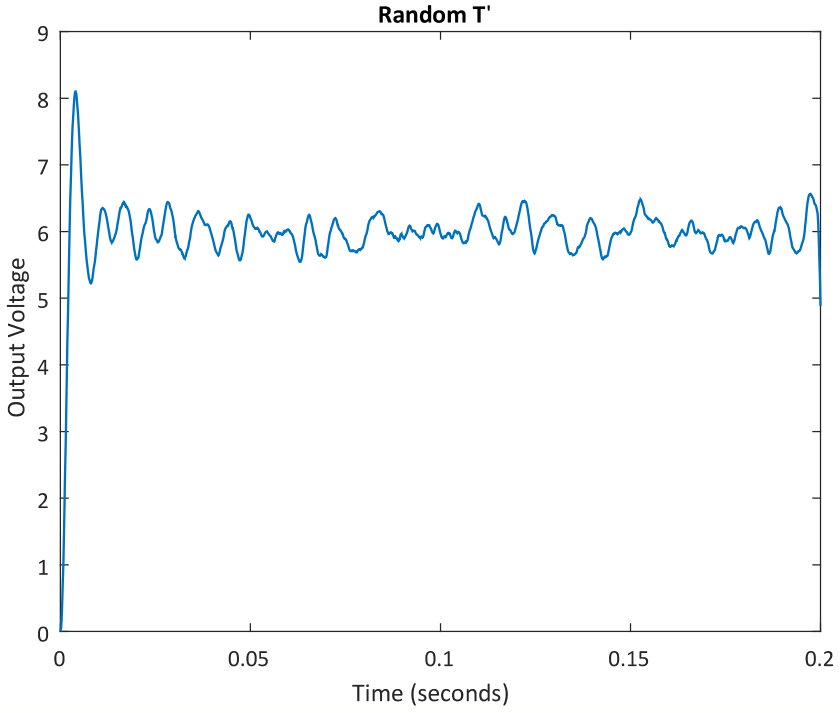

(B) Converter Output voltage conditional random T'

FIGURE 6.6: Waveforms showing RPWM impact on output voltage of a converter when using random T

6.5.5.2 Random Pulse Width

Figure 6.7A shows the resulting random PWM signal for conditional random modulation with the conditional pool of random W'. In the same way, there are no overlapping pulses, and the primary constraints are acceptably obeyed. The same can be said for the secondary constraints with the average output voltage of 5.814V.

6.5.5.3 Random Pulse Position

The random PWM signal for random Δ' is shown in Figure 6.8A. And due to the duty ratio in random Δ not being altered. Both constraints are obeyed as there are nearly no variations in the steady state output voltage of Figure 6.8B, with an average output voltage of 5.991 V.

6.5.5.4 All Random

The random PWM signal for the conditional MaxEnt joint probability is illustrated in Figure 6.9A. The resulting output voltage for this PWM signal is plotted in Figure 6.9B. It is clear also that the primary constraints are fully obeyed since there are no pulses that add up to create magnitudes higher than 1. The secondary constraints can also be said to have sufficiently been obeyed with the average output voltage of 5.9452 V.

TABLE 6.3: Comparison of average output voltages for conditional random modulations in comparison to non-random output of 5.9136 V

RPWM	output average	Error (absolute %)
Random T	6.0164	1.73
Random W	5.995	1.37
Random Δ	5.9919	1.32
All Random	5.9452	0.53

6.5.6 Remarks on Monte Carlo Simulation Results

Using conditional MaxEnt probability distribution has demonstrated the ability to obey all constraints (both primary and secondary). Thus it can be accepted that the MaxEnt PMFs maximally spread out the PSD subject to the time-domain constraints.

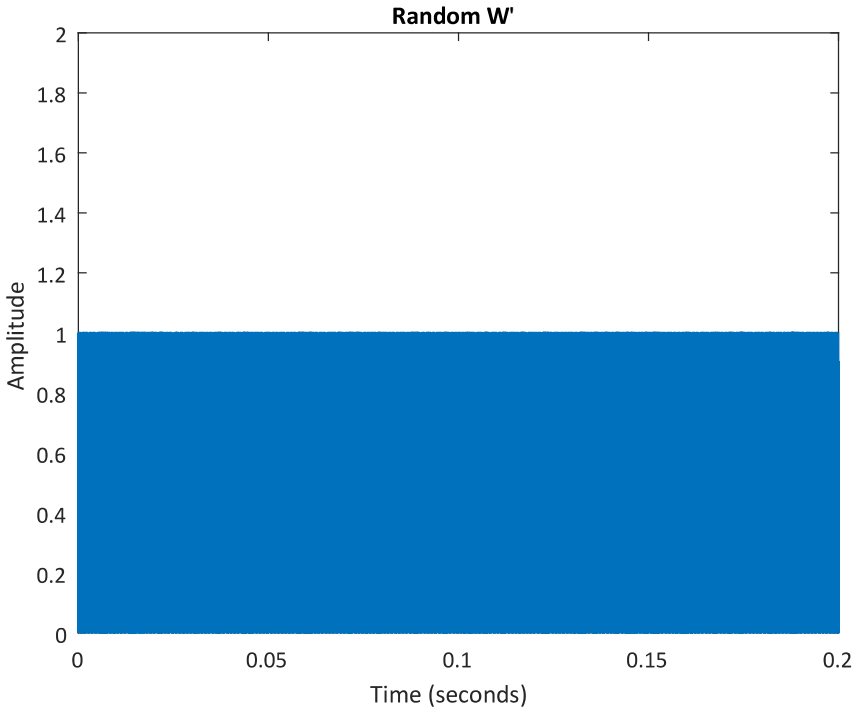

(A) PWM for Random W' conditional PMF (A line with an amplitude of more than 1 indicates the primary constraints are not obeyed. In this case, there is no indication of breaking the primary constraints.)

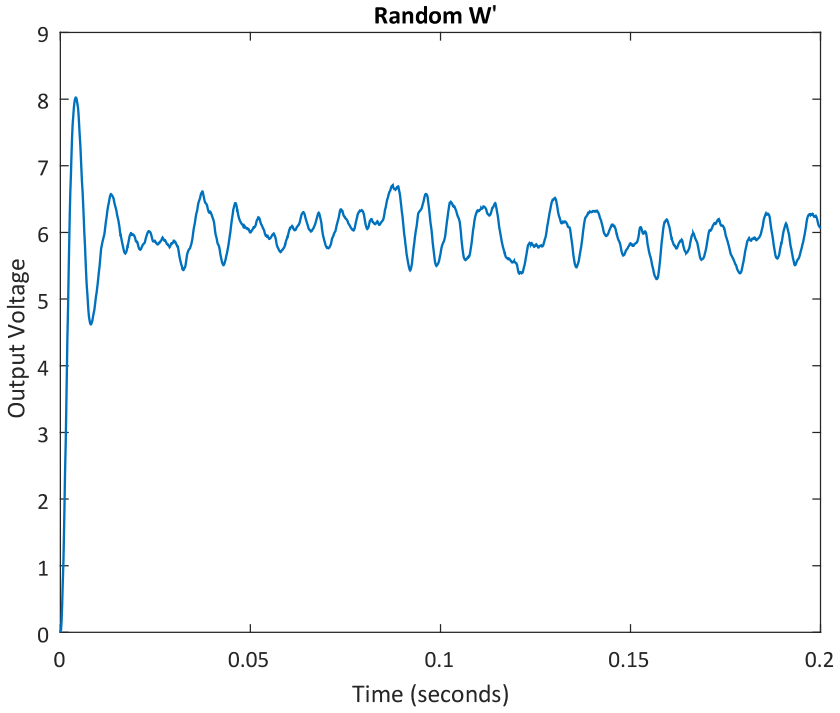

(B) Converter Output voltage Random W' conditional

FIGURE 6.7: Waveforms showing RPWM impact on output voltage of a converter when using Random $\Delta = 0\mu s$ and $T = 40\mu s$, pool $W' = \{8, 20, 25\}\mu s$

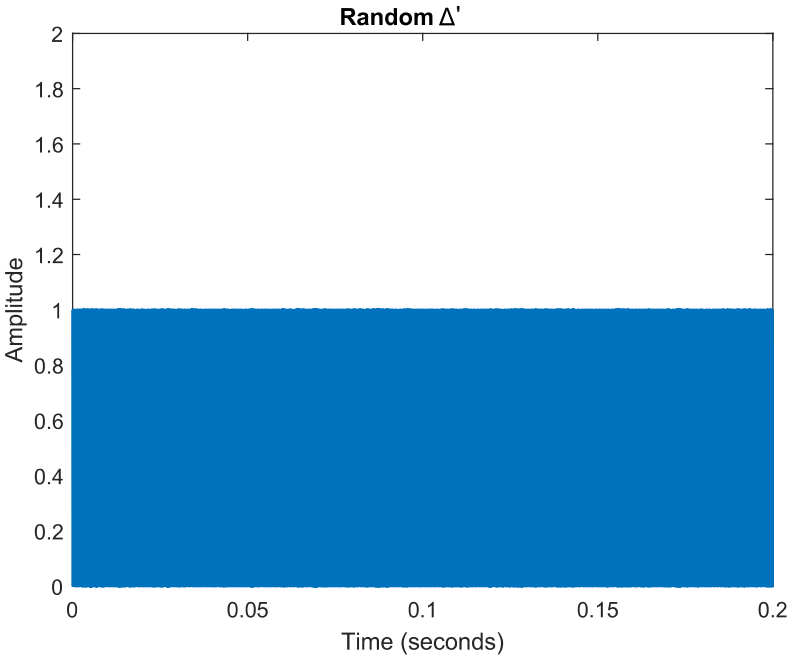

(A) PWM for random Δ' with conditional PMF

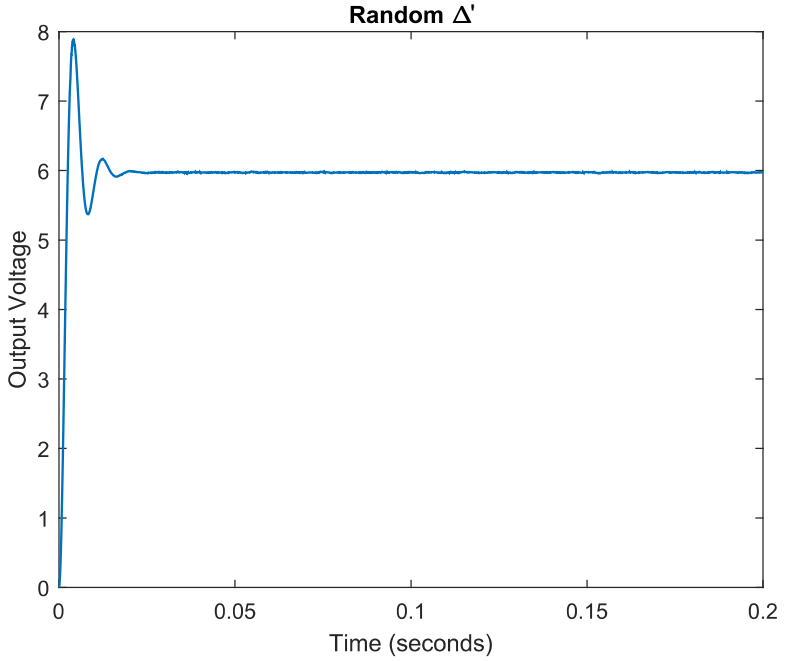

(B) Converter output voltage for Random Δ' with conditional PMF

FIGURE 6.8: Waveforms showing RPWM impact on output voltage of a converter when using random Δ with pool $\Delta' = \{8, 20\}\mu s$ constant parameters $T = 40\mu s$ and $W = 20\mu s$

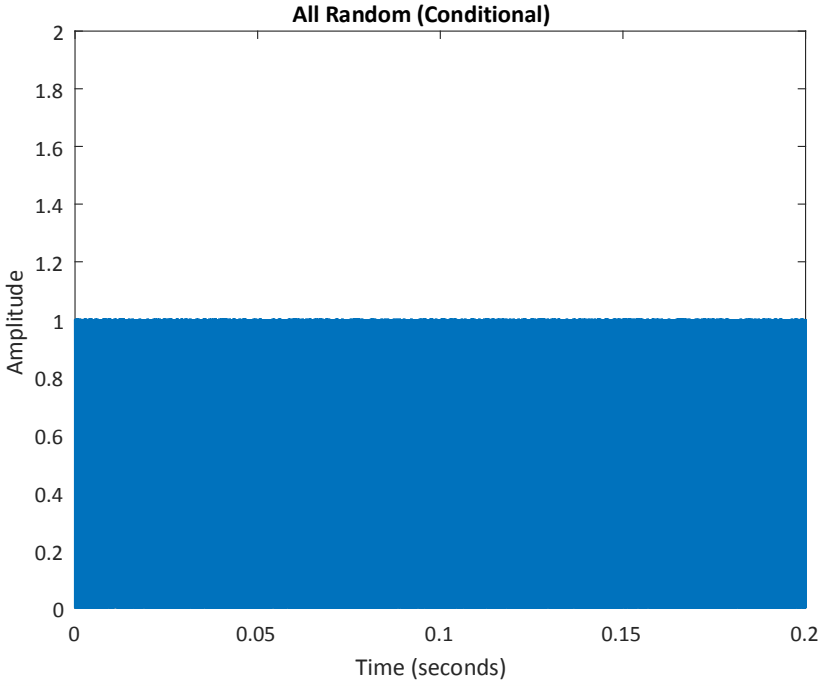

(A) PWM input for conditional PMF and joint random Δ, W and T

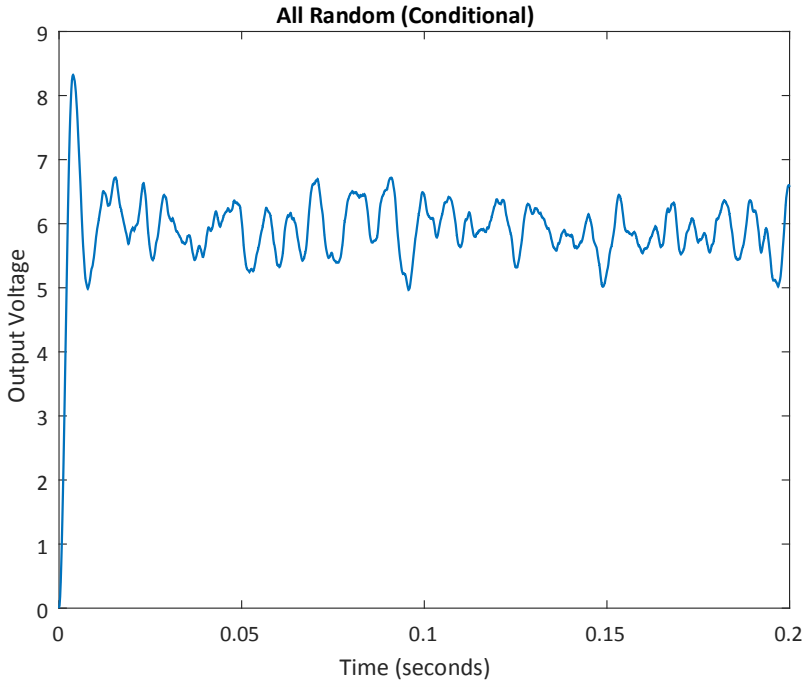

(B) PWM input for conditional PMF and joint random Δ, W and T

FIGURE 6.9: Waveforms showing RPWM impact output voltage for conditional PMF jointly Randomising Δ, W and T

The voltage ripples at the output of the converters are a an indication of the duty ratio jumping from one ratio to another. The magnitude of the jump corresponds to the variations seen However, recall that observing this phenomenon was part of the reason behind the numerical values in the random pool. In practice, the 'jumps' can be reduced by reducing the interval size between in the values the pool.

Furthermore, it should be noted that, Monte Carlo simulations are highly dependant on the number of simulation trials. Thus, the numerical results such as the percentage errors computed, could easily be improved by increasing the simulation trials to extreme numbers. However, the simulation trials in this dissertation where kept to an acceptable number for demonstrating the application of MaxEnt PMFs.

6.6 Impact of Secondary Constraints on Maximum Entropy

Through-out all the given numerical results, the secondary constraints had been fixed. It would be beneficial to investigate how fixing the pool, and computing the MaxEnt PMFs with varying levels/strengths of secondary constraints impact spectral entropy. The objective in this section is to provide a consolidated overview of the limitations of spectral spreading using MaxEnt probabilities, as well as the trade-offs that are associated with these constraints.

The magnitudes of ζ, γ and α are gradually increased from minimum allowable to maximum allowable values respectively. The parameters that are fixed were adjusted so that the primary constraints are always obeyed. Plotting ζ versus λ_1, γ versus λ_2 and α versus λ_3, results in a plot indicating all the allowable constraints. Varying the constraints changes the value of the Lagrange multipliers. This then changes the MaxEnt value of the resulting PMF, which when used to generate a RPWM signal, affects the maximal spreading in the PSD.

6.6.1 Random Pulse Period

Figure 6.10A is a plot of the average values of T (or ζ) for the whole pool $T = \{8, 20, 25, 40, 50\}\mu s$ as a function of λ_1 (Equation 6.69 below). Observe that as λ_1 increases, the value of ζ asymptotically approaches $8\mu s$, and when λ_2 decreases, the value of ζ asymptomatically reaches $50\mu s$. At both these extreme points, the Lagrange

multiplier approaches $\pm\infty$. Therefore, if the value of the Lagrange multiplier is substituted into the MaxEnt probability formula for random T (Equation 6.14), then the resulting PMF approaches deterministic probability.

$$\frac{\sum_{i=1}^{5} e^{-\lambda_1 T_i} T_i}{\sum_{i=1}^{5} e^{-\lambda_1 T_i}} = \zeta. \tag{6.69}$$

At the point with the red-dot, $\zeta = 0.286\mu s$. At this point $\lambda_1 = 0$. This corresponds to a uniform probability distribution. Ultimately this curve shows what can be perceived as different strengths of secondary constraints. The extreme ends $\zeta \to 08\mu s$ and $\zeta \to 50\mu s$ are points with strongest constraints, as they result in determinism PMF, which means no randomisation and an probability entropy of 0. And the midpoint at $\zeta = 0.286\mu$ is a point of the 'weakest' constraint as the resulting PMF is a uniform distribution, which is the 'most' random PMF with the highest entropy.

Now Figure 6.10B was plotted by varying the value of ζ, solving for the corresponding value of λ_1 and inserting the resulting value into the MaxEnt PMF formula for random T. The resulting PMF is then used to generate a random PWM signal, and the associated spectral entropy is estimated. i.e. the vertical axis of Figure 6.10A is the horizontal axis in Figure 6.10B.

The curve plotted in orange shows different maximum spectral entropies as determined by the average outcome of T. In other words, the curve is an indication of how maximum spectral entropy changes when the constraints change from the strongest constraints to the weakest constraints.

Considering this, it can be said that for random T, as the MaxEnt probability moves from deterministic to uniform (which is the turning point of the blue curve), then the spectral entropy also increases accordingly. Which is an expected relationship. But the blue curve indicates that probability entropy is not unique to one distribution because of its parabolic shape. This shows that multiple distributions can result in the same spectral entropy.

6.6.1.1 Random Pulse Width

The Equation 6.70 for random W is plotted in Figure 6.11A, and the corresponding spectral entropy curve is in Figure 6.11B. In this case, the spectral entropy curve shows no correlation to the probability entropy curve in blue. This is obviously due to the increasing average of W, that results from the changing average total power. This

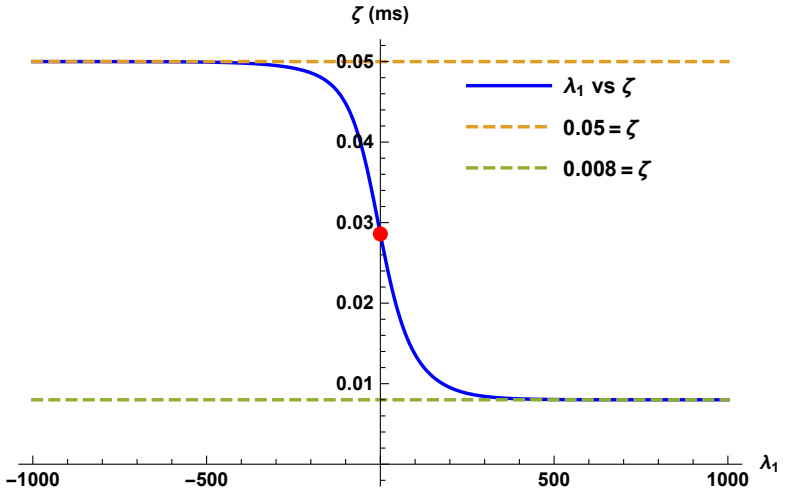

(A) Lagrange Multiplier versus allowable averages for Random T

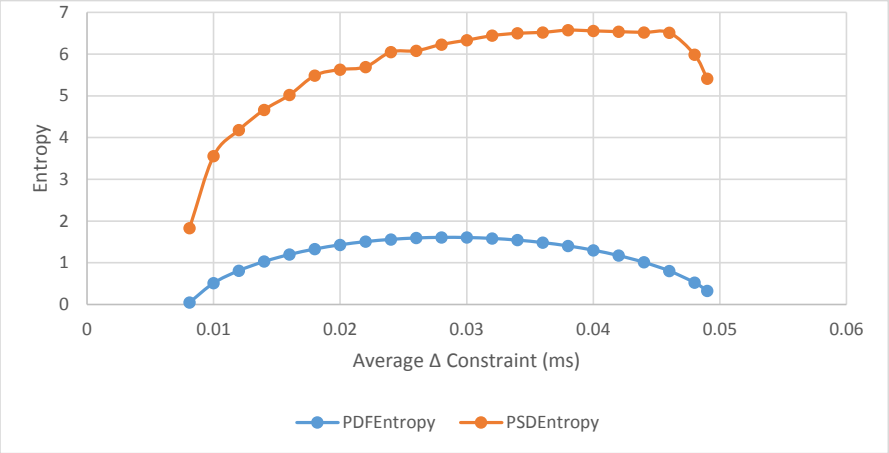

(B) Lagrange Multiplier versus constraints/allowable averages

FIGURE 6.10: Showing how Secondary Constrains (average values) impact the entropy or the spreading out capabilities of the PSD for Random T

then causes the spectral entropy calculation result to decrease, since spectral entropy is inversely proportional to the total power average.

$$\frac{\sum_{r=1}^{5} e^{-\lambda_2 W_r} W_r}{\sum_{r=1}^{5} e^{-\lambda_2 W_r}} = \gamma \tag{6.70}$$

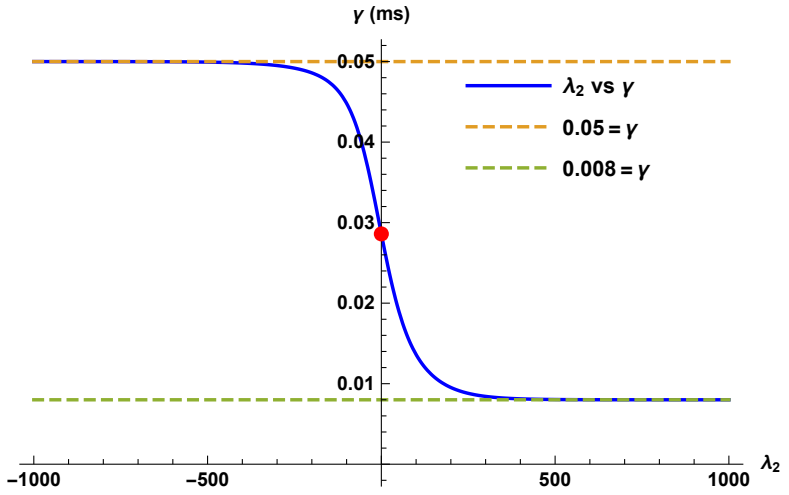

(A) Lagrange Multiplier versus allowable averages

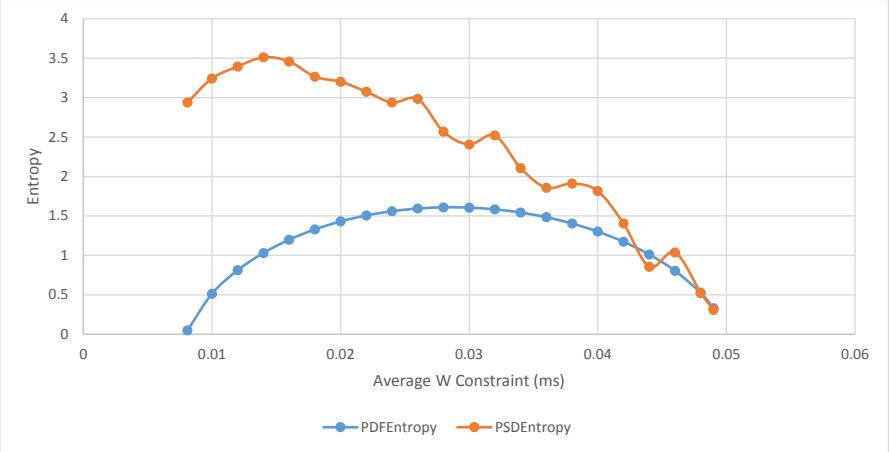

(B) Lagrange Multiplier versus constraints/allowable averages RPW Modulation

FIGURE 6.11: Showing how constrains (average values) impact the entropy or the spreading out capabilities of the PSD for Random W

6.6.1.2 Random Pulse Position

In the case of random pulse position, the relationship between the PMF maximum entropy and PSD entropy Figure 6.11B show a correlation, since, similar to random T the average total power is unaffected.

$$\frac{\sum_{j=1}^{5} e^{-\lambda_3 \Delta_j} \Delta_j}{\sum_{j=1}^{5} e^{-\lambda_3 \Delta_j}} = \alpha \tag{6.71}$$

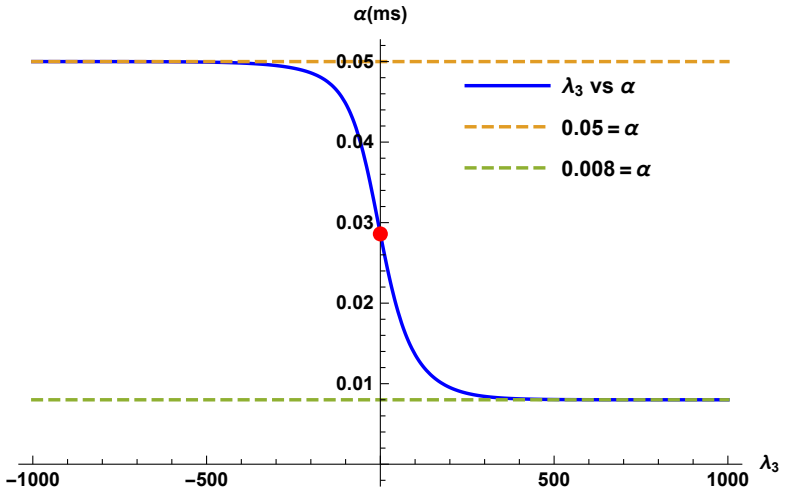

(A) Lagrange Multiplier versus constraints/allowable averages for Random Δ

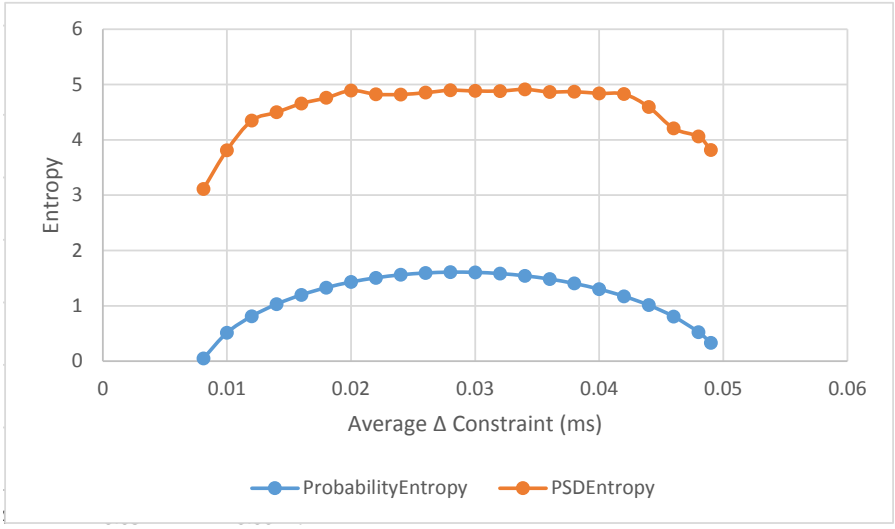

(B) Lagrange Multiplier versus constraints/allowable averages

FIGURE 6.12: Showing how constrains (average values) impact the entropy or the spreading out capabilities of the PSD for Random Δ

6.6.2 Constraints and Spreading out Trade-offs

The most important conclusion that can be made from the given plots is that, as the constraints become 'strong' the PMF approaches deterministic PMF, i.e. no randomisation. This results in a deterministic PSD even though, according to the relationship between spreading in the PMF and PSD, is a maximally spread PSD.

And as the constraints become 'weak', the PMF becomes a uniform distribution. At This point, the PSD is maximally spread out. This is a clear indication of the trade-off

between spectral spreading and the strengths of secondary constraints.

With a fixed pool, any distribution that meets the specified constraints is the most spread out possible, and when applied to RPWM, leading to the most spread out spectrum - possible.

Another important factor is that the spreading in the PMFs and the PSDs are not a one-to-one mapping.

It can then be concluded that, under the assumption of a limited pool, the main limiting factors to spectral spreading are the time domain constraints specified for the random PWM to follow in order to produce a certain output voltage in a DC-DC converter. Nevertheless, MaxEnt probabilities, can result in maximally spread out PSD, given those constraints.

6.7 Conclusion

This chapter has presented three important discussions. Firstly, the method for computing MaxEnt PMFs for univariate and trivariate randomisations was presented. In each case, the MaxEnt PMFs were computed in general and the condition through which the primary and secondary constraints were obeyed were presented. Secondly, the MaxEnt PMFs were used to demonstrate their impact on spreading the harmonic power in the PSD of univariate and trivariate cases, as well as the extent to which the time-domain constraints were obeyed. From this, it was concluded that, given that the constraints are sufficiently obeyed, then the MaxEnt PMFs truly maximally spread out the PSD while obeying random PWM constraints. The spectral entropy measure for spectral spreading was used to compare the extent to which the PSDs are spread. It was shown to sufficiently represent the visually observable spread-spectrum effects. However, the reliability of this measure relies on having a common average total power for each random strategy. Or at least, average total powers that are close enough, since the closer these are, the better the representation of spreading. Lastly the strengths (from weak to strong) of secondary constraints were explored in order to determine the limitations of maximal harmonic spreading. This was done by changing the magnitude of the expected average outcome for each randomisation strategy. From this, it was found that the main limitation that prevents the PSD from spreading any further, are the secondary constraints that are typically specified for DC-DC conversion.

Chapter 7

Conclusions and Recommendations

7.1 Conclusions

In this research, a method that uses maximum entropy probability distributions to maximally spread out harmonic power in the power density spectrum of a random PWM signal was developed. The major benefit the reduction of high amplitude harmonics that cause conducted EMI in DC-DC converters. The developed method allows for the use of a random PWM signal that maximally spreads out harmonic power, thereby reducing high amplitude harmonics, yet maintaining the time-domain constraints associated with PWM signals.

The research question was stated as "What is the relationship between spreading out of probability and spreading out of the power density spectrum of a random PWM signal? To what extent do maximum entropy probability distributions of random PWM, subject to constraints, result in a maximally spread out PSD?". A number of means were taken in order to answer the research question.

In order to measure the extent to which probabilities in general, spread out the harmonic power in the PSD, it was necessary to introduce a reasonably reliable measure of spreading in the PSD. The concept of spectral entropy was then presented as a proper measure of spreading out and spectral performance, provided the average total power of the random PWM signal is not significantly affected by the randomisation.

The random PWM signal was then characterised by PMFs, that describe the randomisation of the three fundamental PWM parameters: Pulse Width, Pulse Period, and Pulse Position. This allowed for generally describing the random PWM in terms of randomisation of the three parameters, given a pool of possible values that the parameters could take.

The relationship between probability spreading and spectral spreading had to be established, before maximum entropy could be employed. Given that probability entropy and spectral entropy had been accepted as a proper measures of probability and spectral spreading respectively, the relationship between the two could be established. This allowed for the investigation of how the spreading out of probability results in spreading out in the power density spectrum of a random PWM signal. Through a rigorous argument, the conclusion that, on average, there exists an increasing monotonic relationship between spectral entropy (spectral spreading) and probability entropy (probability spreading), was established.

This then means that, if one maximally spreads the probability distribution, given some constraints, then the resulting power density spectrum is also a maximally spread out one. This gave way for the use of the Method of Maximum Entropy probabilities for maximally spreading the power density spectrum, given time-domain constraints. A DC-DC simulated buck converter was then used to illustrate how maximum entropy probabilities are solved, given constraints, and applied to RPWM signal.

Since now the ability to obtain a maximally spread out power density spectrum was developed, the research question could then be answered in full. By changing the random PWM time-domain constraints, and keeping a limited and fixed random PWM pool, the limitations to spectral spreading could be pointed out. From this, it was found that the main limitation that prevents the PSD from spreading any further, are the secondary constraints that are typically specified for DC-DC conversion.

The contributions that came as a result of the process of answering the research question are:

- A framework for measuring the impact of probability distributions on PSD of a RPWM signal. This framework is based on the entropy of the PMFs and spectral entropy, which quantifies the spreading in both.
- The relationship between spreading out of probability and spreading out of harmonic power in the PSD of a RPWM signal. This relationship was found to be that

spreading out in probability of RPWM causes more spectral spreading, and that there is – on average – an increasing monotonic relationship between the spreading out probability and spreading out in the PSD.

- A method for maximally spreading PSD given time-domain RPWM constraints. Which is the use of Maximum Entropy PMFs for RPWM parameters. A method that can be employed by designers requiring to maximally spread out RPWM PSDs to reduce conducted EMI, while maintaining DC-DC time domain converter constraints.

- Illustration of factors that limit spreading out of harmonic power in the PSD of RPWM signals. These are the time-domain constraints, where strong constraints reduce spectral spreading even when using MaxEnt PMFs. Knowledge of these factors open up an opportunity to create more custom designed RPWM techniques given limited resources, that also make use of the MaxEnt PMFs.

- A method for jointly randomizing all three parameters that describe a random PWM signal while maintaining timed-main constraints.

Overall, this dissertation provided a further understanding and framework on how the PMFs of RPWM techniques relate to time-domain constraints of a DC-DC converter and the PSD.

7.1.1 Future Recommendations

The relationship between spectral spreading and probability spreading was argued for using simulated data and some analytical arguments. A further step that could be explored is the development of an analytical proof of this relationship. This would result in a closed-form solution where, given the entropy of probability and some constraints, the spectral entropy can be mapped. A closed-form solution presents an opportunity to map this relation.

Unlike randomising W and T, randomising the pulse width W presented problems when comparing the spectral entropies, as randomising W without ensuring that the average W is constrained, makes the resulting spectrum entropy an inaccurate measure of the spreading. Concepts such as relative entropy can be revisited in order to establish a better measure between different spectra with different features.

On the same topic, relative entropy may be worth investigating in order to reinforce how spectral performance is measured. For example, an ideal spectral spreading reference point could be established so that all possible spectra of RPWM signals can be compared against the ideal spectral entropy measure.

One of the important time-domain constraints that has not been included is the output ripple voltage of a DC-DC converter. This quantity is largely affected by how randomly choosing a value for T , or W results in the duty ratio jumping from one value to another. Thus, by adding the ripple voltage as one of the time-domain constraints, the maximum entropy probability could result in a reduced ripple voltage without having to change the values in the random modulation pool.

Lastly, the general method for obtaining MaxEnt PMFs that was presented using trivariate randomisation case could be improved. The presented method is procedural. It would be of great benefit to explore the possibility of obtaining a more generalized method using continuous probability distributions and as well eliminate the need for a discrete perspective. This would also reduce procedural steps such as eliminating elements that disobey constraints, to a continuous equation that handles primary constraints.

Appendix A

A.1 MODEL PROBLEM

The intention of this model problem is to provide intuition to the research problem presented in this the dissertation. It thus models the process of analysing a random PWM signal in both the time-domain and frequency domain. However, in this case, the random PWM is replaced by a simple sinusoid that has a hopping frequency. The frequency that the signal 'hops' to is chosen at random (at fixed intervals) from a predetermined probability distribution. In other words, the probability distribution governs the likelihood of choosing a particular frequency from a range of possible frequencies. Once the signal is generated, its power density spectrum (PSD) is computed and plotted. The PSD is also approximated analytically given the probability distribution function of the random frequencies.

A.1.1 Frequency Hopping

A simple sinusoid $s(t)$ has an amplitude A and a frequency ω_o as given

$$s = A\sin(\omega_0 t) \tag{A.1}$$

If the frequency w_0 is fixed, the Fourier Transform $S(\omega)$ can be determined and plot its magnitude and frequency spectra. We know that the spectrum is a Dirac delta function weighted at A at the frequencies $-\omega_0$ and ω_0.

Now if the frequency periodically changes after some fixed period $t = k\tau$ $(k = 0, 1, 2\ldots)$, then the signal has a frequency that 'hops' from one frequency to another.

If the frequency that the signal will hop to is uncertain, then it can be represented by a probability distribution.

We then ask *what is the frequency spectrum of this signal $s(t)$ given that ω_0 is uncertain? And how does the probability distribution of ω impact this frequency spectrum?*

In order to answer this question we consider finding a model that can link probability distribution to the frequency spectrum. This will allow us to understand the relationship and even predict the power density spectrum from the probability distribution.

A.1.2 Finding Frequency Spectrum of a Random Frequency Sine Wave

The frequencies are chosen at random and at fixed time intervals. The time stamps (in seconds) of these intervals are $t = k\tau$ where $k \in \mathbb{Z}$ and τ is the hopping time interval in seconds. One can think of this experiment in the following way; a dice is rolled at every time τ seconds (say each side of the dice maps to a specified frequency), the outcome of this dice determines the frequency that the signal will have. The signal will posses this frequency for a period of τ seconds. Afterwards, the dice is rolled again, and the outcome determines the next frequency. We define the signal as

$$s(t) = \sum_{k=0}^{N} A \sin\left(W\left(t - kT\right)\right) \operatorname{rect}\left(\frac{t - \frac{T}{2} - k\tau}{T}\right) \tag{A.2}$$

where W is a random radial frequency variable with the possible values

$$W \in \{\omega_1, \omega_2, \ldots, \omega_n\} \tag{A.3}$$

Thus W is randomly selected for every time $t = k\tau$ with a probability distribution $\Pr(W|K)$ (K some prior scope or knowledge). In the case of rolling a dice, the weight of each side of the dice is still to be determined. T is the width of the rectangular pulse. The signal $s(t)$ has the following constraints.

1. The possible frequencies in (A.3) must be integer multiples of the least 'hopping' frequency $2\pi/\tau$.
2. τ must be greater than all the possible periods of the sine wave (i.e. hopping frequency must be smaller or equal to the possible frequencies)
3. $N\tau \leq t_f$, i.e. the sum all of the sine wave portions must fit in the time of observation t_f

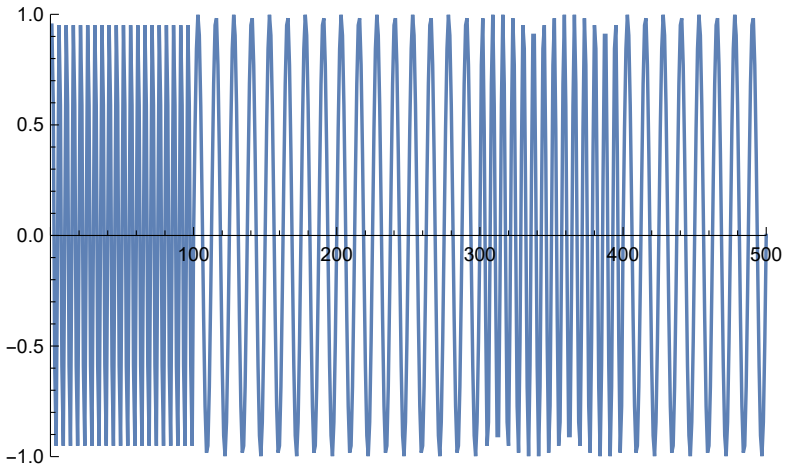

FIGURE A.1: An example of a sine wave with randomly varied frequencies

Constraint 1 ensures that the consecutive sine waves have zero phase shift. This allows a 'smoother' transition to another frequency. Constraint 2 follows from constraint 1, it allows the sine to always have a complete period/cycle of 2π. Figure A.1 shows an example of this signal. Note that the magnitudes of each window varies due to the different frequencies in each window, the sampling frequency 'misses' some peaks. This could obviously be avoided via coherent sampling (see 5.4.4.3). This is easily reflected by the PSD plots containing some spectral leakage. However, this was left as is to limit the complexity in the model problem. The actual magnitude of all the peaks is 1. Since $s(t)$ is a stochastic process, what is required is the Fourier transform of the Expected value of $s(t)$.

We know from the product rule that the joint distribution of s and W is

$$\Pr(s, W \mid K) = \Pr(s \mid W, K)\ \Pr(W|K) \tag{A.4}$$

The variable K also includes the time dependency.

If we can marginalize over all W, then we can obtain the probability distribution of s that is not conditional on W as shown below.

$$\Pr(s \mid K) = \sum_{W} \Pr(s, W \mid K) \tag{A.5}$$

If W is known or given, then the probability distribution of s is the probability modelled by a dirac delta function δ:

$$\Pr\left(s \mid W, K\right) = \delta\left(s - \sum_{k=0}^{N} A\sin\left(W\left(t - kT\right)\right)\operatorname{rect}\left(\frac{t - \frac{T}{2} - k\tau}{T}\right)\right) \tag{A.6}$$

Substituting equation (A.6) into (A.5) gives

$$\Pr(s|K) = \sum_{W}\Pr(W|K)\delta\left(s - \sum_{k=0}^{N} A\sin\left(W\left(t - kT\right)\right)\operatorname{rect}\left(\frac{t - \frac{T}{2} - k\tau}{T}\right)\right) \tag{A.7}$$

We then take the expectation of the above

$$\langle s\rangle = \int_{-\infty}^{\infty} s\Pr\left(s \mid K\right)ds \tag{A.8a}$$

$$\langle s\rangle = \int_{-\infty}^{\infty} s\sum_{W}\Pr(W|K)\delta(s - \sum_{k=0}^{N} A\sin(W(t - k\tau))\operatorname{rect}(\frac{t - \frac{T}{2} - k\tau}{T}))ds \tag{A.8b}$$

$$\langle s\rangle = \sum_{W}\Pr\left(W \mid K\right)\sum_{k=0}^{N}\left(A\sin\left(W\left(t - kT\right)\right)\operatorname{rect}\left(\frac{t - \frac{T}{2} - k\tau}{T}\right)\right) \tag{A.8c}$$

Taking the Fourier transform of equation (A.8c)

$$\mathcal{F}\left[\langle s\rangle\right] = \int_{-\infty}^{\infty}\sum_{W}\Pr\left(W \mid K\right)\sum_{k=0}^{N} A\sin\left(W\left(t - kT\right)\right)\operatorname{rect}\left(\frac{t - \frac{T}{2} - k\tau}{T}\right)\mathrm{e}^{-j\omega t}dt \tag{A.9a}$$

$$\therefore \mathcal{F}\left[\langle s\rangle\right] = A\sum_{W}\sum_{k=0}^{N}\Pr(W|K)\frac{\pi}{j}[\delta(\omega - W)+ \delta(\omega + W)]\mathrm{e}^{-j\omega k\tau} * T\,\mathrm{sinc}(\frac{\omega T}{2})e^{-j\omega(\frac{T}{2}+k\tau)} \quad \text{(A.9b)}$$

The symbol * denotes convolution. Solving the convolution integral gives

$$f(\omega) * g(\omega) = \int_{-\infty}^{\infty} f(p)\, g(\omega - p)\, dp$$

where

$$f(p) = \frac{\pi}{j}\left[\delta(p - W) + \delta(p + W)\right]\mathrm{e}^{-jpk\tau}$$

$$g(\omega - p) = T sinc\left(\frac{(\omega - p)\,T}{2}\right)\ \mathrm{e}^{-j(\omega-p)(\frac{T}{2}+k\tau)}$$

results in

$$\therefore \mathcal{F}\left[\langle s\rangle\right] = A\frac{\pi T}{j}\sum_{W}\sum_{k=0}^{N}\Pr(W|K) \left[\mathrm{sinc}\left(\frac{(\omega - W)\,T}{2}\right)\mathrm{e}^{-j(\frac{\omega T}{2}+\omega k\tau-\frac{WT}{2})}+ \mathrm{sinc}(\frac{(\omega + W)T}{2})\mathrm{e}^{-j(\frac{\omega T}{2}+\omega k\tau+\frac{WT}{2})}\right] \quad \text{(A.10)}$$

This is the model that will be used to model the magnitude spectrum which we will refer to as the PSD.

A.1.3 Simulation Experiments

In these results, we compare the PSD of the random experiment with the PSD that the analytical solution predicts.

The experiment is conducted as follows:

A frequency is randomly chosen from n possible frequencies. This experiment is done N number of times so that each outcome is assigned to the k^{th} portion of $s(t)$ from $k = 1$ to $k = N$.

According to the law of large numbers, if N is large, for a uniform distribution, on average, each of the possible frequencies will be chosen an equal number of times (approximately). For a Gaussian distribution, then the PSD will also follow a Gaussian shape.

The impact of changing the probability distribution $\Pr(W|K)$ is investigated by performing 3 sets of tests. The first 2 tests use a uniform PDF and a Gaussian PDF respectively. For each PDF, the resulting spectrum from the random experiment and the analytical model is plotted. In the last test, constraint 1 is disobeyed by changing the 'hopping' period τ to be smaller than the smallest possible periods. Each discrete PDF has 5 possible frequencies in Hz. Thus the PDF is denoted $\Pr(F|K)$ here. Table A.1 shows the parameters used.

TABLE A.1: Parameters for the 3 sets of tests performed

Parameters	Value
test 1 τ	0.02s
test 2 τ	0.02s
test 3 τ	0.005
N	100
A	1
T	τ
$(f_1, f_2, f_3, f_4, f_5)$	(100,200,300,400,500) Hz

Figure A.3B and A.3C show the spectrum of the random experiment and analytical solution respectively, when a Uniform PDF (shown in Figure A.3A) is used. Figure A.2B and A.2C show the spectrum of the random experiment and analytical solution respectively, when a Gaussian PDF (shown in Figure A.2A) is used. Figure A.4 shows the resulting spectrum if constraint 1 is not imposed.

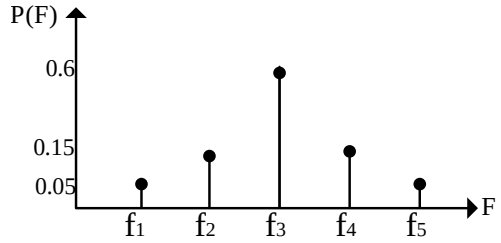

(A) Gaussian probability distribution input function.

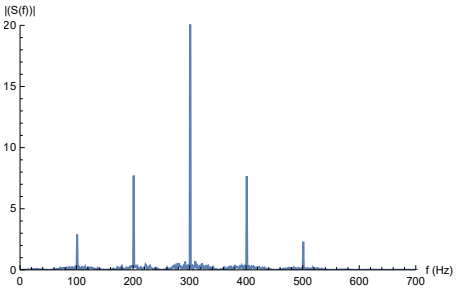

(B) Spectrum for Gaussian Probability Distribution from random experiment.

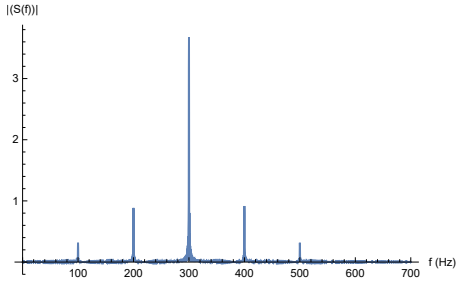

(C) Spectrum for Gaussian Probability Distribution predicted by model (equation A.10).

FIGURE A.2: Spectrum for Gaussian Probability Distribution from random trials and predicted result.

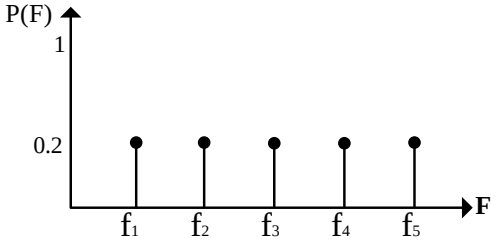

(A) Uniform probability distribution input function

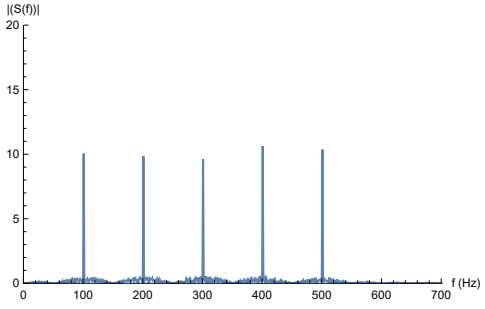

(B) Spectrum for Uniform Probability Distribution from random experiment

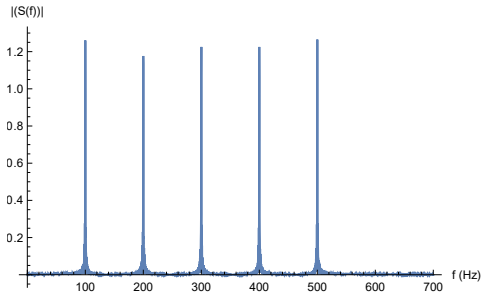

(C) Spectrum for Uniform Probability Distribution predicted by model (equation A.10)

FIGURE A.3: Spectrum for Uniform Probability Distribution from random trials and predicted result

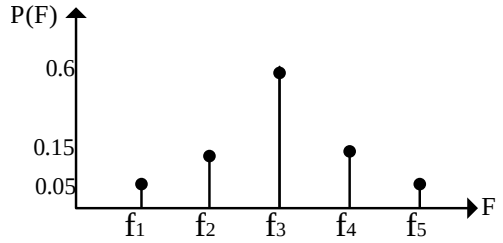

(A) Gaussian probability distribution input function

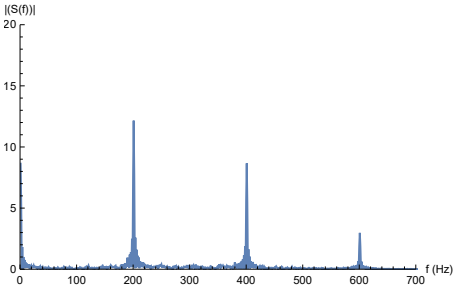

(B) Random experiment Spectrum for Gaussian Probability Distribution without following constraints.

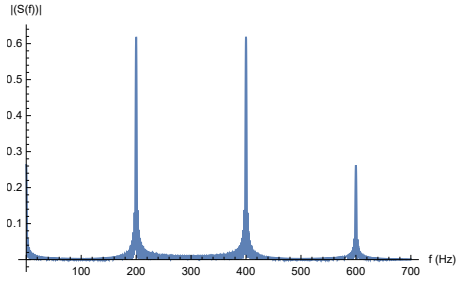

(C) Predicted Spectrum for Gaussian Probability Distribution without following constraints.

FIGURE A.4: Spectrum for Gaussian Probability Distribution without following constraints.

A.1.4 Results Discussion

As expected, the analytical solution predicts the generic shape of the PSD. However, it is unable to predict the actual magnitudes of each of the 'harmonics'. The difference in magnitude differs for each frequency in a non-linear manner and also differs for different PDFs. The nature of the error in that regard would have to be investigated further.

One may assert that the magnitudes in the PSD assumes that the width T is much longer than some multiples of the period. This is true. Recalling that several portions (or windows) of s will have the a common frequency. Thus if one were to lump up together the portions with common frequency, their combined width is more than T. As a result, their magnitude becomes more than the analytically predicted magnitude. A possible solution is to use Welch's periodogram method of estimating the PSD in simulation (see Section 4.3.2), as it can normalize the magnitude by averaging all windows that contain a common frequency over a fixed time T (i.e. an ensemble average) instead of lumping up (or adding up) the windows in time. In any case, the intention is approximate the PSD in order to view shape of the PSD governed by the probability distribution. Due to this, the vertical scales have been adjusted to show the shape of the PSD.

From Figure A.4, we see that once the constraint 1 is disobeyed, then we loose the ability to control the shape of the PSD using the probability distributions since a Gaussian shaped spectrum was expected. The high amplitudes were also supposed to be located at the possible set of frequencies. Instead, these amplitudes are located at multiples of the 'hopping' frequency of 200 Hz. This is due to consecutive sine waves being out of phase, so there is a non-smooth transition between consecutive sine waves with different frequencies. This transition then 'forces' the integer multiples of the 'hopping' frequency $1/\tau$ to appear in the frequency spectrum.

From here, it can be concluded that in order to be able to shape the spectrum using a PDF, the possible frequencies must be integer multiples of hopping frequency. This will prevent the hopping frequency from dominating the spectrum.

Appendix B

Appendix B

B.1 Definition of Spreading

This appendix aims to define what is meant by 'spreading' out of probability and of the harmonic power in the Power Spectral Density.

Spreading out of probability happens in two ways. The first one is an increase in the distribution of probability among available inputs, chances or choices. For discrete probabilities, this phenomenon is depicted by Figure 3.1 and 3.2. The entropic values where calculated using Equation 3.1.

The entropy of the probability in Figure 3.1 is greater than the entropy in Figure 3.2 as shown in the respective Figures. Thus entropy increases without affecting the number of possible outcomes. The distribution of probability 'spreads' out due to the normalization condition $\sum p_i = 1$ (p_i are the discrete probabilities) that probabilities must obey.

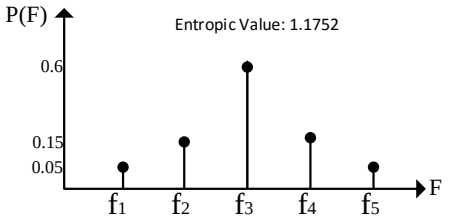

FIGURE B.1: Example of PDF will less spreading

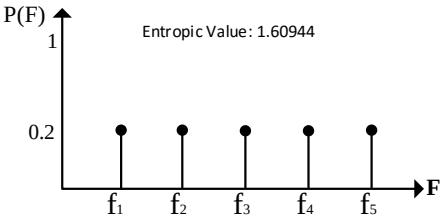

FIGURE B.2: Example of PDF will more spreading

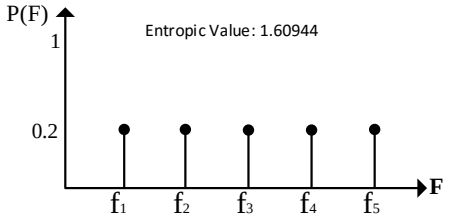

FIGURE B.3: Example of PDF will less spreading

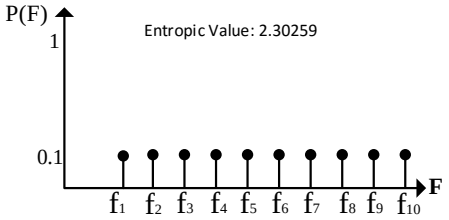

FIGURE B.4: Example of PDF will more spreading

Spreading out can also be described as increase in the number of possible outcomes. When this happens, it means the probability will be more distributed or more spread out because of the normalization condition.

This is demonstrated by Figure 3.3 and 3.4.

It is obvious that the combination of the two types of spreading will increase the entropic value even more.

This description of spreading out also applies to the power density spectrum. The power density spectrum holds the condition that the total harmonic power remains unchanched when changing the shape of the distribution [7].

B.2 Use of entropy in the Model problem

It has already been shown how spreading out of probability can be quantified by entropy. This section seeks to show how for the model problem, increase in probability distribution leads to a more spread out PSD, and this spreading out is quantifiable by using entropy. Table B.1 tabulates the entropy of probability distribution as the spreading out of probability is increased as well as the entropy of the resulting PSD. The probabilities of the possible frequencies where chosen so as to increase the spreading out of probability. The increase in this case is of the first type as discussed in section B.1, where the number of possible outcomes is kept the same. The relationship is shown in Figure B.5.

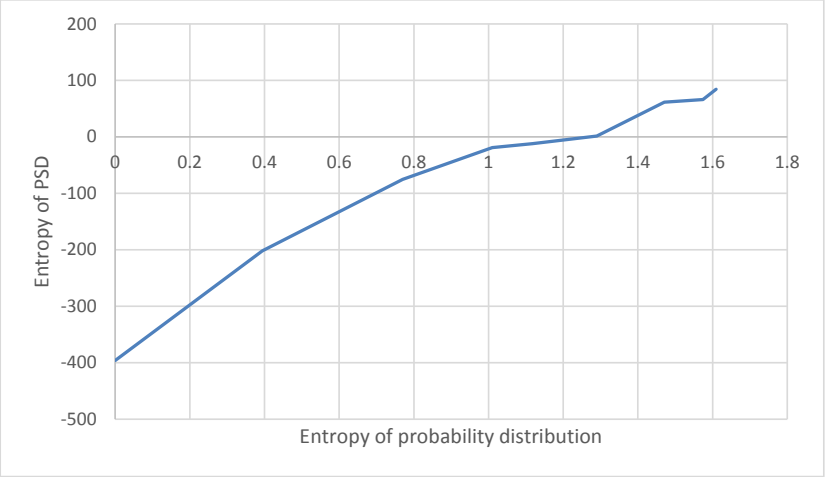

FIGURE B.5: Plot showing increase in spreading of probability distribution leads to increase of spreading in PSD as measured by respective entropic values

TABLE B.1: Entropic values of probability distributions and PSD

Pr(f1)	Pr(f2)	Pr(f3)	Pr(f4)	Pr(f5)	Prob Entropy	PSD Entropy
0	0	1	0	0	0	-396.119
0	0.05	0.9	0.05	0	0.394398	-202
0.05	0.05	0.8	0.05	0.05	0.77	-75.2159
0.05	0.1	0.7	0.1	0.05	1.00976	-19.013
0.05	0.15	0.6	0.15	0.05	1.11752	-12.0643
0.05	0.2	0.5	0.2	0.05	1.28992	1.452
0.1	0.2	0.4	0.2	0.1	1.47081	61.2932
0.15	0.2	0.3	0.2	0.15	1.5741	66.3383
0.2	0.2	0.2	0.2	0.2	1.60944	84.358

In this case, there is a direct proportionality between the entropy in PDF and entropy in the PSD, provided the constraint in A.1.2 is obeyed. This is the type of result we seek to find in the main research question for this research.

There are many other factors that can be discussed for this model problem. However, its aim has been only to help further understand the scale and the direction that this research is taking.

Bibliography

[1] S. Sivakumar, M. Jagabar Sathik, P. S. Manoj, and G. Sundararajan. An assessment on performance of DCDC converters for renewable energy applications. volume 58, pages 1475–1485, May 2016.

[2] A. Tomaszuk and A. Krupa. High efficiency high step-up DC/DC converters - a review. volume 59, January 2011.

[3] Alfred Hesener. Electromagnetic Interference (EMI) in Power Supplies. In *Fairchild Semiconductor Power Seminar*, volume 2011, pages 1–16, 2010.

[4] A. Carlosena, Wing-Yee Chu, B. Bakkaloglu, and S. Kiaei. Randomized carrier PWM with exponential frequency mapping. In *2006 IEEE International Symposium on Circuits and Systems*, pages 4 pp.–, May 2006.

[5] A. Elrayyah, K. MPK Namburi, Y. Sozer, and I. Husain. An Effective Dithering Method for Electromagnetic Interference (EMI) Reduction in Single-Phase DC/AC Inverters. volume 29, pages 2798–2806, June 2014.

[6] M. Kchikach, A. Elhasnanoui, K. Zazi, and Z. M. Qian. The Electromagnetic Interference (EMI) affect on power supply of Telecom equipment. In *2010 Asia-Pacific International Symposium on Electromagnetic Compatibility*, pages 83–86, April 2010.

[7] A. M. Trzynadlowski, F. Blaabjerg, J. K. Pedersen, R. L. Kirlin, and S. Legowski. Random pulse width modulation techniques for converter-fed drive systems - a review. volume 30, pages 1166–1175, September 1994.

[8] D. Gonzalez, J. Balcells, A. Santolaria, J. C. Le Bunetel, J. Gago, D. Magnon, and S. Brehaut. Conducted EMI Reduction in Power Converters by Means of Periodic Switching Frequency Modulation. volume 22, pages 2271–2281, November 2007.

[9] R. Boopathi, P. Muthukumar, P. Melba Mary, and S. Jeevananthan. Investigations on harmonic spreading effects of SVPWM switching patterns in VSI fed AC drives. In *2012 International Conference on Advances in Engineering, Science and Management (ICAESM)*, pages 651–656, March 2012.

[10] C. M. Liaw, Y. M. Lin, C. H. Wu, and K. I. Hwu. Analysis, design, and implementation of a random frequency PWM inverter. volume 15, pages 843–854, September 2000.

[11] S. H. Na, Y. G. Jung, Y. C. Lim, and S. H. Yang. Reduction of audible switching noise in induction motor drives using random position space vector PWM. volume 149, pages 195–200, May 2002.

[12] G. Wang, L. Yang, B. Yuan, B. Wang, G. Zhang, and D. Xu. Pseudo-Random High-Frequency Square-Wave Voltage Injection Based Sensorless Control of IPMSM Drives for Audible Noise Reduction. volume 63, pages 7423–7433, December 2016.

[13] G. Ala, G. C. Giaconia, G. Giglia, M. C. Di Piazza, M. Luna, G. Vitale, and P. Zanchetta. Optimized design of high power density EMI filters for power electronic converters. In *2016 AEIT International Annual Conference (AEIT)*, pages 1–6, October 2016.

[14] G. Ala, G. C. Giaconia, G. Giglia, M. C. Di Piazza, M. Luna, G. Vitale, and P. Zanchetta. Computer aided optimal design of high power density EMI filters. In *2016 IEEE 16th International Conference on Environment and Electrical Engineering (EEEIC)*, pages 1–6, June 2016.

[15] M. M. Bech, J. K. Pedersen, F. Blaabjerg, and A. M. Trzynadlowski. A methodology for true comparison of analytical and measured frequency domain spectra in random PWM converters. volume 14, pages 578–586, May 1999.

[16] M. M. Bech, F. Blaabjerg, and J. K. Pedersen. Random modulation techniques with fixed switching frequency for three-phase power converters. volume 15, pages 753–761, July 2000.

[17] Michael M. Bech. *Analysis of random pulse-width modulation techniques for power electronic converters*. PhD thesis, Institute of Energy Technology, Aalborg University, 2000.

[18] R. L. Kirlin, M. M. Bech, and A. M. Trzynadlowski. Analysis of power and power spectral density in PWM inverters with randomized switching frequency. volume 49, pages 486–499, April 2002.

[19] R. L. Kirlin, S. F. Legowski, and A. M. Trzynadlowski. An optimal approach to random pulse width modulation in power inverters. In *, 26th Annual IEEE Power Electronics Specialists Conference, 1995. PESC '95 Record*, volume 1, pages 313–318, June 1995.

[20] R. L. Kirlin, C. Lascu, and A. M. Trzynadlowski. Shaping the Noise Spectrum in Power Electronic Converters. volume 58, pages 2780–2788, July 2011.

[21] K. K. Tse, H. S. H. Chung, S. Y. R. Hui, and H. C. So. A comparative study of using random switching schemes for DC/DC converters. In *Applied Power Electronics Conference and Exposition, 1999. APEC '99. Fourteenth Annual*, volume 1, pages 160–166, March 1999.

[22] A. M. Stankovic, G. E. Verghese, and D. J. Perreault. Analysis and synthesis of randomized modulation schemes for power converters. volume 10, pages 680–693, November 1995.

[23] T. S. Kiran and K. N. Pavithran. Novel approach for harmonic reduction with random PWM technique for multilevel inerters. In *2015 International Conference on Power, Instrumentation, Control and Computing (PICC)*, pages 1–6, December 2015.

[24] R. L. Kirlin, S. Kwok, S. Legowski, and A. M. Trzynadlowski. Power spectra of a PWM inverter with randomized pulse position. In *, 24th Annual IEEE Power Electronics Specialists Conference, 1993. PESC '93 Record*, pages 1041–1047, June 1993.

[25] A. M. Trzynadlowski, M. M. Bech, F. Blaabjerg, J. K. Pedersen, R. L. Kirlin, and M. Zigliotto. Optimization of switching frequencies in the limited-pool random space vector PWM strategy for inverter-fed drives. volume 16, pages 852–857, November 2001.

[26] R. L. Kirlin and A. M. Trzynadlowski. Spectral Design of Randomized Pulse Width Modulation in DC to AC Converters. In *, IEEE Seventh SP Workshop on Statistical Signal and Array Processing*, pages 387–391, June 1994.

[27] P. Clarke. Self-commutated thyristor DC-to-DC converter. volume 6, pages 10–15, March 1970.

[28] Kevin Lee, Guangtong Shen, Wenxi Yao, and Zhengyu Lu. Performance characterization of random pulse width modulation algorithms in industrial and commercial adjustable speed drives. pages 2003–2010. IEEE, March 2016.

[29] K. K. Tse, H. S. H. Chung, S. Y. Huo, and H. C. So. Analysis and spectral characteristics of a spread-spectrum technique for conducted EMI suppression. volume 15, pages 399–410, March 2000.

[30] H. Li, Y. Liu, J. L, T. Zheng, and X. Yu. Suppressing EMI in Power Converters via Chaotic SPWM Control Based on Spectrum Analysis Approach. volume 61, pages 6128–6137, November 2014.

[31] K. S. Kim, Y. G. Jung, and Y. C. Lim. A New Hybrid Random PWM Scheme. volume 24, pages 192–200, January 2009.

[32] L. Premalatha and A. Thanuja. Generation of chaos and EMI reduction in current controlled boost converter using Random modulation. In *2011 International Conference on Recent Advancements in Electrical, Electronics and Control Engineering (ICONRAEeCE)*, pages 211–215, December 2011.

[33] K. K. Tse, Henry Shu-Hung Chung, S. Y. Ron Hui, and H. C. So. A comparative study of carrier-frequency modulation techniques for conducted EMI suppression in PWM converters. volume 49, pages 618–627, June 2002.

[34] Michael Mller Bech. Comparative Investigation of Random PWM Techniques with Variable Switching Frequency and Pulse Position for Inverter-fed Induction Motors. 1997.

[35] P. C. Loh, D. M. Vilathgamuwa, F. Gao, C. J. Gajanayake, L. W. Gay, and P. F. Leong. Random Pulse-Width Modulated Neutral-Point-Clamped Inverter With Reduced Common-Mode Switching. In *2005 International Conference on Power Electronics and Drives Systems*, volume 2, pages 1435–1440, November 2005.

[36] S. Y. R. Hui, S. Sathiakumar, and K. K. Sung. Novel random PWM schemes with weighted switching decision. In *1996 Sixth International Conference on Power Electronics and Variable Speed Drives (Conf. Publ. No. 429)*, pages 348–353, September 1996.

[37] Bor-Ren Lin. High power factor AC/DC/AC converter with random PWM. volume 35, pages 935–943, July 1999.

[38] S. Bhattacharya, D. Mascarella, G. Joos, and G. Moschopoulos. A discrete random PWM technique for acoustic noise reduction in electric traction drives. In *2015 IEEE Energy Conversion Congress and Exposition (ECCE)*, pages 6811–6817, September 2015.

[39] L. Mathe, F. Lungeanu, D. Sera, P. O. Rasmussen, and J. K. Pedersen. Spread Spectrum Modulation by Using Asymmetric-Carrier Random PWM. volume 59, pages 3710–3718, October 2012.

[40] S. Y. Oh, Y. G. Jung, S. H. Yang, and Y. C. Lim. Harmonic-Spectrum Spreading Effects of Two-Phase Random Centered Distribution PWM (DZRCD) Scheme With Dual Zero Vectors. volume 56, pages 3013–3020, August 2009.

[41] Y. L. Familiant and A. Ruderman. Discussion of #8220;A Variable Switching Frequency PWM Technique for Induction Motor Drive to Spread Acoustic Noise Spectrum With Reduced Current Ripple #8221;. volume 52, pages 5355–5355, November 2016.

[42] A. C. B. Kumar and G. Narayanan. Variable-Switching Frequency PWM Technique for Induction Motor Drive to Spread Acoustic Noise Spectrum With Reduced Current Ripple. volume 52, pages 3927–3938, September 2016.

[43] S. T. S, J. J. S, and A. K. C. Intensive random carrier pulse width modulation for induction motor drives based on hopping between discrete carrier frequencies. volume 9, pages 417–426, 2016.

[44] Bin Huo, A. M. Trzynadlowski, I. Panahi, A. Mohammed, and Zhenyu Yu. Novel random pulse width modulator with constant sampling frequency based on the TMS320f240 DSP controller. In *The 25th Annual Conference of the IEEE Industrial Electronics Society, 1999. IECON '99 Proceedings*, volume 1, pages 342–347, 1999.

[45] Aleksandar Mihajla Stankovi. *Random pulse modulation with applications to power electronic converters.* Thesis, Massachusetts Institute of Technology, 1993.

[46] E. T. Jaynes. Information Theory and Statistical Mechanics. volume 106, pages 620–630, May 1957.

[47] R. L. Kirlin, M. M. Bech, and A. M. Trzynadlowski. Power spectral density analysis of randomly switched pulse width modulation for DC/AC converters. In *Proceedings of the Tenth IEEE Workshop on Statistical Signal and Array Processing (Cat. No.00TH8496)*, pages 373–377, 2000.

[48] Thomas M. Cover and Joy A. Thomas. *Elements of Information Theory (Wiley Series in Telecommunications and Signal Processing).* Wiley-Interscience, 2006.

[49] Y. C. Lim, S. O. Wi, J. N. Kim, and Y. G. Jung. A Pseudorandom Carrier Modulation Scheme. volume 25, pages 797–805, April 2010.

[50] T. Tanaka, H. Hamasaki, and H. Yoshida. Random-switching control in DC-to-DC converters: an implementation using M-sequence. In *Telecommunications Energy Conference, 1997. INEC 97., 19th International*, pages 431–437, October 1997.

[51] G. A. Covic and J. T. Boys. Noise quieting with random PWM AC drives. volume 145, pages 1–10, January 1998.

[52] Pierre Bremaud. *Markov Chains: Gibbs Fields, Monte Carlo Simulation, and Queues*. Springer Science & Business Media, March 2013. Google-Books-ID: jrPVBwAAQBAJ.

[53] J. R. Norris. *Markov Chains*. Cambridge University Press, July 1998. Google-Books-ID: qM65VRmOJZAC.

[54] Dean L. Urban and David O. Wallin. Introduction to Markov Models. In *Learning Landscape Ecology*, pages 129–142. Springer, New York, NY, 2017. DOI: 10.1007/978-1-4939-6374-4_8.

[55] Vijay P. Singh. *Entropy Theory and its Application in Environmental and Water Engineering*. John Wiley & Sons, January 2013.

[56] Edwin T. Jaynes. *Probability theory: The logic of science*. Cambridge university press, 2003.

[57] Ariel Caticha. Lectures on Probability, Entropy, and Statistical Physics. July 2008. arXiv: 0808.0012.

[58] A.E. Abbas. Entropy methods for joint distributions in decision analysis. volume 53, pages 146–159, February 2006.

[59] Constrained Optimization and Lagrange Multiplier Methods - 1st Edition.

[60] Kevin Davey. What Is Gibbss Canonical Distribution? volume 76, pages 970–983, December 2009.

[61] R. L. Kirlin, S. Legowski, A. M. Trzynadlowski, Y. Cui, and S. Kwok. Power spectra of a three-phase inverter with random pulse width modulation modes. In *[Proceedings] 1992 IEEE Workshop on Computers in Power Electronics*, pages 265–267, 1992.

[62] S. Legowski, J. Bei, and A. M. Trzynadlowski. Analysis and implementation of a grey-noise PWM technique based on voltage space vectors. In *Applied Power*

Electronics Conference and Exposition, 1992. APEC '92. Conference Proceedings 1992., Seventh Annual, pages 586–593, February 1992.

[63] N. C. Sevktekin and A. C. Singer. I.I.D. stochastic analysis of PWM signals. In *2014 48th Asilomar Conference on Signals, Systems and Computers*, pages 1885–1889, November 2014.

[64] David Solomon George and M. R. Baiju. Space vector based Random Pulse Width Modulation scheme for a 3-level inverter in open-end winding induction motor configuration. In *2012 IEEE International Symposium on Industrial Electronics*, pages 742–747, May 2012.

[65] Dennis W. Ricker. *Echo Signal Processing.* Springer Science & Business Media, February 2003.

[66] P. Welch. The use of fast Fourier transform for the estimation of power spectra: A method based on time averaging over short, modified periodograms. volume 15, pages 70–73, June 1967.

[67] David Middleton. *An introduction to statistical communication theory.* McGraw-Hill, 1960.

[68] Athanasios Papoulis. *Probability, Random Variables, and Stochastic Processes.* McGraw-Hill, 1991.

[69] K. K. Tse, H. S. H. Chung, S. Y. R. Hui, and H. C. So. A comparative investigation on the use of random modulation schemes for DC/DC converters. volume 47, pages 253–263, April 2000.

[70] Debabrata Mukher jee and Makarand V. Ratnaparkhi. On the functional relationship between entropy and variance with related applications. volume 15, pages 291–311, January 1986.

[71] H. Misra, S. Ikbal, H. Bourlard, and H. Hermansky. Spectral entropy based feature for robust ASR. In *2004 IEEE International Conference on Acoustics, Speech, and Signal Processing*, volume 1, pages I–193–6, May 2004.

[72] T. Yingthawornsuk. Spectral Entropy in Speech for Classification of Depressed Speakers. In *2016 12th International Conference on Signal-Image Technology Internet-Based Systems (SITIS)*, pages 679–682, November 2016.

[73] B. Yang and A. Zhang. Power spectral entropy analysis of EEG signal based-on BCI. In *Proceedings of the 32nd Chinese Control Conference*, pages 4513–4516, July 2013.

[74] Changqing Yin, W. Li, Yuanqing Luo, and Li-Chuan Tseng. Robust online music identification using spectral entropy in the compressed domain. In *2014 IEEE Wireless Communications and Networking Conference Workshops (WCNCW)*, pages 128–133, April 2014.

[75] David Stone and Barry Chambers. The Effect of Carrier Frequency Modulation of PWM Waveforms on Conducted EMC Problems in Switched Mode Power Supplies. volume 5, pages 32–37, January 1996.

[76] Charles Marsh. *Introduction to continuous entropy*. 2013.

[77] Manuel Duarte Ortigueira. The comb signal and its Fourier transform. volume 81, pages 581–592, 2001.

[78] Werner Krauth. *Statistical mechanics: algorithms and computations*. Number 13 in Oxford master series in physics Statistical, computational, and theoretical physics. Oxford Univ. Press, Oxford, 2006. OCLC: 254061236.

[79] George Casella, Christian P. Robert, and Martin T. Wells. *Generalized Accept-Reject sampling schemes*. Institute of Mathematical Statistics, 2004. DOI: 10.1214/lnms/1196285403.